NASA Technical Paper 1737

Evaluation of Flow Quality in Two Large NASA Wind Tunnels at Transonic Speeds

William D. Harvey, P. Calvin Stainback, and F. Kevin Owen

DECEMBER 1980

NASA

NASA Technical Paper 1737

Evaluation of Flow Quality in Two Large NASA Wind Tunnels at Transonic Speeds

William D. Harvey and P. Calvin Stainback
Langley Research Center
Hampton, Virginia

F. Kevin Owen
COMPLERE, Inc.
Pala Alto, California

National Aeronautics
and Space Administration

**Scientific and Technical
Information Branch**

1980

SUMMARY

Wind-tunnel testing of low-drag airfoils and basic transition studies at transonic speeds are designed to provide high-quality aerodynamic data at high Reynolds numbers. This requires that the flow quality in facilities used for such research be excellent. To obtain a better understanding of the characteristics of facility disturbances and identification of their sources for possible facility modification, detailed flow-quality measurements were made in two prospective NASA wind tunnels. This paper presents experimental results of an extensive and systematic flow-quality study of the settling chamber, test section, and diffuser in the Langley 8-Foot Transonic Pressure Tunnel (TPT) and the Ames 12-Foot Pressure Wind Tunnel (PWT). Results indicate that the free-stream velocity and pressure-fluctuation levels in both facilities are low ($\leq$ 0.1 percent) at subsonic speeds and are so high as to make it difficult to conduct meaningful boundary-layer control and transition studies at transonic speeds.

INTRODUCTION

One of the largest economic problems facing the airlines industry today is the rapid rise in fuel cost. Recognizing the importance of fuel efficiency, the NASA Langley Research Center and industry are currently trying to define and demonstrate a practical, reliable, and maintainable boundary-layer suction system for viscous drag reduction through laminar flow control. As a part of these efforts, an advanced laminar flow control (LFC) airfoil has been designed, and plans have been made to confirm experimentally its performance at high-chord Reynolds numbers in a wind tunnel of acceptable flow quality. This work is intended to establish a technology data base for long-range commercial transports of the 1990's.

Aside from other considerations, it is particularly important, when measurements are obtained on low-drag airfoils whose boundary layers remain laminar over long lengths, not to adversely influence the laminar boundary layer by facility disturbances. Although wind-tunnel wall effects on experimental data have long been recognized, little is presently known about the influence of free-stream turbulence on steady and dynamic measurements in wind tunnels at transonic speeds. Indeed, few measurements have been made of the characteristics of free-stream unsteadiness in transonic wind tunnels. The result is that information is lacking on velocity and pressure fluctuations and their amplitude and spectra. This information is needed in order to assess the relationship between wind-tunnel and flight transition behavior. Furthermore, characteristic source disturbances must be identified for proper facility modification to achieve the anticipated improvement in flow quality.

Perhaps the major open question is the influence of free-stream disturbances on model boundary-layer transition. The effect of turbulence is to

reduce the boundary-layer transition Reynolds number to values which depend, in an almost unknown manner, on the characteristics of free-stream turbulence. Earlier results at subsonic speeds have shown the effects of free-stream disturbance on transition. (See refs. 1 to 4.) Recent developments in boundary-layer transition research, particularly those of the NASA Transition Study Group (ref. 5), have stressed the dominant role that free-stream fluctuations have on model boundary-layer stability at transonic and supersonic speeds. Not only do the external fluctuation amplitudes influence transition, but their energy spectra are particularly significant. However, a significant quantity of available data have been compiled recently which shows that the beginning of transition on simple models is influenced both by free-stream disturbances (broadband) and local conditions, and the data collapse along a single curve for a wide range of test conditions and wind tunnels (ref. 6). In general, acceptable values for the mean-velocity variations within the test section of most wind tunnels are about $\pm 0.1^{\circ}$. These variations correspond to about four times the rms turbulent fluctuations normally aimed at. However, design for low turbulence in wind tunnels should ensure adequate uniformity of mean velocity, since the techniques for reducing turbulence and spatial variation are similar. Previous LFC experiments (ref. 7) have shown that the characteristics of these low-drag airfoils can be successfully measured only in low-turbulence tunnels. Figure 1 illustrates the effect of environmental disturbance level (broadband) on maintaining laminar flow on low-drag wings and bodies of revolution with suction in several wind tunnels and flight (ref. 8) for $0 \leq M_{\infty} \leq 0.3$ and $0.4 \leq M_{\infty} \leq 0.8$, respectively. Tunnels whose broadband level of turbulence is very small ($\tilde{u}/\bar{u} \approx 0.05$ percent) are required to achieve laminar flow on wings for large chord Reynolds numbers approaching flight conditions. This objective becomes increasingly difficult when testing models at transonic Mach numbers, since the results and their accuracy may be influenced by free-stream turbulence (vorticity), acoustical disturbances (noise or sound), low-frequency pressure fluctuations, temperature fluctuations, and mechanical vibrations. These disturbances can influence either the steady flow over a test model or introduce fluctuations in dynamic force measurements. In general, the stream turbulence is established by the tunnel drive system, settling chamber and components, and by the contraction to the test section. Acoustical disturbances can be expected from the drive system, perforated or slotted transonic walls, reentry of air at slots, model support, and diffuser. Some facility disturbances are unavoidable, such as wall boundary noise and separated flow conditions. However, the noise level that would be radiated by the turbulent boundary layer on solid-wall test sections in a subsonic or transonic facility may be considered as an irreducible minimum.

The need for transonic wind tunnels with low disturbance levels has been recognized, and work is being done to develop such tunnels (refs. 9 and 10). Based on very limited information, which indicates good flow quality in both facilities, the Langley 8-Foot Transonic Pressure Tunnel and Ames 12-Foot Pressure Wind Tunnel were selected for flow-quality evaluation for possible future laminar flow control (LFC) research. In order to obtain a better understanding of the characteristics of the disturbances and identification of their sources (refs. 11 and 12) for possible modification, detailed flow-quality measurements were made in both facilities. This paper presents experimental results of an extensive and systematic flow-quality study made in the settling chambers, test

sections, and diffusers of the Langley 8-Foot and Ames 12-Foot Tunnels over a range of operating conditions.

SYMBOLS

a	speed of sound
C_L	lift coefficient
C_p	pressure coefficient
c	model chord
d	diameter
f	frequency
K	screen resistance (pressure-drop) coefficient
l	length
M	Mach number
n	number of screens
p	pressure
q_l	local dynamic pressure
q_t	tunnel dynamic pressure
R	unit Reynolds number
R_c	Reynolds number based on wing chord
R_{xy}	cross-correlation function
T	temperature
t	thickness
u	velocity
x	axial distance or distance from wall slot origin
α	angle of attack
γ	ratio of specific heats

ρ density

τ time

Subscripts:

avg average

s screen

sep separation

t total conditions

∞ free stream

1,2 before and after, respectively

Superscripts:

$\bar{}$ mean value

$\sim$ rms value of fluctuating component

FACILITIES, INSTRUMENTATION, AND TEST CONDITIONS

Facilities

Langley 8-Foot Transonic Pressure Tunnel (TPT). A sketch of the Langley 8-Foot Tunnel circuit is shown in figure 2(a). The circles with crosses in them indicate where measurements were made. Figures 2(b), (c), and (d) show details of the various instrumented regions which are discussed subsequently. The test section has a rectangular cross section (fig. 2(c)) with slotted top and bottom walls. The Langley 8-Foot Tunnel is similar to most transonic tunnels except for the presence of a cooler (fig. 2(b)), consisting of eight staggered rows of finned tubes, located in the corner just upstream of the 10.97-m diameter settling chamber. Because of the large pressure drop across the cooler ($\Delta p/q_1 \approx 8$), it is assumed that the flow leaves the cooler normal to the plane of the cooler and at 45° with respect to the undisturbed free-stream direction in the settling chamber. Together, the cooler and the 45° turning vanes downstream of the cooler (fig. 2(b)) turn the flow through the 90° corner. There are no turbulence suppression screens in the settling chamber, and the nozzle contraction ratio is 20:1. The rectangular test section ($l/d \approx 3$) is formed by a transition section ($l/d \approx 0.33$) from circular to rectangular at its entrance and the reverse at its exit. For comparison purposes with the Ames 12-Foot Tunnel, which has solid test-section walls, the Langley 8-Foot Tunnel test-section wall slots were covered with 0.635-cm thick metal plates which were beveled and mounted over the slots (fig. 2(c)). Except when noted, the slot covers were in place for the present tests. The cooler was operational for the present tests and the total temperature was 322 K for all Mach numbers except $M_\infty = 0.2$, where the temperature was as low as 319 K.

Ames 12-Foot Pressure Wind Tunnel (PWT).- A sketch of the Ames 12-Foot Tunnel circuit is shown in figure 3. The circles with crosses in them indicate where measurements were made (fig. 3(a)). Figures 3(b) and (c) show details of the various instrumented regions in the test section and diffuser, respectively, and are discussed in the section "Instrumentation." The Ames tunnel has a rapid expansion section (Area ratio = 2) ahead of the 18.29-m diameter settling chamber with 8 screens in series about 20.32 cm apart. The most upstream screen has a mesh of 16 and is followed by 7 screens with a mesh of 12. Porosity of the screens is 0.462 and 0.490, respectively. The contraction ratio of the nozzle is 25:1, which is exceptionally good for turbulence reduction. The new tunnel-model support strut in the Ames 12-Foot Tunnel is shown in figure 3(b) and is located at the circular-test-section exit and high-speed-diffuser entrance. The geometry of the new strut is very similar to that of the previous strut. However, the blockage area is greater by a factor of about 1.5. Except when noted, the present tests were conducted with 0.1588-cm thick cover plates mounted over the existing strut slots to eliminate flow-generated disturbances in and out of the normally exposed through slots. The strut is provided with vertical slots for translation of the centerbody sting mount.

Instrumentation

General.- For consistency, the measuring probes and dynamic recording instrumentation were identical insofar as possible in each of the facilities. Constant-temperature hot-wire anemometry techniques were used with probes having tungsten wires with $\ell/d \geq 50$. Individual wires were calibrated for the test range. The data-reduction methods used are similar to those previously used by Rose and McDaid (ref. 13) for transonic speeds. Value of $\tilde{u}$ presented herein were reduced from simultaneous measurements of the mass-flow fluctuations ($\rho\tilde{u}/\rho\bar{u}$) from the hot wires and pressure fluctuations from the acoustic probes, assuming negligible total-temperature fluctuations (ref. 13). Pressure transducers, cavity mounted within ogive-cylinder (acoustic) probes were used to measure the fluctuating static pressures. The pressure transducers and data-reduction methods were similar to those described in reference 14. The probes were either individually or rake mounted as required for measuring spatial variations. Surface thin-film gages (operated at constant overheat) were also used to measure relative rather than absolute values of the chordwise flow disturbances over the model support struts in each facility.

Langley 8-Foot.- A single hot-wire probe was mounted immediately ahead of and 0.6096 m downstream of the cooler (fig. 2(b)) on the tunnel centerline. Two rakes were used in the settling chamber; one with four hot-wire probes was mounted just downstream of the turning vanes (fig. 2(b)), and another with a single hot-wire and acoustic probe was mounted in the center of the settling chamber on a 0.6096-m diameter ring supported by crossed cables ahead of the contraction section and 7.315 m downstream of the rake at the vanes. Hot-wire and acoustic probes were sting mounted on the centerline of the existing test-section strut (fig. 2(c)). Fluctuating pressure transducers were flush mounted on one vertical sidewall and located in the test section at values of ℓ/d of approximately -0.14 and -0.8 ahead of the wall slot origin (fig. 2(c)) to measure pressure fluctuations beneath the turbulent boundary layer. Thin-film gages were flush mounted on the circular-arc strut at $x/c \approx 0.25$ and 0.75 to

monitor the flow dynamics over the strut. A rake with several pitot tubes and a single acoustic probe was located on the diffuser sidewall at the exit (fig. 2(d)) to measure diffuser mean total pressure and local disturbance levels, respectively.

Ames 12-Foot.- A rake of several hot-wire and acoustic probes was sting mounted in the test section of the Ames 12-Foot Tunnel ahead of the strut ($l/d = 1.7$) and on the centerline (fig. 3(b)). Thin-film gages were flush mounted on the strut slot cover plates beneath the turbulent boundary layer to measure the flow characteristics over the strut at $x/c \approx 0.19$ and 0.65. Multitube static pressure strips were located along both sides of the strut for its total chord (fig. 2(b)) and had 25 pressure orifices on each side to measure the pressure distribution. The same ogive-cylinder probe used by Dods and Hanly (ref. 15) for wind-tunnel flow-quality and flight measurements was used to measure the pressure fluctuations in the diffuser entrance (fig. 3(b)) at a distance $l/d = 1.87$ from the strut trailing edge. To measure fluctuating static pressure, a flush-mounted transducer was located at a distance of about 4 probe diameters from the tip. Hot-wire probes were located approximately on the tunnel centerline just ahead of the first screen in the settling chamber and several hundred screen meshes downstream of the last screen (fig. 3(a)). The pressure drop (Δp) across the eight screens was also simultaneously measured with total and static pressure probes. Both the hot-wire and pressure-drop results were used to evaluate the turbulence-reduction factor for the screens. Figure 3(c) shows both pitot and static pressure probes at the diffuser exit located on the turning-vane support structure. These probes were used to measure the average diffuser-exit total pressure and to evaluate losses.

Test Conditions

A comparison of the maximum operating characteristics of the Langley 8-Foot Tunnel with the Ames 12-Foot Tunnel is shown in figure 4. The normal operating capability of each facility limits a direct, wide-range unit Reynolds number comparison for constant Mach number. Therefore, the present results reflect nearly the maximum unit Reynolds number capability for each tunnel. However, for the Langley 8-Foot Tunnel with the slots covered, the maximum Mach number capability is limited to $M_\infty \approx 0.9$. Tests were conducted in the Langley 8-Foot Tunnel over a range of Mach numbers from 0.2 to 0.9 (up to 1.2 with slots open) and unit Reynolds numbers from 2.0×10^6 to 2.0×10^7 m^{-1}. Corresponding tests were conducted in the Ames 12-Foot Tunnel for Mach numbers from 0.26 to 0.82 and unit Reynolds numbers from 2.0×10^6 to 2.6×10^7 m^{-1}.

RESULTS AND DISCUSSIONS

Test Section

Free-stream velocity fluctuations.- Hot-wire measurements on the centerline of the test-section free stream in the Langley 8-Foot Tunnel are shown in figure 5 for a range of Mach and unit Reynolds numbers. The results show an increasing turbulence level $\tilde{u}/\bar{u}$ with increases in both Mach and unit Reynolds numbers. Velocity fluctuations for $0.2 \leq M_\infty \leq 0.8$ at maximum unit Reynolds

numbers with the tunnel wall slots open increase above the turbulence levels with slots closed at the higher Mach numbers. Measured spectra indicated that these higher levels with slots open, generated primarily by shear between the moving air in the test section and the air in the surrounding plenum chamber, are broadband with no obvious edge tones. Based on a plane-wave assumption (fixed source), velocity fluctuations were calculated from measured pressure fluctuations, using the relationship $\tilde{u}/\bar{u} = \tilde{p}/\gamma\bar{p}M$, for results obtained in the Langley 8-Foot Tunnel with slots open. Figure 5 also shows that these results agree with the measured velocity fluctuations from hot-wire data at the high Mach numbers, but disagree at $M_\infty = 0.2$. This discrepancy between measured velocity fluctuations and those inferred from the fluctuating pressure measurements (fig. 5) is probably due to the fact that the directly measured hot-wire mass-flow fluctuation levels at $M_\infty \approx 0.2$ were considerably higher than the corresponding pressure fluctuations. Progressive agreement between the mass-flow and pressure-fluctuation levels occurred with increasing Mach number and was probably caused by the dominance of sound being measured in either case. Therefore, the effect of $\tilde{p}/\bar{p}$ on $\tilde{u}/\bar{u}$ was very small at $M_\infty \approx 0.2$. Since both the hot-wire and acoustic probes respond to vorticity and pressure fluctuations, it remains difficult to completely separate these characteristic flow disturbances, especially at transonic speeds. Although the hot-wire and acoustic probes respond primarily to vorticity and sound, it is believed that sound is dominant in these facilities at high speeds.

Free-stream velocity fluctuations obtained from hot-wire measurements made in the Ames 12-Foot and Langley 8-Foot Tunnels are compared in figure 6. At low subsonic speeds ($M_\infty \approx 0.2$) the turbulence levels in the Ames tunnel are low, less than 0.1 percent at the highest unit Reynolds number tested, and decrease to 0.04 percent at the lowest Reynolds number. At Mach 0.6, the turbulence levels in the Ames tunnel are still low (≈0.1 percent). For $0.2 \leq M_\infty \leq 0.8$, the turbulence level in the Langley 8-Foot Tunnel is always a factor of 2 to 2.5 times greater than in the Ames 12-Foot Tunnel over the Reynolds number range. The difference in turbulence level between the two tunnels (fig. 6) is, however, less than expected since there are no turbulence suppression screens currently in the Langley 8-Foot Tunnel.

There are many sources of disturbances in conventional, closed-circuit, fan-driven wind tunnels (ref. 10). Aside from mechanical sources, flow disturbances are generated. Their level can be expected to increase with tunnel power and may dominate in different regions of the circuit. In fan-driven wind tunnels, it can be expected that pressure waves are created by the passage of rotor blades past stator blades, which produces velocity fluctuations. The noise produced by the several blades of the compressor stages can include a number of narrow-band frequencies. With increased power, this noise source can radiate upstream and downstream from the fan and influence test-section fluctuation levels. In an effort to gain insight and identify potential disturbance sources, velocity fluctuations obtained from the hot wire and calculated from the pressure fluctuations in the test sections of the Langley 8-Foot and Ames 12-Foot Tunnels were compared with tunnel power variations. Figure 7 shows a comparison of the variation of $\tilde{u}/\bar{u}$ with measured tunnel drive power divided by the cross-sectional area of the test section. In general, the velocity fluctuations obtained from the hot wire (fig. 7(a)) tend to collapse along a constant value of $\tilde{u}/\bar{u} \approx 0.1$ percent with increasing power for $M_\infty \leq 0.6$ and

increase above this level with increasing power for $M_\infty \geq 0.6$. A similar trend to that shown in figure 7(a) is observed in figure 7(b) for the velocity fluctuations calculated from $\tilde{p}/\bar{p}$. The results shown in figure 7 demonstrate that significant increases in the test-section fluctuation levels can be correlated with tunnel drive power, whether they are generated directly or indirectly by sound sources from the compressor.

Free-stream pressure fluctuations.- The static pressure fluctuations measured in the test sections of the Langley and Ames tunnels are shown and compared in figure 8 for the range of Mach and unit Reynolds numbers previously shown for the velocity fluctuations in figure 6. At $M_\infty \approx 0.2$, the fluctuating pressures in both tunnels are considered to be low ($\tilde{p}/\bar{p} \approx 0.01$ percent). At $M_\infty \approx 0.2$, the Langley tunnel results are slightly lower than the Ames tunnel results; however, both facilities apparently have low levels of sound propagation upstream at these speeds from the diffuser or around the circuit. At $M_\infty = 0.2$, a comparison of $\tilde{p}/\bar{p}$ levels with $\tilde{u}/\bar{u}$ levels from figure 6 supports the dominance of vorticity rather than pressure fluctuations in the test section of the Langley tunnel. However, a similar comparison in the Ames 12-Foot Tunnel indicates less vorticity at $M_\infty = 0.26$. At $0.6 \leq M_\infty \leq 0.8$ and low Reynolds numbers, the levels of $\tilde{p}/\bar{p}$ in the Ames 12-Foot Tunnel are lower than those in the Langley 8-Foot Tunnel. However, increasing power in the Ames tunnel to obtain maximum Reynolds number at $M_\infty \geq 0.6$ caused a significant increase in fluctuating pressure level. For $M_\infty = 0.62$, a representative comparison of the fluctuating pressure level in the test-section free stream was made in the Ames tunnel at the maximum test Reynolds number with strut slots open and closed (fig. 3(b)). These results are shown in figure 8 and demonstrate that significant disturbances are also produced by the slots in the strut and can be reduced by suitable covers. Pressure fluctuations in the Ames tunnel test section with strut slots open can apparently approach or exceed the measured levels in the Langley tunnel at high Mach and Reynolds numbers, as indicated by the limited comparison shown in figure 8. Therefore, exposed slots in wind-tunnel struts can be considered a serious source of flow disturbance and should be avoided.

Assuming that the pressure fluctuations (fig. 8) measured in both wind tunnels are plane waves and unidirectional, the velocity fluctuation levels can be calculated ($\tilde{u}/\bar{u} = \tilde{p}/\gamma M\bar{p}$) for a range of tunnel total pressures in the Ames 12-Foot and Langley 8-Foot Tunnels. Variations of the calculated free-stream velocity fluctuations with unit Reynolds number are compared in figure 9 for the Ames and Langley tunnels. It should be noted that variations with Mach number are not evident in figure 9 because of the different operating characteristics of each tunnel (fig. 4); i.e., M_∞ remained constant with varying total pressure in the Langley tunnel and varied with constant pressure in the Ames tunnel. Figure 9 shows that the results from the Ames tunnel agree quite well with previous data (ref. 16) and with unpublished data obtained by Werner Pfenninger, currently with George Washington University.

Low-frequency disturbances (pressure fluctuations) can be generated at specific frequencies that are associated with the characteristics of a given tunnel drive system. These low-frequency disturbances may be related essentially to fluctuations in total pressure that influence the fluctuation of the mean free-stream properties. For example, oscillations in total pressure could

generate a wave moving through the test section with subsequent fluctuations in static and dynamic pressure. Free-stream velocity and density fluctuations may be expressed by the simple wave equations as

$$\frac{\tilde{u}}{\bar{u}} = \frac{\tilde{p}}{\gamma M \bar{p}} \quad \text{and} \quad \frac{\tilde{\rho}}{\bar{\rho}} = \frac{\tilde{u}}{a} = \frac{\tilde{u}}{\bar{u}} M$$

Hence, fluctuations in dynamic pressure are as follows:

$$\frac{\tilde{q}_l}{\bar{q}_l} = \frac{\tilde{\rho}}{\bar{\rho}} + 2\frac{\tilde{u}}{\bar{u}} = (2 + M)\frac{\tilde{u}}{\bar{u}} = \frac{(2 + M)}{\gamma M}\left(\frac{\tilde{p}}{\bar{p}}\right)$$

For $0.2 \leq M_\infty \leq 0.8$, values of $\tilde{u}/\bar{u}$ range from about 0.04 to 0.2 percent in the Ames 12-Foot Tunnel and from about 0.1 to 0.4 percent in the Langley 8-Foot Tunnel (figs. 6, 7, and 9). These values correspond to calculated values of $\tilde{q}_l/\bar{q}_l$ from 0.091 to 0.564 percent and 0.22 to 1.12 percent and values of $\tilde{\rho}/\bar{\rho}$ from 0.0104 to 0.164 and 0.02 and 0.32, respectively. Furthermore, variations of the Mach number due to total pressure fluctuations may be evaluated by using the following equation:

$$\frac{\tilde{M}}{\bar{M}} = \frac{\tilde{u}}{\bar{u}} - \frac{\tilde{a}}{\bar{a}}$$

Since $a = \sqrt{\gamma p/\rho}$, it can be shown that

$$\frac{\tilde{a}}{\bar{a}} = \frac{1}{2}\left(\frac{\tilde{p}}{\bar{p}} - \frac{\tilde{\rho}}{\bar{\rho}}\right) = \frac{1}{2}\left(\frac{\tilde{p}}{\bar{p}} - \frac{1}{\gamma}\frac{\tilde{p}}{\bar{p}}\right)$$

Hence,

$$\frac{\tilde{M}}{\bar{M}} = \left(\frac{1}{\gamma M} - 0.143\right)\frac{\tilde{p}}{\bar{p}} = (1 - 0.143\gamma M)\frac{\tilde{u}}{\bar{u}}$$

Therefore, for $0.2 \leq M_\infty \leq 0.9$, values of $\tilde{p}/\bar{p}$ vary from about 0.006 to 0.6 percent in the Langley 8-Foot Tunnel and from about 0.008 to 0.2 percent

in the Ames 12-Foot Tunnel (fig. 8). These values correspond to variations in Mach number of about 0.02 to 0.39 and 0.02 to 0.15, respectively.

A comparison of the present measured free-stream pressure fluctuations in the Langley 8-Foot and Ames 12-Foot Tunnels with results obtained from a large number of wind tunnels (ref. 6) is shown in figure 10 for a wide range of Mach numbers ($0.2 \leq M_\infty \leq 50$). The results from reference 6 represent solid-, perforated-, and slotted-wall transonic tunnels and solid-wall supersonic and hypersonic tunnels. Data scatter for the reference results is primarily due to unit Reynolds number effects other than characteristic facility disturbances. The present data agree in trend with the reference results and are considerably lower than other transonic tunnels, especially at low speeds. This comparison suggests that the flow quality in both the Langley 8-Foot and Ames 12-Foot Tunnels is very good relative to most other similar facilities. However, based on the results of figures 1 and 10, the Langley and Ames tunnels currently have disturbance levels in the test section that are considered so high as to make it difficult to conduct meaningful low-drag airfoil research and basic transition research at high subsonic Mach numbers without suitable modification.

Spectra.- As mentioned previously, not only do fluctuation amplitudes affect model performance and transition studies in wind tunnels, but spectral characteristics are also important. Attempts were made to gain a better understanding of the disturbance environment and sources in the Langley 8-Foot and Ames 12-Foot Tunnels. This was done by recording stationary spectra at several locations in the circuit. (See figs. 2 and 3.)

Representative variations of the free-stream spectra from hot-wire measurements at $M_\infty = 0.8$ in the Langley 8-Foot Tunnel are shown in figure 11 for several unit Reynolds numbers. Although there is an increased high-frequency (small-scale) contribution with increasing Reynolds number, the energy contribution is an order of magnitude (10 dB) lower than the peak value, even at low frequencies, and there are no significant peaks for frequencies up to 7 kHz. The rapid decay in energy with frequency is typical of most subsonic wind tunnels. Integrated fluctuation values are included in figure 11 to illustrate the increased levels with increases in Reynolds number. Hot-wire autocorrelations obtained in the free stream of the Langley 8-Foot Tunnel test section for $0.2 \leq M_\infty \leq 0.8$ are shown in figure 12 and indicate an increase in the time scale of turbulence for small time intervals as Mach number is increased. This is supported by a more rapid decay of the correlation near the origin with time delay. The results presented in figure 12 imply that the bandwidths of the spectra decrease at lower Mach numbers.

Representative variations of the free-stream spectra from the measured pressure fluctuations at $M_\infty = 0.8$ in the Langley 8-Foot Tunnel are shown in figure 13 for a range of unit Reynolds numbers. Again, integrated fluctuation values are shown to illustrate the increased levels with increase in Reynolds number. These pressure spectra (fig. 13) once again show, apart from the identifiable probe cavity resonance at $f \approx 1.4$ kHz, similar rapid decay and spectra trends with frequency as shown in figure 11 for the hot-wire results. As shown in figures 11 and 13, most of the energy in the spectra occurs at low frequency ($f < 1$ kHz), which indicates probable mechanical or acoustical type source generation in the circuit rather than typical high-frequency low-energy

sources from the turbulent boundary layer. Furthermore, calculated fundamental fan-blade frequencies are shown in figure 13 for comparison with possible corresponding peaks in the spectra. As seen in the figure, no significant peaks are present in the measured spectra corresponding to the calculated fundamental blade passing frequencies or their multiples.

Representative variations of the spectra obtained in the free stream of the Ames 12-Foot Tunnel test section with the hot wire and pressure probes are shown in figures 14 and 15 for $0.26 \leq M_\infty \leq 0.82$. Also shown are calculated fundamental fan-blade frequencies and integrated fluctuation levels. The hot-wire broadband spectra (fig. 14) indicate a significant increase in relative energy at higher frequencies as the Mach number increases. There are several discrete frequencies present in the spectra shown in figure 14. These are probably the result of the greatly reduced signal at the lower turbulence levels in the Ames 12-Foot Tunnel. Below $f = 2.5$ kHz, spectra obtained with the pressure probe in the Ames 12-Foot Tunnel (fig. 15) for $M_\infty \geq 0.62$ show several discrete frequencies other than the smaller peaks, which are possibly the result of probe resonance and calculated fan-blade frequencies between 0.2 and 0.317 kHz. These discrete frequencies are probably due to acoustic disturbances from the strut and diffuser propagating upstream into the test section and are discussed subsequently. The large discrete peak in the pressure spectra at $M_\infty = 0.62$ (fig. 15) has not been identified and, along with the other discrete frequencies below $f = 2.5$ kHz, does not appear at corresponding frequencies in the hot-wire spectra of figure 14. The spectra shown in figures 14 and 15 for the Ames 12-Foot Tunnel indicate that there is less relative energy at the higher frequencies in the Langley tunnel than in the Ames tunnel. Again, this is probably due to the strut-diffuser flow interactions for the Ames facility.

Simple area ratio analysis and tunnel-wall boundary-layer calculations in the test section of the Ames 12-Foot Tunnel indicate that the flow may be choked at the strut, prohibiting noise generation downstream from propagating upstream. Figure 15 shows that the discrete frequency for $f \approx 2.5$ kHz at $M_\infty = 0.62$ in the test section was not evident at $M_\infty = 0.82$, possibly because of the choking effect. However, discrete frequencies of the spectra (fig. 15) for $M_\infty = 0.82$ were found to be different upstream for the pressure spectra with significant peaks at $f \approx 0.5$ kHz and 1 kHz. Subsequent results presented herein obtained on the strut and diffuser entrance tend to support these observed spectra changes.

Simple stability analysis indicates that the observed high-frequency peaks shown in figure 15 are within the critical Tollmien-Schlichting type wave range for instability of the laminar boundary layer and should be eliminated for basic transition and low-drag suction airfoils tested in the Ames tunnel or any facility having similar disturbance characteristics. The frequency sensitivity of a laminar boundary layer to known external acoustical disturbances has recently been evaluated (ref. 17); however, further experimental data are required to establish fundamental relationships involved in the energy transfer between applied acoustic fields and the vorticity mode associated with boundary-layer stability and receptivity. Furthermore, identification of characteristic energy spectra between wind tunnel and flight are required for proper stability analysis simulation.

Tunnel-wall pressure fluctuations.- Pressure fluctuations beneath the turbulent boundary layer on the tunnel wall were measured only in the Langley 8-Foot TPT. The data were obtained from two gages flush mounted on one of the vertical sidewalls (fig. 2(c)). The gages were located at stations ahead of the slot origin in the tunnel and had a spatial separation of 1.42 m. Cross-correlations of the outputs of the two gages are shown in figure 16 for $0.70 \leq M_\infty \leq 0.95$. The downstream gage (fig. 2(c)) was delayed with respect to the other gage as indicated in the figure. Figure 16 shows that cross-correlation peaks occur for $\tau \leq 50$ msec and decrease in level with increasing M_∞ until the peak diminishes to nearly zero for $M_\infty = 0.95$. These results indicate that upstream propagation of sound waves exists in the test section at lower Mach numbers, and that when the flow was choked by increasing tunnel power to $M_\infty = 0.95$, there is a negligible correlation peak at the wall.

Support Strut-Surface Flow Fluctuations

Thin-film gages were mounted flush on the surface of the model support struts in the Langley 8-Foot and Ames 12-Foot Tunnels (figs. 2(c) and 3(b), respectively) to measure relative values of the local flow fluctuations and spectra. A comparison of the strut flow fluctuations in the two tunnels is shown in figure 17 for a range of tunnel dynamic pressures and for two representative Mach numbers. Although there is good agreement between the strut data for the two tunnels at $M_\infty \approx 0.2$, higher irregular rms fluctuating values occur and are probably due to unsteadiness or intermittent separation over the strut in the Ames tunnel at $M_\infty = 0.8$. This observation is further supported by the spectra obtained in the Ames tunnel for $0.26 \leq M_\infty \leq 0.82$ and shown in figure 18. Significant peaks occur (fig. 18) over the frequency range with increasing M_∞ on the Ames tunnel strut and suggest the existence of flow unsteadiness with possible separation as Mach number increases. Representative strut spectra are compared for both tunnels in figure 19 where the energy levels are represented in terms of decibels (dB) lower than the peak value. The results are for the most rearward chordwise measurement station x/c on each strut. Figure 19 indicates that, while a significant energy level exists at $M_\infty = 0.80$, with relatively small scale fluctuations on the Langley tunnel strut, there exist lower frequency ($f < 3$ kHz) and larger scale fluctuations on the Ames tunnel strut at $M_\infty = 0.80$. If the flow over either strut is turbulent and unseparated, it would be expected that significant energy at high frequencies typical of such flows would exist as seen in figure 19 for the Langley tunnel strut.

Additional measurements were made on the Ames 12-Foot Tunnel strut simultaneously with the previously discussed thin-film measurements. Surface static-pressure strip-tubes were located on either side of the strut (fig. 3(b)) to evaluate the local pressure distribution and possible flow separation. Variations of the chordwise surface pressure coefficient C_p on the Ames tunnel support strut for several Mach numbers are shown in figure 20. The free-air predictions were calculated by Dennis Allison and Perry Newman of Langley Research Center, using the method of reference 18. These predictions include boundary-layer effects. The predictions are not expected to completely agree in level, only in trend. This is because the input conditions were not matched exactly to experiment for the calculations which were conducted prior to testing

and because the tunnel static-pressure gradient was not represented in the calculations. However, it is believed that the present data-theory comparison is sufficient to illustrate the possible existence of strut flow separation. In general, the predictions agree in trend and level in the strut forebody region (fig. 20) for $x/c \leq 0.3$ and $0.25 \leq M_\infty \leq 0.83$. Aside from differences between data and theory test conditions, the agreement in trend and disagreement in level for $x/c \geq 0.3$ over the same Mach number range is probably due, as indicated by the pressure distributions, to the inadequate theoretical simulation of the strut aft boundary layer and the positive static-pressure gradient in the expanding area in the diffuser. For $M_\infty = 0.83$ (fig. 20(d)), the pressures indicate that sonic flow exists in the forebody region.

Depending upon the extent of sonic flow on the strut, interference with the tunnel wall could possibly occur in the Ames 12-Foot Tunnel at $M_\infty \geq 0.8$. It should also be noted that, for a given value of x/c, some disagreement exists (fig. 20) for the measured pressure distributions on the north (right) and south (left) sides of the strut, which indicates variable-flow asymmetry. Analysis of video film records clearly demonstrated that tufts, grid-mounted on the north side of the strut surface above the centerbody, revealed very irregular and unsteady flow phenomena over the rearward portion of the strut ($x/c > 0.5$) above $M_\infty = 0.6$ and separation for $x/c \geq 0.95$ at $0.3 \leq M_\infty \leq 0.83$.

A summary of the chordwise location of flow separation $(x/c)_{sep}$ on the Ames tunnel strut is shown in figure 21 for the upper and lower surfaces over the Mach number range tested. The data and theoretical results shown correspond to variations in unit Reynolds numbers indicated in figure 20. The predictions represent a range of input flow incident angles relative to the strut leading edge from 0° to 3° and were obtained by using reference 18. The data points were obtained from the measured distributions of C_p versus x/c shown in figure 20 and have no direct reference to incident flow angularity. The locations for separation from the data were chosen with knowledge of the previously discussed video tuft study and knowledge of where the trend of the measured pressure distributions first deviated from that which was expected without separation. In general, the agreement between data and theory (fig. 21) is within about 2 percent over the speed range. Apparently, the flow around the strut is alternating about the left and right surfaces at high Mach numbers. Aside from flow separation for $x/c \geq 0.95$, unsteady flow at the higher transonic speeds could also interact with the diffuser flow and cause large, low-frequency disturbances that could propagate forward.

Apparent slight rounding of the existing Ames 12-Foot Tunnel strut trailing edge causes some separated flow to occur. However, current location of the strut blockage relative to the test-section physical minimum (fig. 3(b)), as indicated previously by a boundary-layer analysis, causes flow unsteadiness at the higher speeds and power tests. It is recommended that future tests be conducted in the Ames 12-Foot PWT to evaluate possible elimination of strut separation by extending the length and changing the trailing-edge shape.

Diffuser

Free-stream pressure fluctuations.- Pressure fluctuations were measured in the Ames 12-Foot Tunnel diffuser at a location about 1.9 entrance diameters downstream of the strut (fig. 3(b)) and about 3.6 diameters from the test-section measurement station. In the Langley 8-Foot Tunnel, pressure fluctuations were measured at the diffuser exit at a distance of about 5 entrance diameters from the strut or about 6.7 diameters from the test-section measurement station. A comparison of the pressure fluctuations in the Ames tunnel diffuser with those measured in the test-section free stream are shown in figure 22 for a range of Mach numbers and constant unit Reynolds number. Both the diffuser and test-section data increase with increasing Mach number until the test-section results decrease for $M_\infty \geqq 0.75$. For $M_\infty \leqq 0.5$, the diffuser fluctuations in the Langley tunnel are considerably higher than those measured in the test section of the Ames tunnel. Even though the pressure fluctuation level in the diffuser entrance continues to increase, the decreasing test-section level for $M_\infty \geqq 0.75$ is apparently due to choking of the flow and blockage of disturbance sources moving upstream.

A comparison of the pressure fluctuations in the Langley 8-Foot Tunnel diffuser exit with those in the test section, with wall slots open and closed, is shown in figure 23 for a range of Mach numbers and constant unit Reynolds number. The diffuser results are similar to those previously discussed and shown in figure 22 for the Ames 12-Foot Tunnel; results for the test section, with slots open, decrease and then increase again for $0.85 \leqq M_\infty \leqq 1.2$. The test section results with slots closed indicate a similar change in trend over the Mach number range from 0.2 to 0.95. Also shown (fig. 23) for comparison are results measured in the settling chamber which are an order of magnitude lower than those in the test section and diffuser.

The effect of closing the wall slots on reducing the disturbance level is seen (fig. 23) by comparing the pressure fluctuations when wall slots are open with the fluctuations when the wall slots are closed. Even though the test-section results (slots open or closed) increase in trend similar to that measured in the diffuser exit, they do not approach or exceed the level measured at the exit (fig. 23). However, at low subsonic speeds the test-section level with slots open is nearly equal to the diffuser-exit level. For $M_\infty \geqq 1.0$, the further increase noted in the test-section levels suggests that the contributions from the turbulent boundary layer on the test-section sidewalls are important. It is clear from the measurements made at the entrance region and exit of the diffusers in the Ames tunnel and Langley tunnel, respectively, that diffuser disturbances are higher than in the test section and provide a source that can influence upstream levels for $M_\infty < 1.0$.

Spectra.- A representative spectrum obtained in the Langley 8-Foot Tunnel diffuser exit is shown in figure 24 for $M_\infty = 0.8$. The variation in energy level with frequency shown in figure 24 is again represented by dB lower than the peak value and was again obtained from the pressure fluctuations. Similar to previously discussed test-section spectra (fig. 13) in the Langley tunnel, these results show a decrease of several orders of magnitude and no significant peaks over the indicated frequency range. Most of the energy was located at

low frequency. This result may be expected because of the slowing down of the flow after having entered the diffuser at the test free-stream speeds.

Representative spectra are also shown in figure 25 for the results measured at the Ames 12-Foot Tunnel diffuser entrance region. Variations in level with frequency are shown for several Mach numbers, and large peaks occur at several discrete frequencies. In particular, the peaks increase significantly with M_∞, for example, at $f \approx 3$ kHz and 4 kHz. The sources of these discrete peaks are not known, but the following possibilities may be eliminated: the indicated (fig. 25) low fundamental fan-blade frequencies ($f \leq 300$ Hz); support-strut slots, which were closed; and support-strut vortex shedding, which should vary in frequency with speed and may be undetected because of the proximity of the probe (fig. 3(b)). One possible source of the discrete peaks may be the interaction of strut-separated flow with the diffuser probe. Whatever the sources may be, they are apparently fixed in frequency (or multiples), which increases in amplitude with tunnel speed.

The most intense sound waves at the higher Mach numbers are those moving upstream. This has been confirmed by cross-correlation measurements in both tunnels. For example, the distance between probes (fig. 3(b)) in the Ames 12-Foot Tunnel was sufficient to make the correlations of vorticity negligibly small. Thus, correlations of the acoustic modes can be measured directly. At Mach numbers below 0.8, and with the output of the probe in the diffuser (fig. 25) delayed, it was determined that there were coherent acoustic disturbances which propagated upstream into the test section from the diffuser. (See fig. 15.) The propagation speed, determined from the spatial separation and time delay for optimum correlation, was approximately equal to the speed of sound minus the free-stream velocity. When sonic flow existed over the area of the test section, all correlation disappeared since weak pressure waves moving upstream cannot propagate forward in sonic or supersonic flow. Thus, under these conditions, response of the free-stream transducer is only to pressure waves moving downstream and to noise radiated from the turbulent boundary layers on the tunnel walls ahead of the probe. The observed disappearance of correlation of $M_\infty \approx 0.83$ in the Ames tunnel indicates that the tunnel was fully choked. This result is in contrast with earlier free-stream acoustic measurements in the Ames tunnel with the old strut (ref. 3), which indicated apparent choking at $M_\infty \approx 0.9$ and a corresponding order-of-magnitude reduction in sound pressure level (SPL). The difference in M_∞ where choking occurs for the Ames tunnel is mainly due to the increase in blockage of the new strut over the old strut by a factor of about 1.5.

Total pressure losses.- A comparison of the high-speed diffuser losses over the Mach number range is shown in figure 26 with the old and new model support struts installed in the Ames tunnel and the existing circular-arc strut in the Langley tunnel. An average of the mean-flow measurements obtained from an array of probes (figs. 2(d) and 3(c)) in each tunnel at constant Mach number was ratioed to the test-section values to indicate the total pressure losses at the diffuser exits. It should be noted that measurements in the Ames tunnel were for an ℓ/d station in the diffuser of about twice that in the Langley tunnel. Results from the Langley tunnel are also shown with the test-section slots open and closed in figure 26. The data for both facilities indicate that diffuser pressure recovery decreases with Mach number. The new strut in the Ames tunnel

and the configuration in the Langley tunnel with wall slots open cause greater losses above $M_\infty \approx 0.4$ compared with the old-strut and slot-closed results, respectively. For example, at $M_\infty \approx 0.8$, the losses are about 2 percent higher with the new strut and are probably due to a combination of strut flow separation and diffuser boundary-layer interaction. Similar results occur for the Langley tunnel for slots open or closed and are possibly attributable to flow interaction from control flaps located near the strut at the diffuser entrance (fig. 2(c)). These flaps are normally used with wall slots open. Since tunnel power is proportional to the diffuser losses, present results show that a more rapid increase in both power requirement and generated disturbance level (fig. 7) can be expected at the transonic speed range. This result is supported in figures 22 and 23 by the test-section and diffuser disturbance levels.

Test-Section Choke Configuration

General.- As discussed previously, choking of the flow usually occurs in transonic wind tunnels when the Mach number approaches 1.0. The location where choking occurs while increasing power depends on the aerodynamic flow minimum in a given facility. For example, choking under such conditions may exist far forward in the test section and cause undesired flow ahead of test models. If an effective physical device is applied so as to produce a local area change (throat or centerbody) which causes the local flow Mach number to exceed 1.0, then sound waves downstream do not propagate upstream and only sound leakage through the wall boundary layer is possible. In addition, the choke can be designed for adjustability so as to not only allow selection of location but also to produce area change effectiveness for a range of Mach number testing capability. These desired choke characteristics can best be achieved by application at the wall rather than at a centerbody. Therefore, wall-mounted choke plates were designed to produce a local sonic flow at $M_\infty \approx 0.8$ and were tested previously (ref. 19) in the Langley 8-Foot Tunnel test section for effectiveness in reducing the free-stream pressure fluctuations (fig. 8).

Choked results.- A representative Mach number distribution in the Langley 8-Foot Tunnel test section is shown in figure 27 with choke plates mounted on four walls (corners filled) and with the slots closed. Also included in figure 27 is a sketch of a single choke plate. All four plates were located in the tunnel between $x \approx 1.63$ m and 2.77 m downstream of the slot origin ($x = 0$). The Mach number distribution was obtained from a streamwise array of wall static-pressure measurements and from the assumption that the test-section total pressure and the local static pressure across the boundary layer were constant. Effectiveness of the four-wall choke plates is seen by the sudden increase in M_∞ at the leading-edge region to $M_\infty \approx 1.13$ in the aft region. It should be noted that the mean-flow quality ahead of the choke leading edge was not influenced to within about one-half of a chord length, as evidenced by the nearly constant Mach number distribution with tunnel station up to $x \approx 1.14$ m. This result is a significant improvement in Mach number distribution over that obtained without the choke as reported and shown in reference 19. Furthermore, pressure recovery was reached very rapidly downstream of the shock compared with the unchoked condition, which indicates no degrading of the

diffuser flow when choked. Additional tests were conducted to evaluate effectiveness with the top and bottom wall choke plates removed and are also reported in reference 19. These tests produced results similar to those obtained with the four-wall plates.

A comparison of the measured free-stream pressure fluctuations (ref. 18) ahead of the choke configurations discussed previously is shown in figure 28 for a range of Mach numbers with and without choke plates. Also shown for comparison are simultaneously measured pressure fluctuations in the settling chamber ahead of the contraction to assess the incoming disturbance level when the downstream noise is blocked as a result of choking. Both the two- and four-wall choke configurations block upstream propagation of sound waves and significantly reduce the test-section pressure fluctuations. For example, this reduction is about a factor of 7 for the four-wall choke. Similar results were also obtained without choke plates by simply increasing tunnel power; however, choking occurred far forward in the test section (ref. 18). Figure 28 shows that when choking occurs with or without choke plates, the disturbance level in the test section is reduced to about 0.05 percent over the Mach number range where choking occurred. With the downstream end of the test section choked, it seems reasonable to assume that the remaining disturbances would be those convected through the settling chamber and radiated from the turbulent boundary layer on the walls. With the aforementioned possibilities in mind, an attempt was made to estimate the noise contribution due to the turbulent boundary layer. Contributions of pressure fluctuations due to the turbulent boundary layer in the test section of the Langley tunnel were estimated by linearly extrapolating the measured choked spectra from $f \geq 1$ kHz to $f = 0$. Then the integrated energy level above the extrapolated level for $0 \leq f \leq 1$ kHz was subtracted from the total level obtained by integration over the spectra frequency range. Thus, disturbance levels as radiated from the turbulent boundary layer can be estimated from this simple approach if the assumption is made that the choked energy spectra at high frequencies are dominated by contributions from the turbulent boundary layer and at low frequencies ($f \leq 1$ kHz) by sound-producing source or support vibration. Both of these assumptions are consistent with well-known research results (refs. 20 and 21), and the method applied for the estimate was first suggested by Dr. Werner Pfenninger of George Washington University. The estimated results are shown in figure 28, with and without the choke plates, and indicate that pressure fluctuations from the Langley 8-Foot Tunnel with turbulent boundary layer are very low and decrease with decreasing Mach number. This estimated result is consistent with previous high-speed trends where the boundary-layer-generated sound dominates the disturbance level (refs. 6, 20, and 21), i.e., normalized pressure fluctuations vary proportional to M_∞^2.

Choked-tunnel power requirements.- An evaluation was made of the power requirements for the Langley 8-Foot Tunnel with and without choked flow (ref. 19). A comparison of the measured tunnel drive power variation with Mach number at 1.015×10^5 Pa is shown in figure 29 for wall slots open or closed with and without choke plates. As mentioned previously, the results with slots open correspond to the normal mode of tunnel operation and are very near those with slots closed for $0.2 \leq M_\infty \leq 0.95$. With two choke plates, the results represent minimum power required to just choke the flow; however, the four plates required additional power (≈23 rpm) above that normally required to pro-

duce adequate sonic flow at the choke (fig. 28). This latter power increase was somewhat arbitrary and no effort was made to determine the minimum increase in power that would be required to reduce the fluctuation pressure to 0.05 percent. In general, no severe increase in power is required with or without choke plates to adequately choke the Langley 8-Foot Tunnel.

It is apparent from the results of reference 19 that choking the flow blocks the upstream propagation of sound into the test section. Effectiveness of the choke device located downstream of the test section but ahead of the strut and diffuser significantly improves the flow-quality characteristics. It is expected that introduction of a similar device in most transonic wind tunnels would also improve flow quality. When a choke device is used, further flow-quality improvement can come only from alterations of a given facility ahead of the contraction (screens, honeycomb, and acoustic baffles) or removal of the turbulent boundary layer on the walls. Under choked conditions, vorticity from the settling chamber can have a dominant effect on the disturbance level in the test section. Thus, it becomes important to determine the turbulence characteristics in the settling chamber of both the Langley 8-Foot and Ames 12-Foot Tunnels so that the alterations required upstream of the nozzle to produce a significant reduction in the settling-chamber disturbance level can be determined.

Settling Chamber

Summary of turbulence levels.- Figure 30 shows a summary of the turbulence levels measured with the hot wire at several locations in the settling chamber of the Langley 8-Foot and Ames 12-Foot Tunnels for a range of dynamic pressures. The Langley tunnel results were obtained on the centerline of the tunnel upstream and downstream of the cooler, downstream of the turning vanes, and in the settling chamber ahead of the contraction (fig. 2(a)). The Ames tunnel results were obtained just ahead of the first screen and at several hundred screen-wire-mesh diameters downstream of the last screen (fig. 3(a)). All results shown are for the streamwise or longitudinal component of turbulence.

The cooler in the Langley tunnel produces very high turbulence levels of about 18 percent (fig. 30), which are approximately equal to values measured upstream of the cooler over most of the test range. Downstream of the turning vanes, the turbulence levels are decreased by a factor of about 3. Farther downstream in the settling chamber, the levels of disturbances are about 2 percent or nearly a factor of 7 below the levels measured at the cooler. Corresponding lateral and vertical components of measured turbulence in the Langley 8-Foot Tunnel settling chamber may be found in reference 19. In general, the results presented in reference 19 indicate that the lateral and vertical components of the fluctuations were approximately equal to the streamwise component ahead of the cooler. However, these fluctuating normal-flow components in the settling chamber were somewhat larger than the streamwise component over nearly the same test conditions shown in figure 30. From the present results and the results of reference 19, it is apparent that proper selection of turbulence suppression devices (honeycomb and screens) is required for modification of the Langley tunnel settling chamber in order to reduce all components of turbulence prior to contraction.

The screens in the settling chamber of the Ames 12-Foot Tunnel (fig. 30) reduced the high incoming turbulence levels by a factor of about 8 over the dynamic-pressure range shown. These results clearly demonstrate the importance of screens for turbulence suppression prior to contraction (refs. 22 to 24). However, it is not known what the corresponding levels of lateral or vertical components of turbulence are upstream and downstream of the screens. The absence of screens in the Langley 8-Foot Tunnel is partly responsible for the higher free-stream turbulence levels shown in figure 6. However, the natural decay of small-scale turbulence generated by the cooler with distance in the Langley tunnel settling chamber is apparently almost as effective in reducing the fluctuating levels of turbulence as are the screens in the Ames tunnel.

An assessment was made of the longitudinal turbulence transmissibility through the contraction of both facilities. Figure 31 shows the effect of nozzle contraction on turbulence transmitted in the Langley 8-Foot and Ames 12-Foot Tunnels at three Mach numbers compared with the incompressible theory (ref. 25). In both tunnels the ratio of measured turbulence downstream to that upstream for the respective contraction ratios is seen to increase with Mach number. A comparison of the data with theory (ref. 25) indicates that there is a significant difference in level and trend with Mach number for a given contraction ratio. Figure 31 shows that the theoretical predicted turbulence-reduction factor decreases with increasing Mach number. However, the measured values increase with Mach number in both wind tunnels tested. Surely, all nozzle contraction data are contaminated by sound at transonic speeds, which can influence the aforementioned effects.

Summary of hot-wire autocorrelations.- Figures 32 and 33 show a summary of the autocorrelations measured at several locations in the settling chamber of the Langley 8-Foot and Ames 12-Foot Tunnels. Corresponding turbulence levels measured at these same locations in the settling chambers have previously been shown (fig. 30) and discussed. As a result of the closely spaced fins on the tubes (fig. 2(b)) of the Langley tunnel cooler, integral scales of turbulence behind the cooler were determined from figure 32 to be small ($\approx$0.03 m) compared with upstream scales which are about 0.61 m. A reduction in turbulence level by a factor of about 3 occurs behind the cooler (fig. 30), with an increase in scale of turbulence to about 0.076 m as determined from figure 32. A further reduction in level and increased scale size to about 0.335 m occurs in the settling chamber. In the settling chamber, the increase in scale size is probably due to the addition of large-scale turbulence from the vanes and also to the decay of small-scale turbulence from the cooler. In general, turbulence scales in the Langley 8-Foot Tunnel increase with decreasing dynamic pressure for a given location and increase in size in the downstream direction (fig. 32). Evidently, the cooler tends to manage incoming turbulence of relatively large scale in a manner similar to that of a honeycomb and screen combination. However, the cooler generates noise as a result of the airflow through closely spaced fins and tubes, which has been supported by a low-frequency tone found to emanate from the cooler model located in the circuit of the pilot test facility of reference 26.

The integral scales of longitudinal turbulence both upstream and downstream of the eight screens (fig. 33) in the Ames tunnel also increase with decreasing dynamic pressure. Corresponding turbulence levels ahead of and behind the screens are shown in figure 30. Apparently, the screens are effective in manipulating high-intensity, relatively large-scale turbulence so as to significantly reduce both level and scale prior to contraction. However, screen effectiveness is not completely known for widely varying degrees of input turbulence level and scale. However, the present full-scale tests, in addition to recent results of references 23 and 27 do provide some insight for future design and selection of screen application.

Turbulence level and spectra downstream of turning vanes.- Turbulence measurements were made with a hot-wire rake behind two turning vanes in the Langley tunnel settling chamber (fig. 2(b)). Figure 34 shows the transverse variation of local turbulence level with distance between vanes for several representative test-section dynamic pressures. Representative spectra across the vane wakes are shown in figure 35 for $M_\infty = 0.8$. The local turbulence levels (fig. 34) between vanes on the tunnel centerline increase with increasing dynamic pressure. The intervane spacing of the hot-wire probes indicates that the overall level between vanes remains similar in trend with increasing dynamic pressure. It is not known whether the probe spacing was precisely within the vane wakes and entrainment region. However, a comparison of the $\tilde{u}/\bar{u}$ levels from figure 34 with the hot-wire probe locations and measured spectra behind the vanes (fig. 35) suggests that high-turbulence levels exist in the vane-wake region followed by lower levels between the vanes and increasing again to high levels in the vane-wake entrainment region. This spatial location of the probes and measured variation of turbulence behind the vanes (fig. 34) changes in level by about a factor of 2 and suggests the possibility and source for enhancement of the lateral and vertical components of turbulence and scale. This possibility is supported by the results found in the Langley tunnel settling chamber and reported in reference 19.

Ames tunnel screens.- Variation of the ratio of measured screen pressure drop Δp with local screen dynamic pressure $q_{l,s}$ is shown in figure 36 as a function of test-section dynamic pressure in the Ames 12-Foot Tunnel. Also shown is the screen resistance K or pressure-drop coefficient for the eight screens in series. The upstream screen (16 mesh) and seven downstream screens (12 mesh) are fabricated of 0.0508-cm and 0.0635-cm diameter wire. From these data the following parameters were calculated based on the results of references 28 to 30 for a single screen:

Screen mesh	Wire diameter, cm	Porosity	Resistance coefficient
16	0.0508	0.462	2.514
12	.0635	.490	2.124

The measured pressure drop across the eight screens (fig. 36) is considerably larger than would be expected for the sum of the losses across corresponding individual screens (refs. 28 to 30) and similar flow conditions. This may be explained partly by the fact that the pressure-drop coefficient is a function not only of screen porosity but also of the critical-wire-diameter Reynolds number. Present tests and calculated values of critical-wire-diameter Reynolds number between 60 and 225 for the Ames tunnel screens indicate that there exists a possible pressure-drop effect for critical-wire-diameter Reynolds numbers less than 200. This theory is supported by a comparison of the calculated and measured results.

Figure 37 shows the measured axial turbulence-reduction factor $\tilde{u}_2/\tilde{u}_1$ across the eight screens in the Ames 12-Foot Tunnel as a function of pressure-drop coefficient K. For comparison, the well-known prediction methods (ref. 29) for the isotropic turbulence-reduction factor are also shown. If the eight screens are represented as one screen and the corresponding value of K for a single screen is used over the Δp range, then fortuitous agreement between data and theory is obtained by using the Prandtl theory (ref. 29) of $1/(1 + K)$. However, when accountability is made of all eight screens by use of nK in the same theory, there exists a large disagreement with the data. This latter approach is similar to the summation of the K factors for the screen combination, assuming one equivalent screen with the total K factor or with nK. Furthermore, this method seems to represent the actual case for screens (ref. 26) in series. Disagreement between data and theory using $1/(1 + nK)$ is due partly to known screen contamination accumulated over years of operation and partly to a possible lack of screen porosity optimization for Δp selection during installation. The present results clearly indicate that the measured turbulence levels across the screens are affected by vorticity-generated sound, unsteady large-scale turbulence input to the screens, contamination, or incorrect porosity, all of which can degrade the performance of the Ames tunnel screens. The present simple analysis and measured results suggest that, for a given facility, aribitrarily adding screens in series may or may not provide the expected turbulence reduction across n-screens and that many factors can control effectiveness.

Although the turbulence reduction across the screens in the Ames 12-Foot Tunnel fortuitously agrees with that calculated (ref. 29) for a single screen, it falls well short of that predicted for the same total pressure drop across eight screens in series for the possible reasons previously mentioned. An important aspect of turbulence reduction is the uniformity of the mean-flow velocity ahead of the screens. If the mean velocity has nonuniformities of only a few percent, regeneration of turbulence can occur through a screen and the screen efficiency is reduced (ref. 24). Such small nonuniformities could possibly be produced in the Ames 12-Foot Tunnel by unsteady flow separations downstream of the sudden expansion ahead of the screens. These separations were evident from the hot-wire spectra data ahead of the screens, particularly at high dynamic pressures. It would be more efficient to manage existing large-scale unsteady motions ahead of the screens. This would lead to improved screen efficiency, lower settling-chamber turbulence levels, and consequently even lower values in the test section. Based on results from earlier experience with turbulence suppression devices, analysis suggests that the Ames tunnel

screens may have a solidity that is too high (refs. 22 and 30). Decreasing the solidity could also reduce the test-section turbulence.

CONCLUDING REMARKS

Tests have been conducted in the Langley 8-Foot Transonic Pressure Tunnel and the Ames 12-Foot Pressure Wind Tunnel to measure characteristic disturbance levels and spectra in their respective settling chambers, test sections, and diffusers and to determine the sources of these disturbances. The primary conclusions are as follows:

At all Mach numbers, the Ames facility has superior flow quality level, which is about a factor of 2 below the level for the Langley tunnel for the same test conditions. At high Mach numbers, disturbances from the strut or in the diffuser propagate upstream into the test section, which degrades the flow quality for both tunnels. The present Ames tunnel model support system appears to choke the tunnel at a Mach number of approximately 0.8, and flow unsteadiness or separation, which occurs on the strut at a Mach number equal to or greater than 0.6 is one of the primary causes for the rapid increase of fluctuation levels with Reynolds number at high free-stream Mach numbers.

Although the free-stream velocity and pressure-fluctuation levels in both facilities are low at subsonic speeds, the disturbance levels at transonic Mach numbers are considered so high as to make it difficult to conduct meaningful low-drag airfoil research or basic transition studies.

With the exception of a few discrete peaks in the hot-wire and pressure-fluctuation spectra at the higher Mach numbers in the Ames tunnel test section which are principally caused by upstream propagation of sound due to strut-diffuser flow interactions, no other significant energy peaks were observed in either facility. In general, rapid, smooth decays of energy with frequency, typical of most low-speed tunnels, were observed. Significant energy peaks were observed for the Ames tunnel strut and diffuser spectra that were determined to be caused not by low-frequency energy from the fan blades, but by possible flow interactions.

Pressure-fluctuation levels at the higher Mach numbers in both facilities appeared to account for most of the flow disturbances in the test section. These fluctuations are believed to be primarily the result of strut-diffuser flow interactions in the Ames tunnel and diffuser unsteadiness in the Langley facility, which are propagated upstream into the test section. Because of the open slots on the Ames tunnel strut the test-section disturbances can become more severe in the Ames facility than in the Langley facility at high Mach numbers.

RECOMMENDATIONS

Significant reduction of the disturbance levels in both facilities could be affected by introducing a sonic choke device on the sidewalls downstream of the test section but upstream of the strut and diffuser. The choke device would

prevent strut-diffuser fluctuations from propagating upstream into the test section without significant power increase. Thus, the only remaining test-section disturbances would be relatively low-level pressure fluctuations propagating from the settling chamber and turbulent wall boundary layers and vorticity fluctuations convected from the settling chamber.

The Langley tunnel cooler performs somewhat like a honeycomb-screen combination; however, further reduction of the test-section disturbance levels can be expected as a result of the installation of properly selected honeycomb and screens in the settling chamber, as the present turbulence levels ahead of the contraction are about twice those in the Ames facility. On the other hand, the eight screens in the Ames facility do not perform particularly well for the pressure drops incurred. This lack of screen efficiency is probably due to large-scale unsteady flows associated with nonuniformity of the flow at the sudden expansion, which could produce mean gradients in the flow ahead of the screens, and also to high screen solidity. Screen efficiency could be greatly improved by reducing any incoming sound and the extent of nonuniform flow and by using lower solidity screens, assuming further mean-flow unsteadiness does not occur because of the drive system. The installation of screens would be more efficient in the Langley 8-Foot Tunnel since there are no area-expansion problems downstream of the cooler. Furthermore, the addition of a honeycomb ahead of the screens would reduce both lateral and vertical components of large-scale turbulences entering the screens and would manage large-scale phenomena to some extent.

Langley Research Center
National Aeronautics and Space Administration
Hampton, VA 23665
October 21, 1980

REFERENCES

1. Schubauer, G. B.; and Skramstad, H. K.: Laminar-Boundary-Layer Oscillations and Transition on a Flat Plate. NACA Rep. 909, 1948.

2. Wells, C. Sinclair, Jr.: Effects of Freestream Turbulence on Boundary-Layer Transition. AIAA J., vol. 5, no. 1, Jan. 1967, pp. 172-174.

3. Boltz, Frederick W.; Kenyon, George C.; and Allen, Clyde Q.: The Boundary-Layer Transition Characteristics of Two Bodies of Revolution, A Flat Plate, and an Unswept Wing in a Low-Turbulence Wind Tunnel. NASA TN D-309, 1960.

4. Spangler, J. G.; and Wells, C. S., Jr.: Effects of Freestream Disturbances on Boundary-Layer Transition. AIAA J., vol. 6, no. 3, Mar. 1968, pp. 543-545.

5. Recent Developments in Boundary-Layer Transition Research AIAA J., vol. 13, no. 3, Mar. 1975, pp. 261-314.

6. Harvey, William D.: Influence of Free-Stream Disturbances on Boundary-Layer Transition. NASA TM-78635, 1978.

7. Pfenninger, Werner; and Reed, Verlin D.: Laminar-Flow Research and Experiments. Astronaut. & Aeronaut., vol. 4, no. 7, July 1966, pp. 44-50.

8. Fowell, L. R.; and Antonatos, P. P.: A. Some Results From the X-21A Program. Part 2: Laminar Flow Control Flight Test Results on the X-21A, Recent Developments in Boundary Layer Research - Part IV, AGARDograph 97, May 1965.

9. Cox, R. N.; and Freestone, M. M.: Design of Ventilated Walls With Special Emphasis on the Aspect of Noise Generation. Fluid Motion Problems in Wind Tunnel Design, AGARD-R-602, 1973, pp. 6-1 - 6-7.

10. Timme, Adalbert: Effects of Turbulence and Noise on Wind-Tunnel Measurements At Transonic Speeds. Fluid Motion Problems in Wind Tunnel Design, AGARD-R-602, 1973, pp. 5-1 - 5-12.

11. McCanless, George F., Jr.; and Boone, James R.: Noise Reduction in Transonic Wind Tunnels. J. Acoust. Soc. America, vol. 56, no. 5, Nov. 1974, pp. 1501-1510.

12. Varner, M. O.: Noise Generation in Transonic Wind Tunnels. AEDC-TR-74-126, U.S. Air Force, Apr. 1975. (Available from DTIC as AD A007 688.)

13. Rose, William C.; and McDaid, Edward P.: Turbulence Measurement in Transonic Flow. Proceedings - AIAA 9th Aerodynamic Testing Conference, June 1976, pp. 267-271.

14. Harvey, W. D.; Stainback, P. C.; Anders, J. B.; and Cary, A. M.: Nozzle Wall Boundary-Layer Transition and Freestream Disturbances at Mach 5. AIAA J., vol. 13, no. 3, Mar. 1975, pp. 307-314.

15. Dods, Jules B., Jr.; and Hanly, Richard D.: Evaluation of Transonic and Supersonic Wind-Tunnel Background Noise and Effects of Surface Pressure Fluctuation Measurements. AIAA Paper No. 72-1004, Sept. 1972.

16. Carlson, J. C.: Investigation of the Laminar Flow Control Characteristics of a 33° Swept Suction Wing at High Reynolds Numbers in the NASA Ames 12-Foot Pressure Wind Tunnel in August 1965. NOR-66-58, Northrop Corp., Jan. 1966.

17. Mangiarotty, R. A.; and Bohn, A. J.: Wind Tunnel Study on the Effects of Acoustical Disturbances on Controlled Laminar Flow. AIAA Paper 79-0629, Mar. 1979.

18. Bauer, Frances; Garabedian, Paul; Korn, David; and Jameson, Antony: Supercritical Wing Sections II. Volume 108 of Lecture Notes in Economics and Mathematical Systems, Springer-Verlag, 1975.

19. Brooks, Joseph D.; Stainback, P. Calvin; and Brooks, Cuyler W., Jr.: Additional Flow Quality Measurements in the Langley Research Center 8-Foot Transonic Pressure Tunnel. A Collection of Technical Papers - AIAA 11th Aerodynamic Testing Conference, Mar. 1980, pp. 138-145. (Available as AIAA-80-0434.)

20. Laufer, John: Aerodynamic Noise in Supersonic Wind Tunnels. J. Aerosp. Sci., vol. 28, no. 9, Sept. 1961, pp. 685-692.

21. Laufer, John: Some Statistical Properties of the Pressure Field Radiated by a Turbulent Boundary Layer. Phys. Fluids, vol. 7, no. 8, Aug. 1964, pp. 1191-1197.

22. Bradshaw, P.: The Effect of Wind Tunnel Screens on "Two-Dimensional" Boundary Layers. NPL Aero Rep. 1085, British A.R.C., Dec. 4, 1963.

23. Loehrke, R. I.; and Nagib, H. M.: Experiments on Management of Free Stream Turbulence. AGARD Rep. 598, Sept. 1972.

24. Bradshaw, P.; and Pankhurst, R. C.: The Design of Low-Speed Wind Tunnels. Progress in Aeronautical Sciences, Volume 5, D. Küchemann and L. H. G. Sterne, eds., Macmillan Co., 1964, pp. 1-69.

25. Uberoi, Mahinder S.: Effect of Wind-Tunnel Contraction on Free Stream Turbulence. J. Aeronaut. Sci., vol. 23, no. 8, Aug. 1956, pp. 754-764.

26. Scheiman, James; and Brooks, J. D.: A Comparison of Experimental and Theoretical Turbulence Reduction From Screens, Honeycomb and Honeycomb-Screen Combinations. A Collection of Technical Papers - AIAA 11th Aerodynamic Testing Conference, Mar. 1980, pp. 129-134. (Available as AIAA-80-0433.)

27. Wigeland, Roald A.; Tan-atichat, Jimmy; and Nagib, Hassan M.: Evaluation of a New Concept for Reducing Free-Stream Turbulence in Wind Tunnels. NASA CR-3196, 1979.

28. Wieghardt, K. E. G.: On the Resistance of Screens. Aeronaut. Q., vol. IV, pt. II, Feb. 1953, pp. 186-192.

29. Prandtl, L.: Attaining a Steady Air Stream in Wind Tunnels. NACA TM 726, 1933.

30. Schubauer, G. B.; Spangenberg, W. G.; and Klebanoff, P. S.: Aerodynamic Characteristics of Damping Screens. NACA TN 2001, 1950.

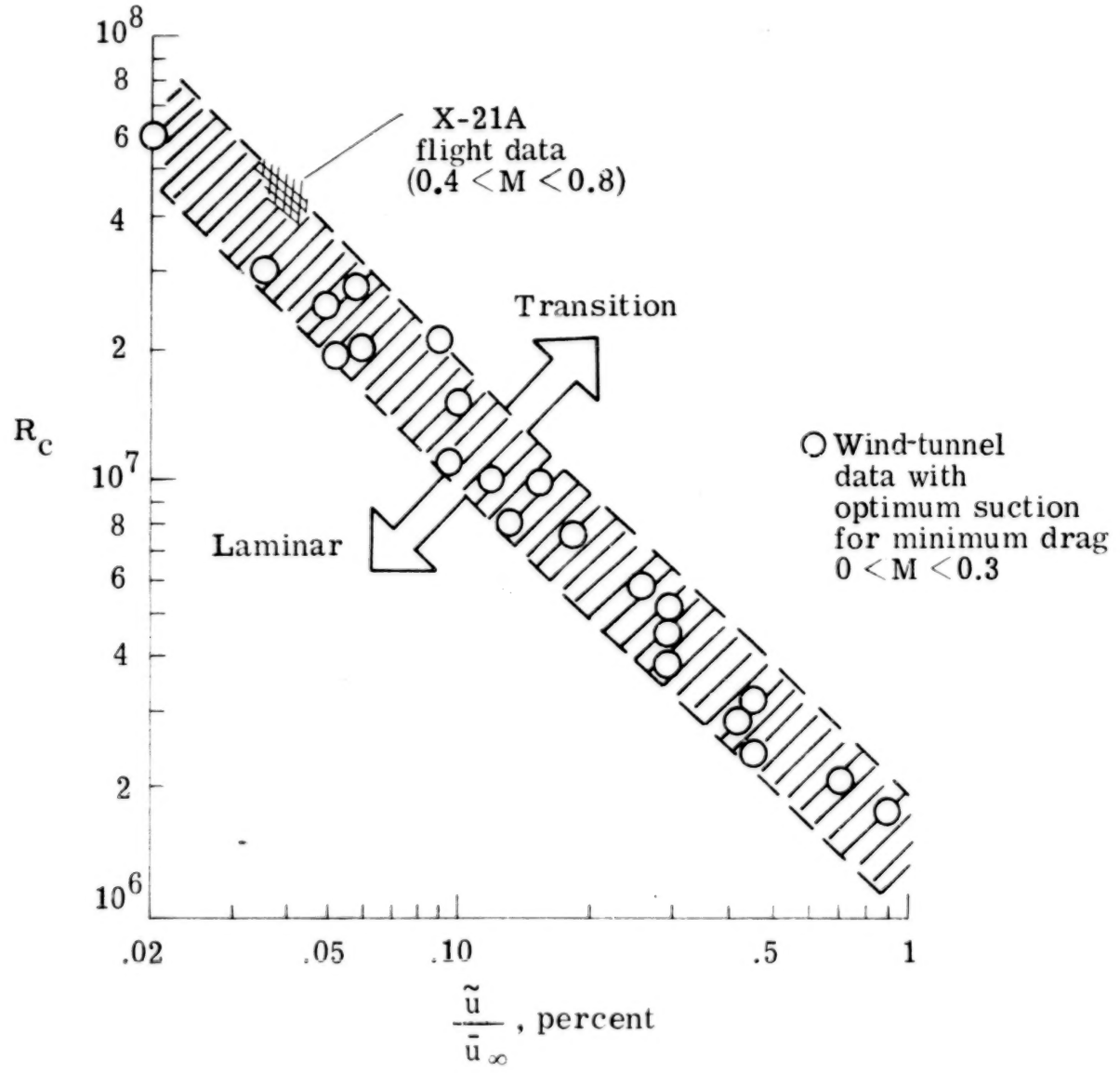

Figure 1.- Effect of turbulence level on transition Reynolds number for transition at trailing edge for wings and bodies of revolution with suction.

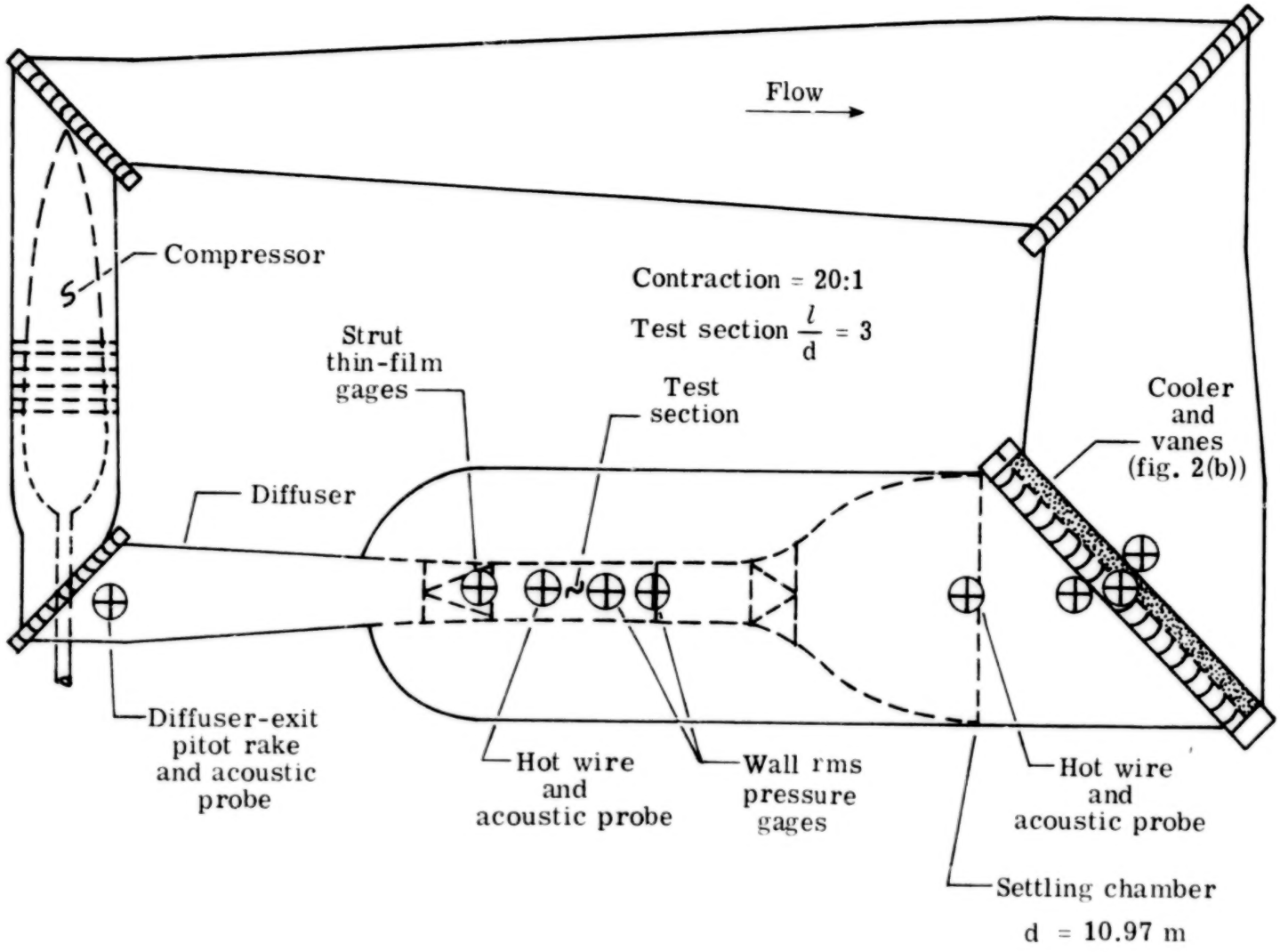

(a) Wind-tunnel circuit.

Figure 2.- Sketch of Langley 8-Foot Transonic Pressure Tunnel and measuring stations.

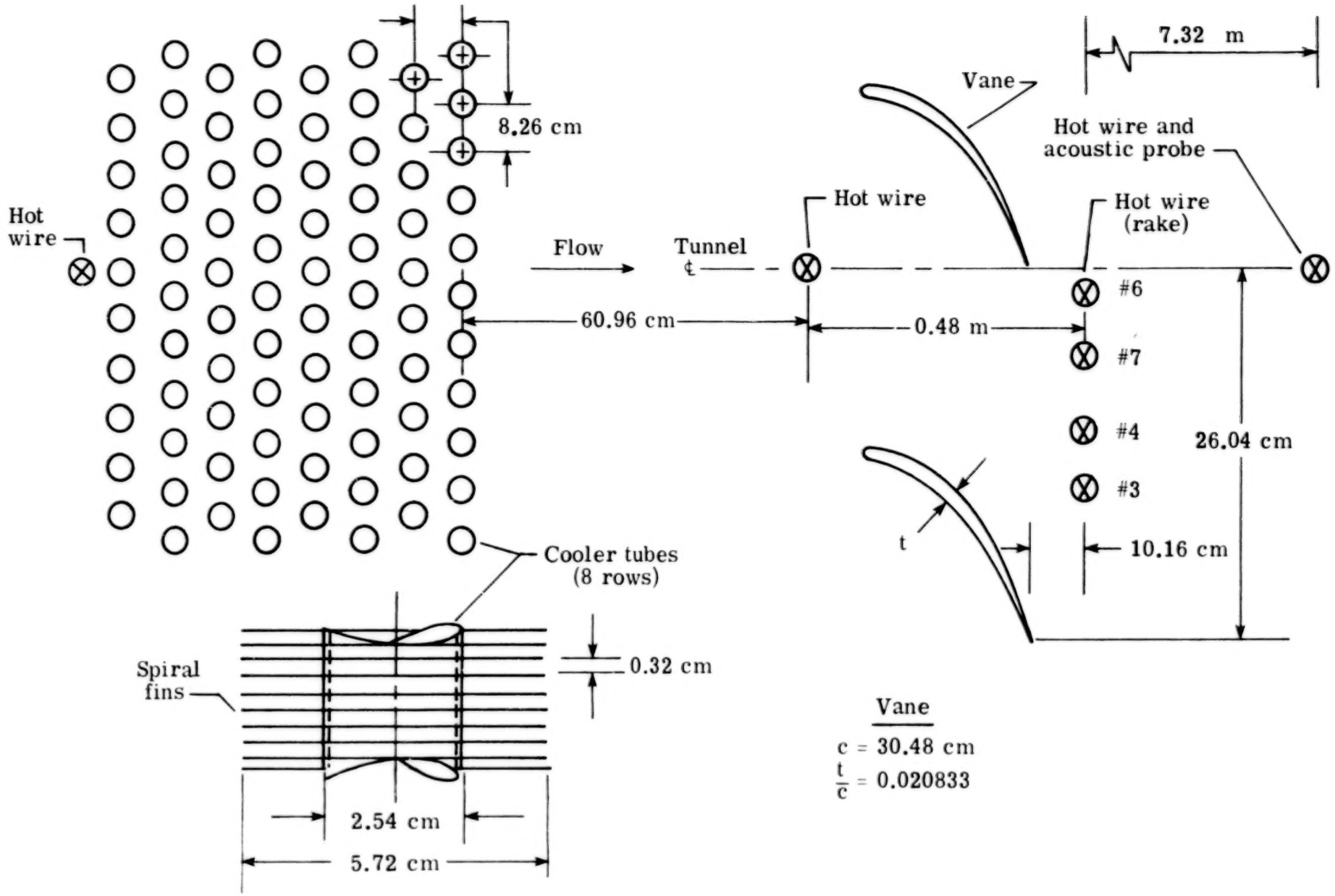

(b) Settling-chamber, cooler, and turning-vane instrumentation.

Figure 2.- Continued.

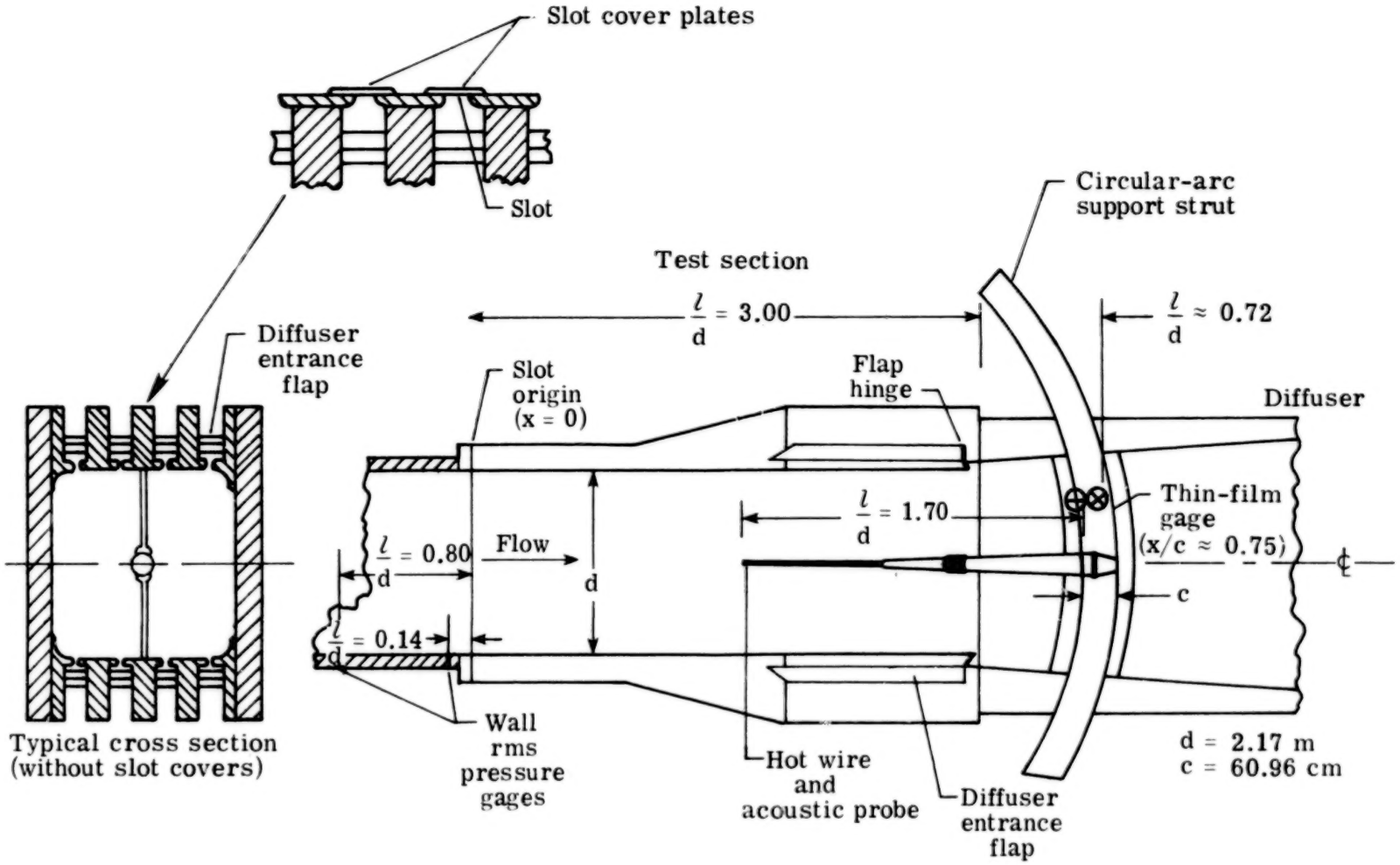

(c) Test-section and strut instrumentation.

Figure 2.- Continued.

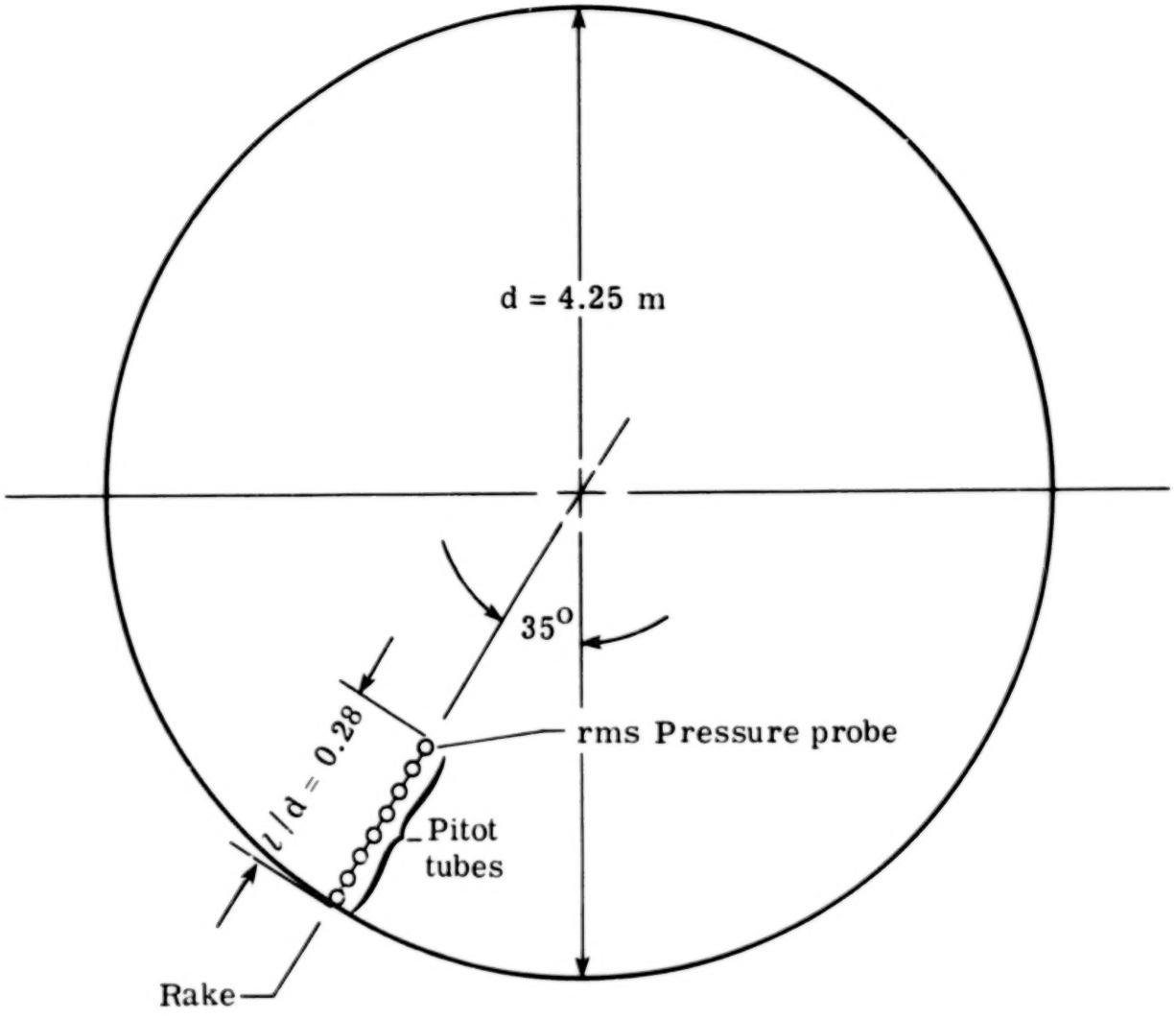

(d) Diffuser-exit instrumentation.

Figure 2.- Concluded.

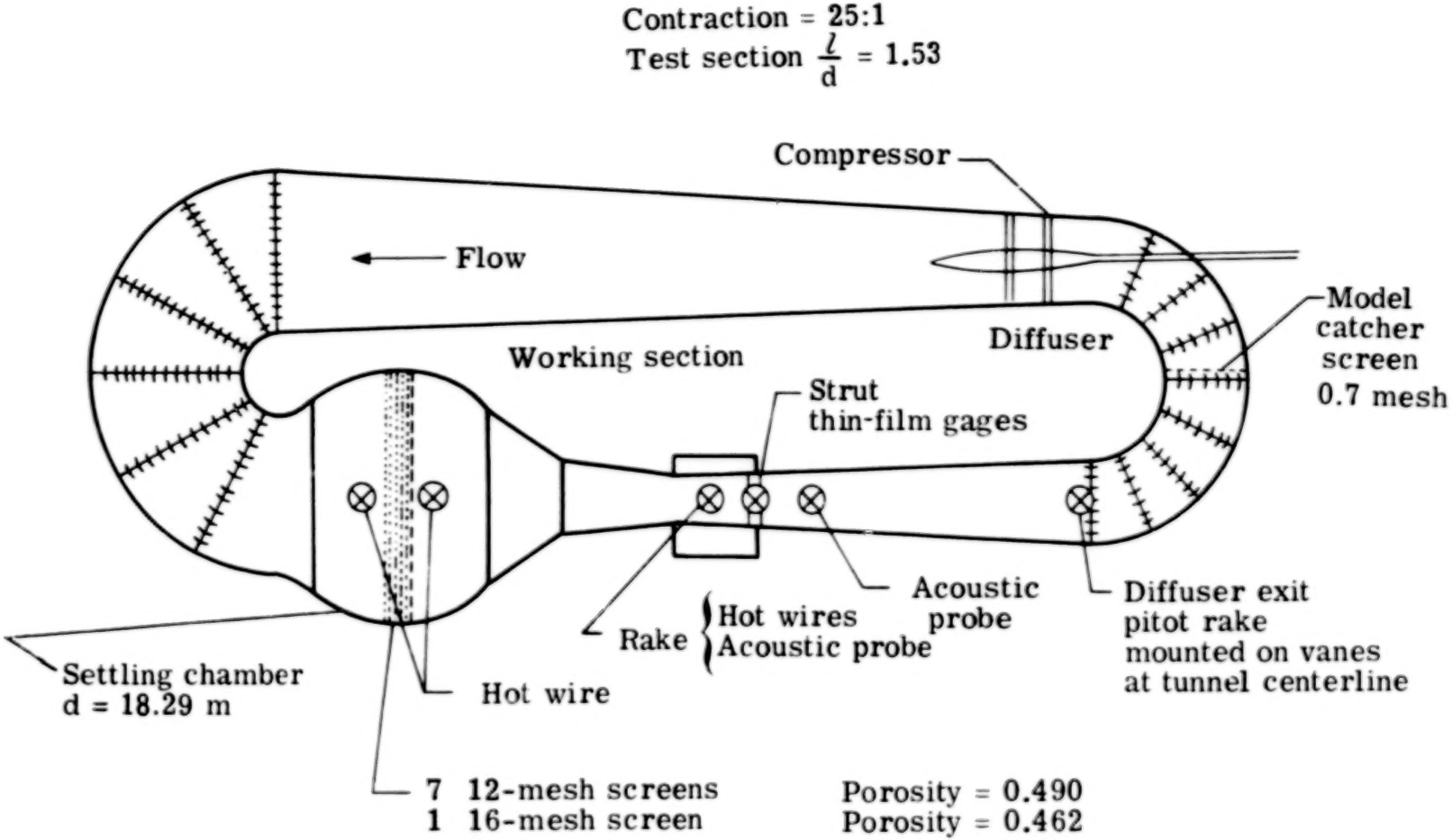

(a) Wind-tunnel circuit.

Figure 3.- Sketch of Ames 12-Foot Pressure Wind Tunnel and measuring stations.

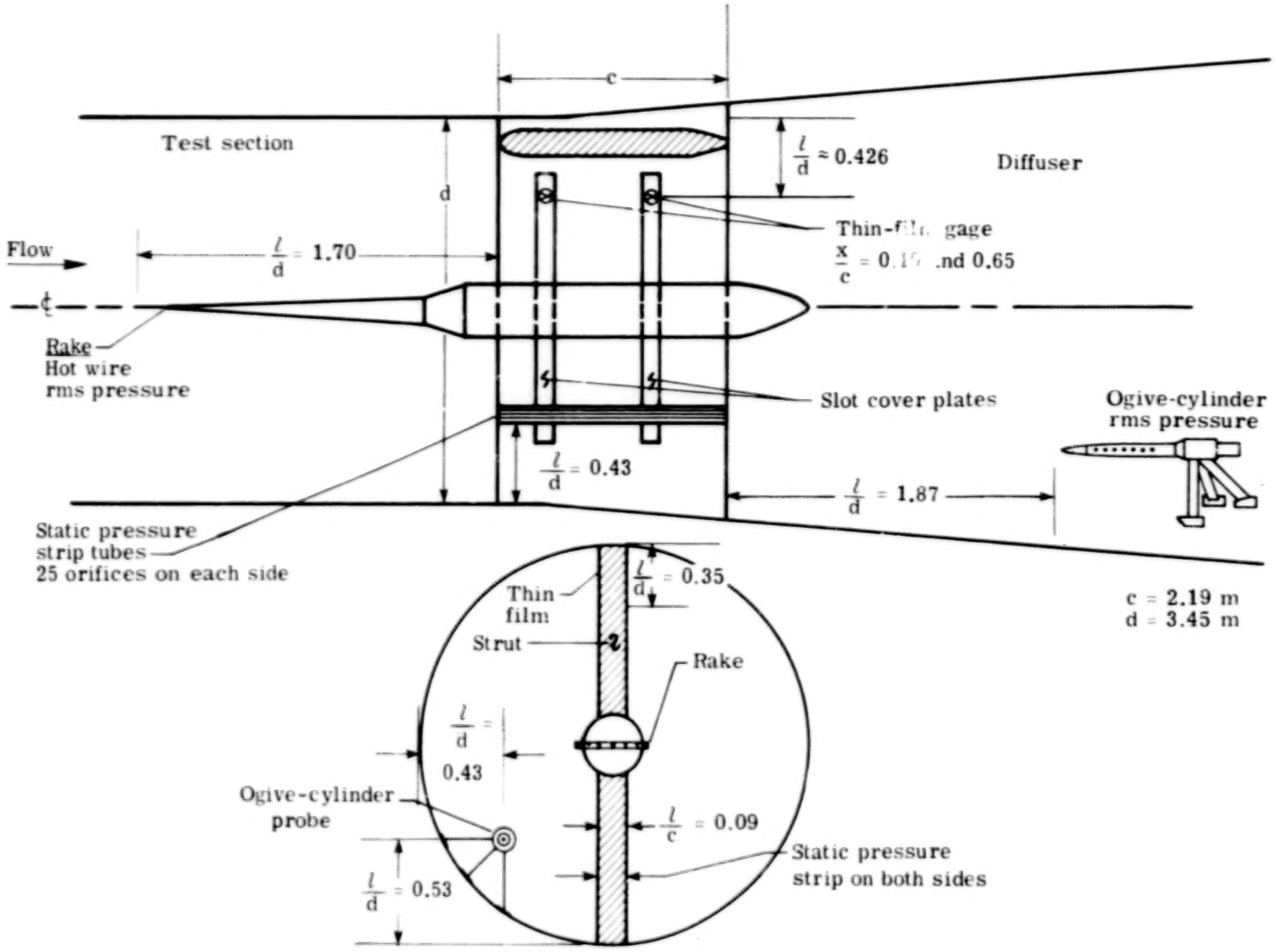

(b) Model support strut and instrumentation.

Figure 3.- Continued.

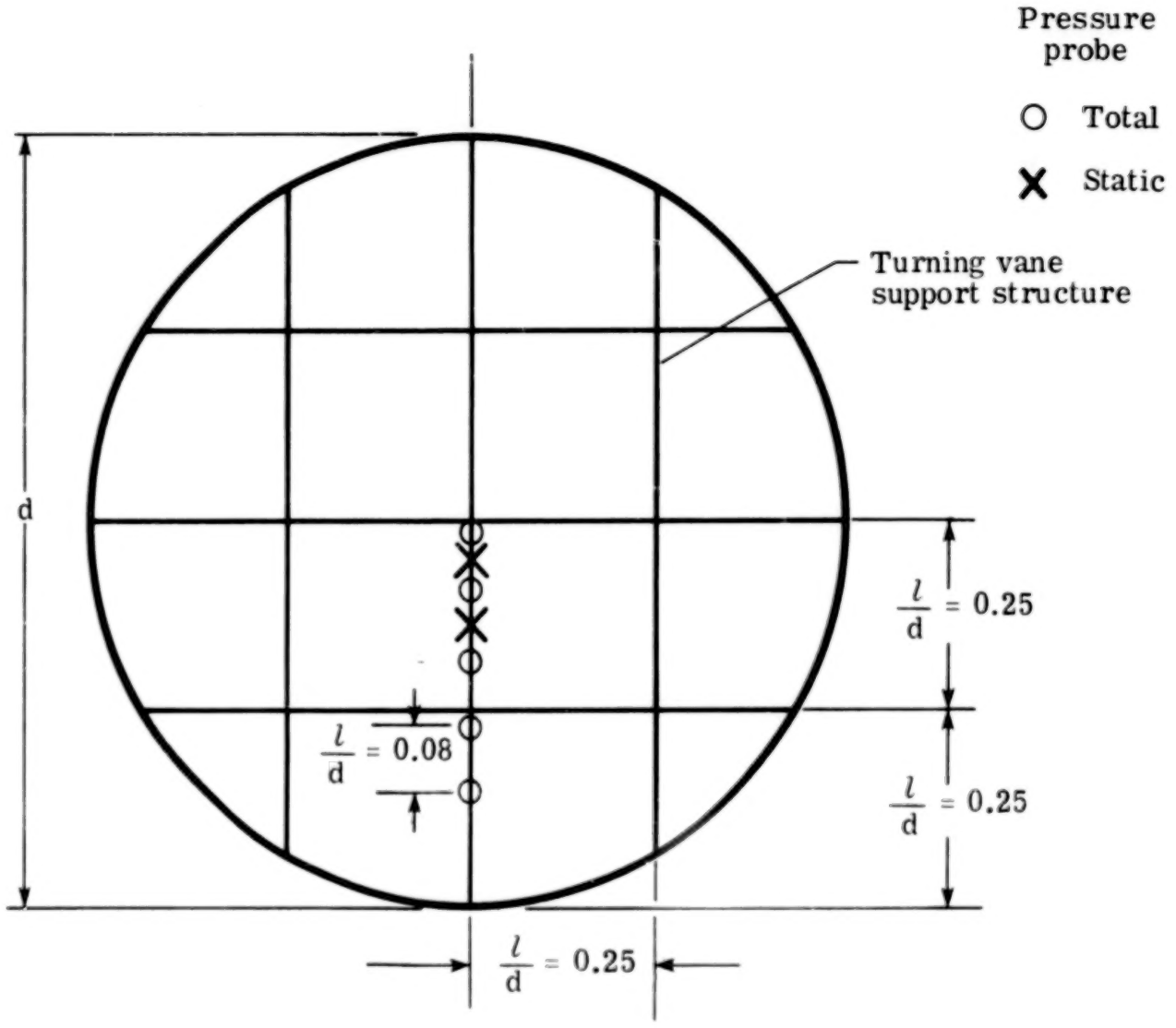

(c) Diffuser-exit instrumentation.

Figure 3.- Concluded.

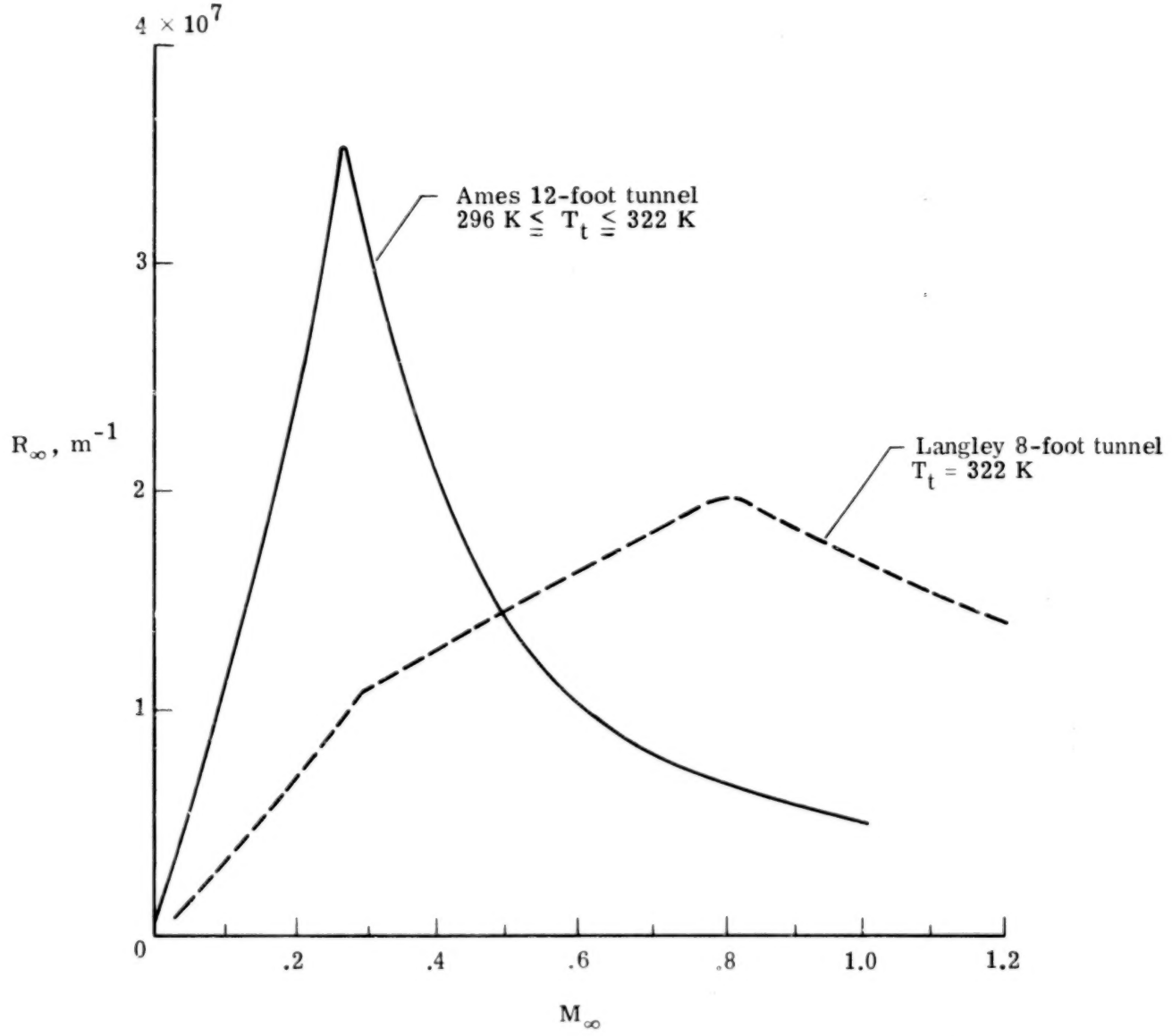

Figure 4.- Maximum operating characteristics of the Langley 8-Foot and Ames 12-Foot Tunnels.

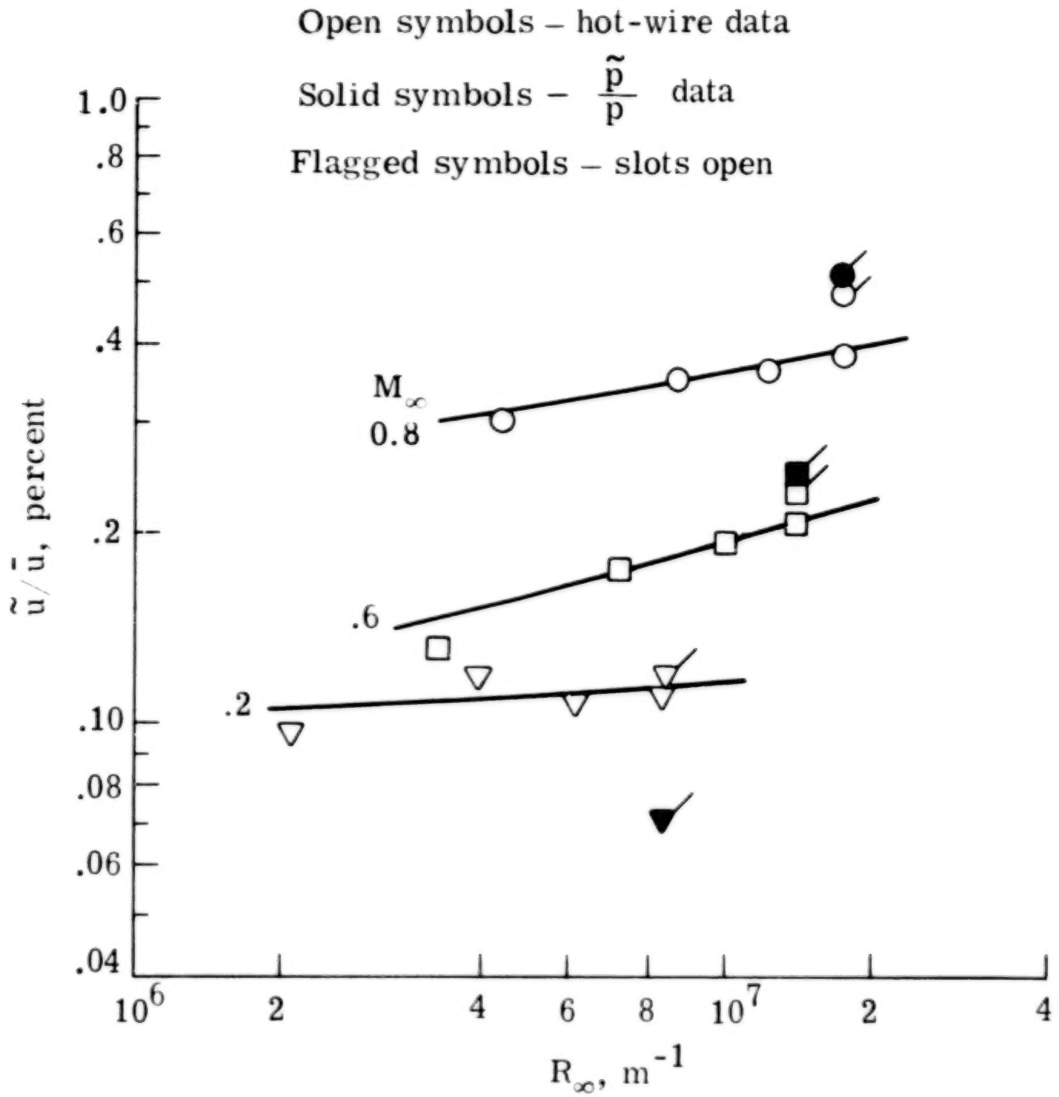

Figure 5.- Velocity fluctuation levels in test section of Langley 8-Foot Tunnel.

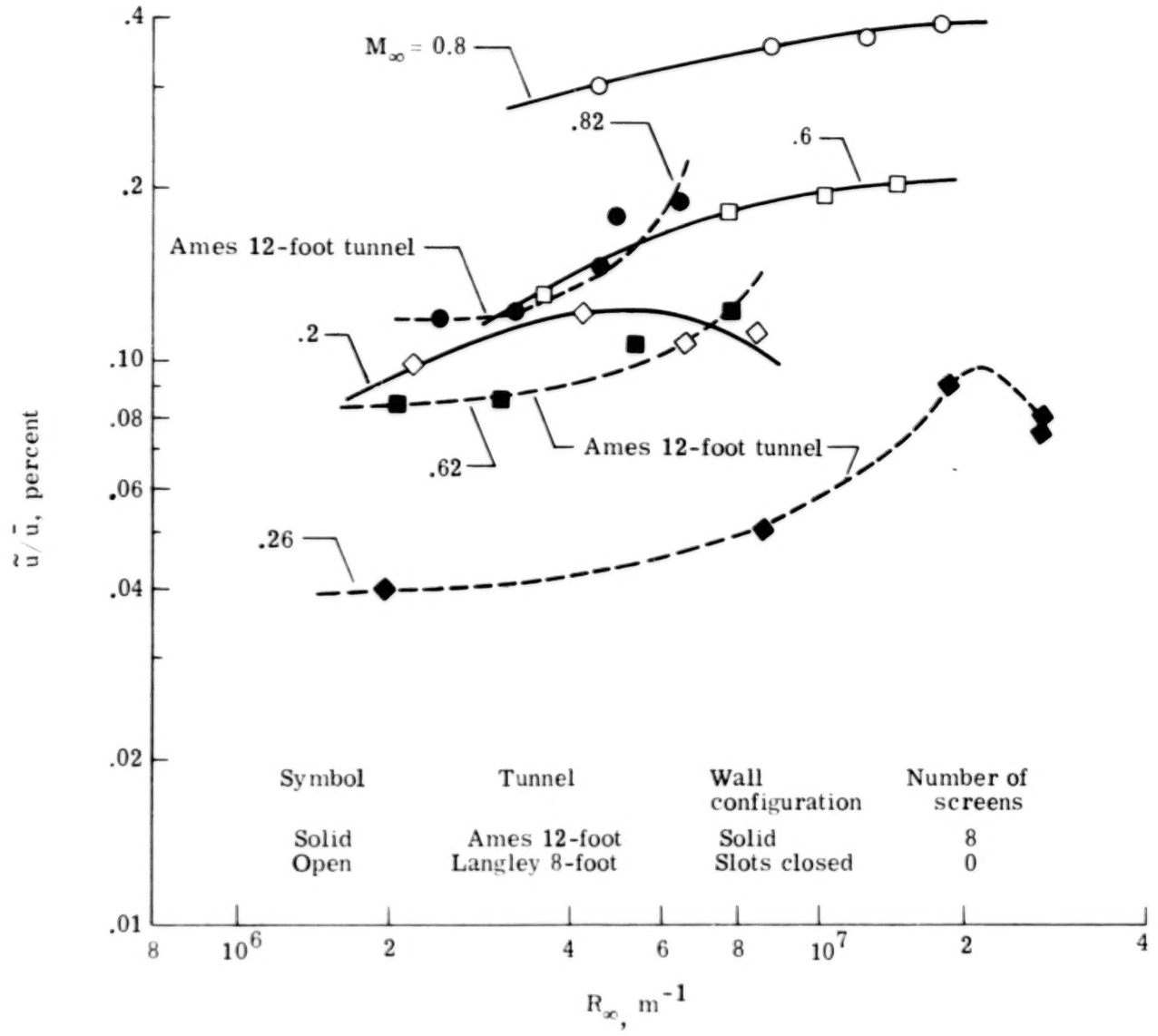

Figure 6.- Comparison between velocity fluctuations in test sections of Ames 12-Foot and Langley 8-Foot Tunnels.

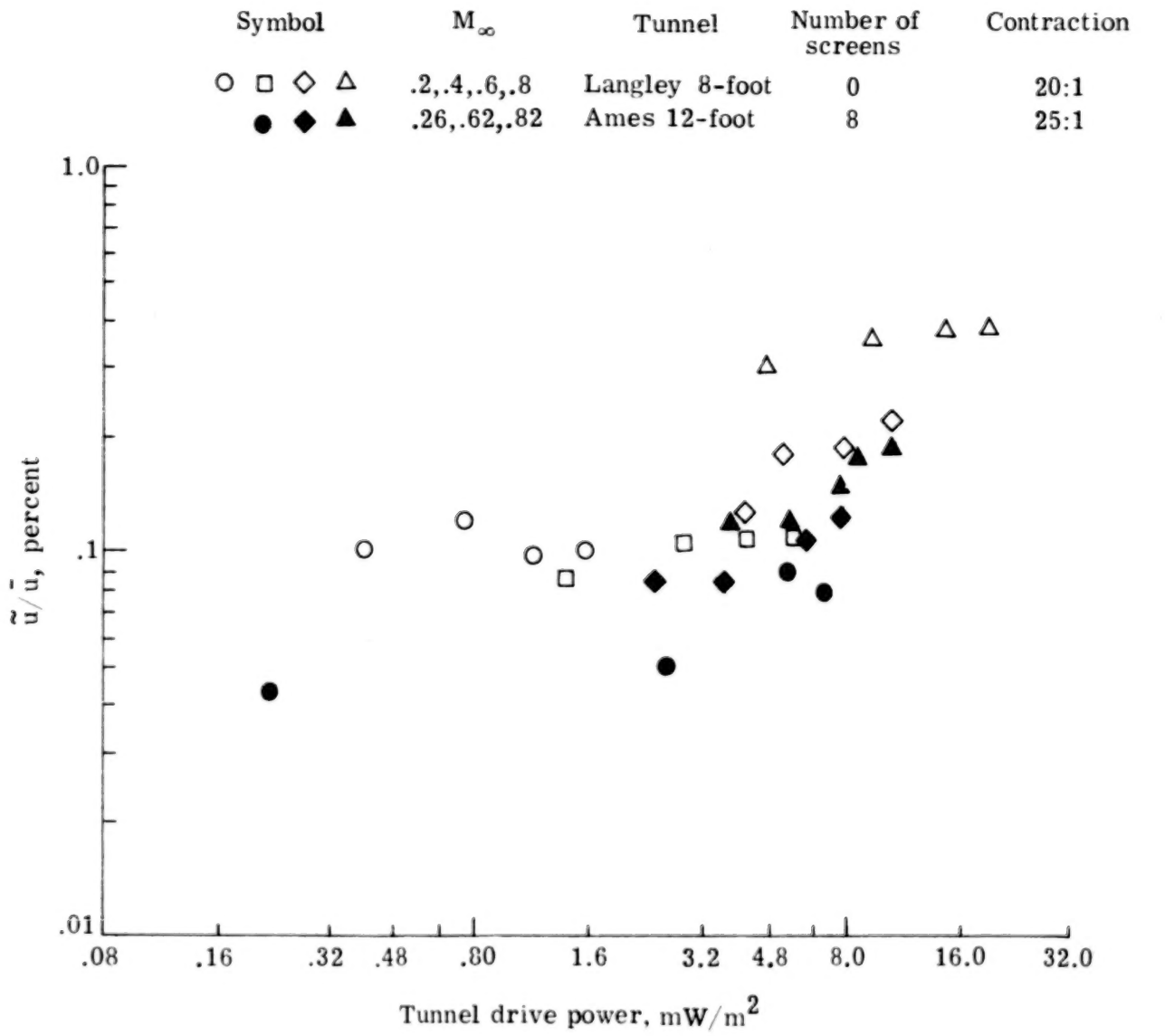

(a) Hot-wire data.

Figure 7.- Comparison of turbulence level with tunnel power for Langley 8-Foot and Ames 12-Foot Tunnels.

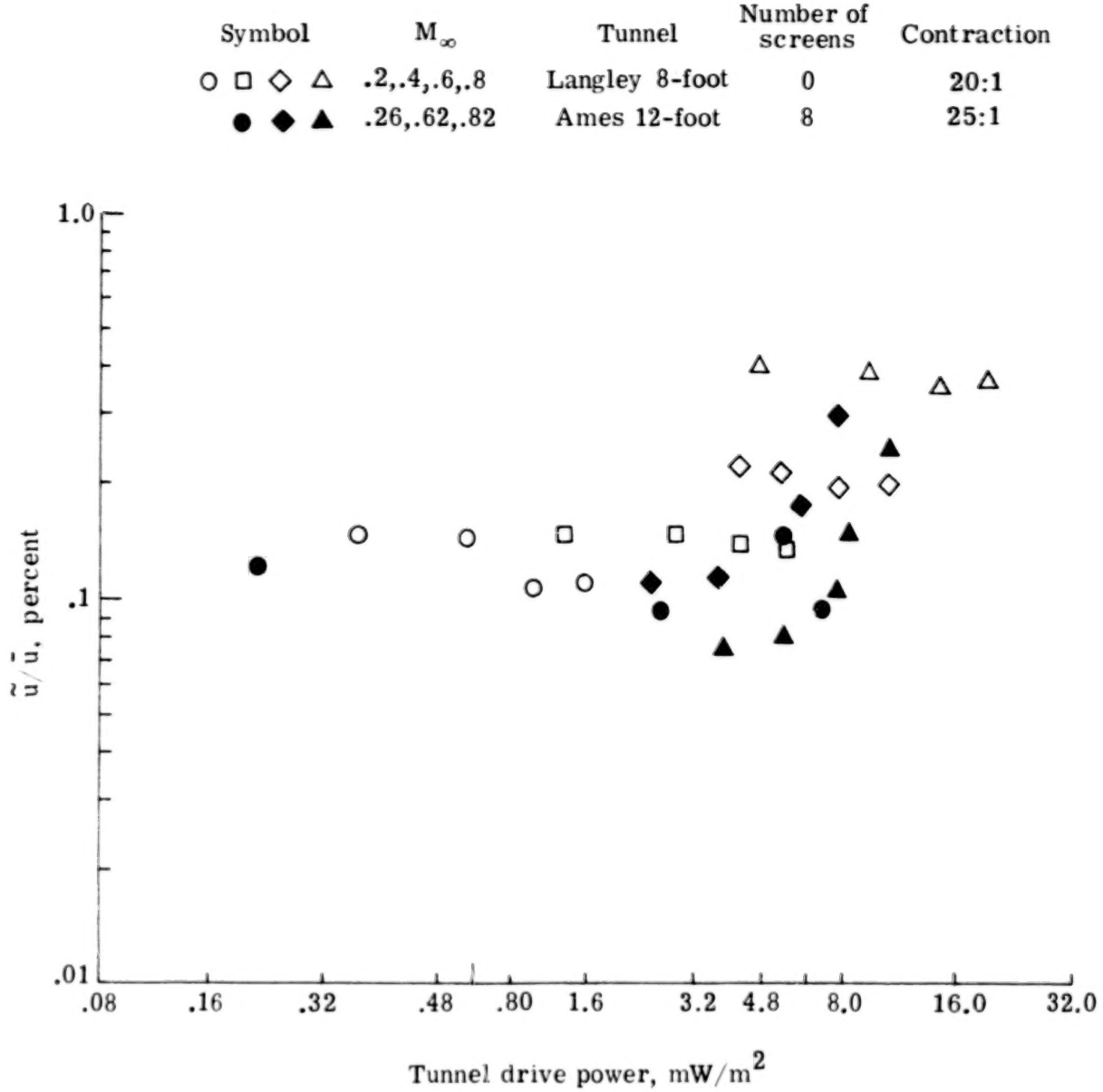

(b) Calculated from $\tilde{p}/\bar{p}$.

Figure 7.- Concluded.

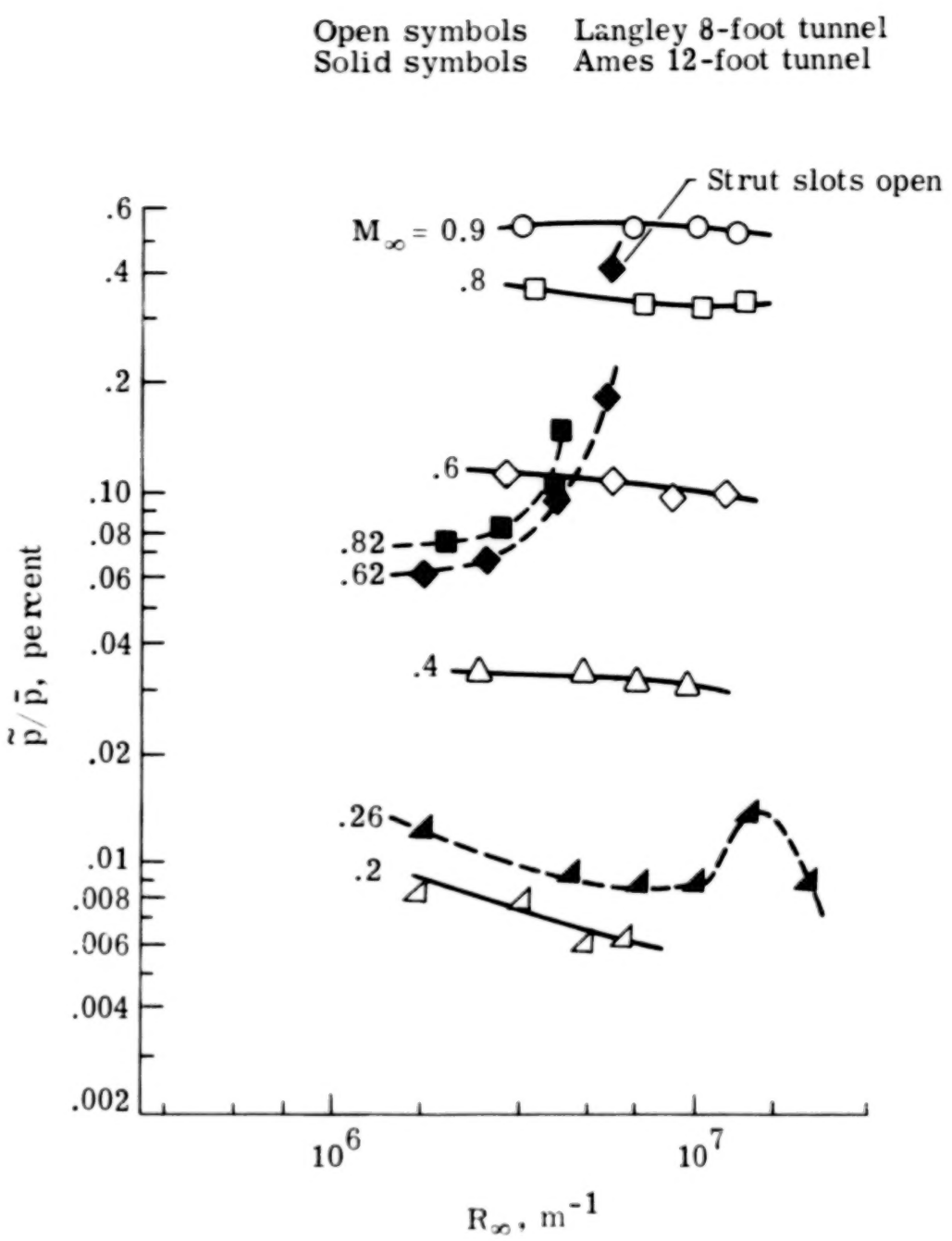

Figure 8.- Comparison between static pressure fluctuations in test sections of Ames 12-Foot and Langley 8-Foot Tunnels.

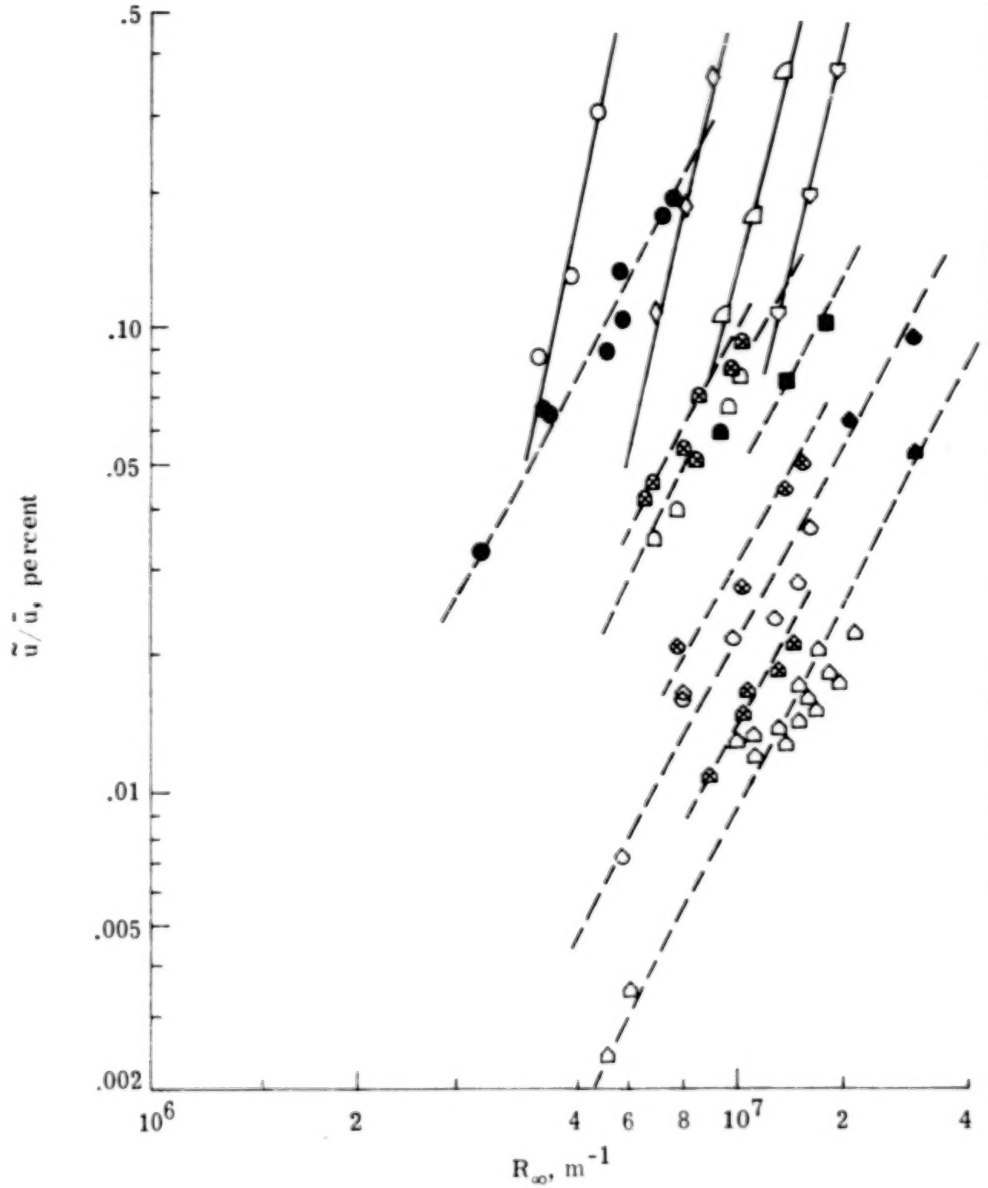

Symbol	Atmospheres	Tunnel	Date	Reference
◈	≈5	Ames 12-foot	10/65	W. Pfenninger (unpublished)
⊗	≈3	↓	↓	↓
⊠	≈1.5			
△	≈5	Ames 12-foot	1/66	16
◇	≈3	↓	↓	↓
□	≈1.5			
◆	≈5	Ames 12-foot	4/78	Present
⬟	≈3	↓	↓	↓
■	≈2.4			
⬢	≈1.5			
●	≈ .5	↓	↓	↓
▽	≈1.42	Langley 8-foot	5/78	
◺	≈1.04	↓	↓	
◊	≈ .7			
○	≈ .35	↓	↓	

Figure 9.- Velocity fluctuations obtained from pressure fluctuations in Ames 12-Foot and Langley 8-Foot Tunnels. 1 atm = 101.3 kPa.

BLANK PAGE

BLANK PAGE

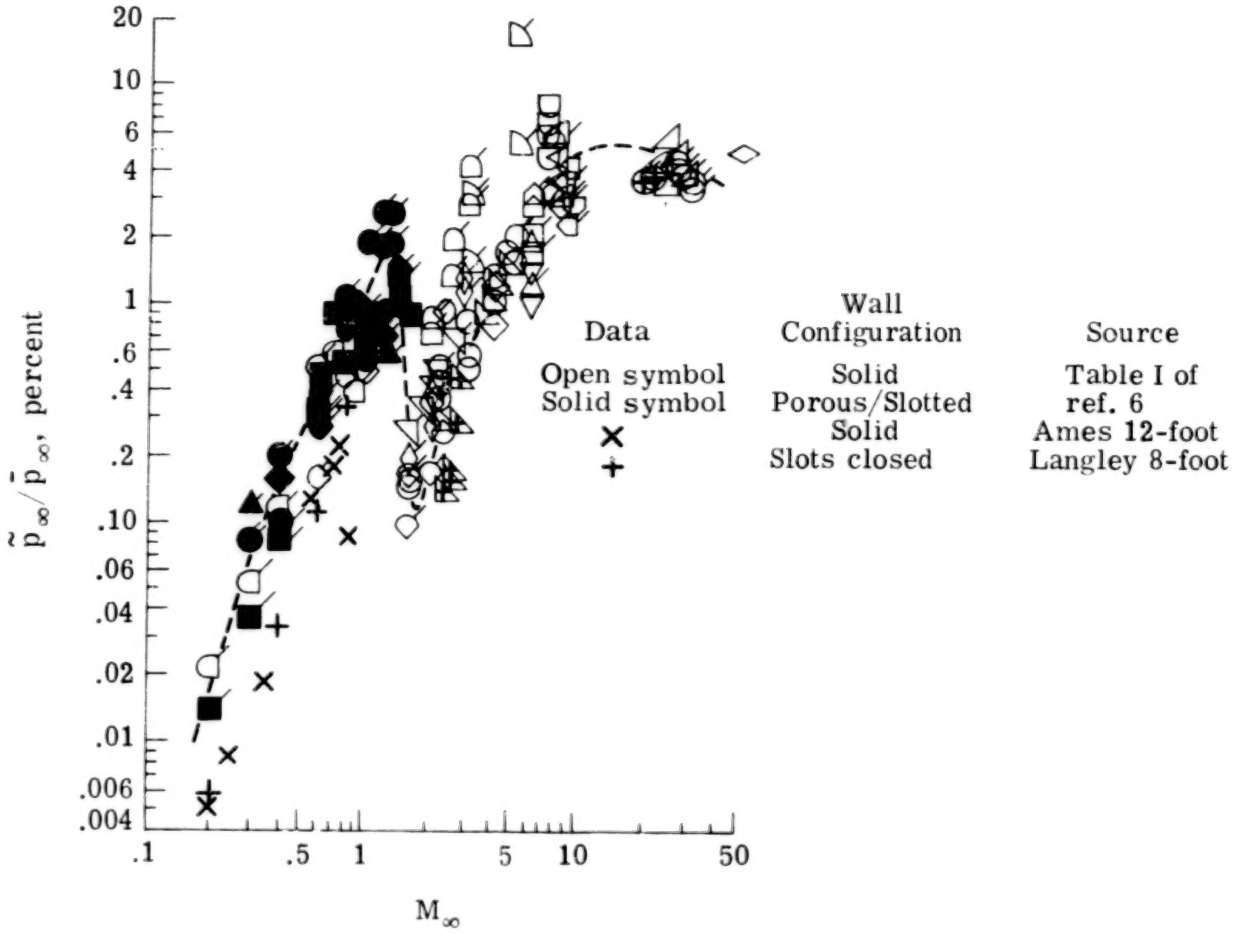

Figure 10.- Comparison of present results with test-section pressure fluctuation in several wind tunnels.

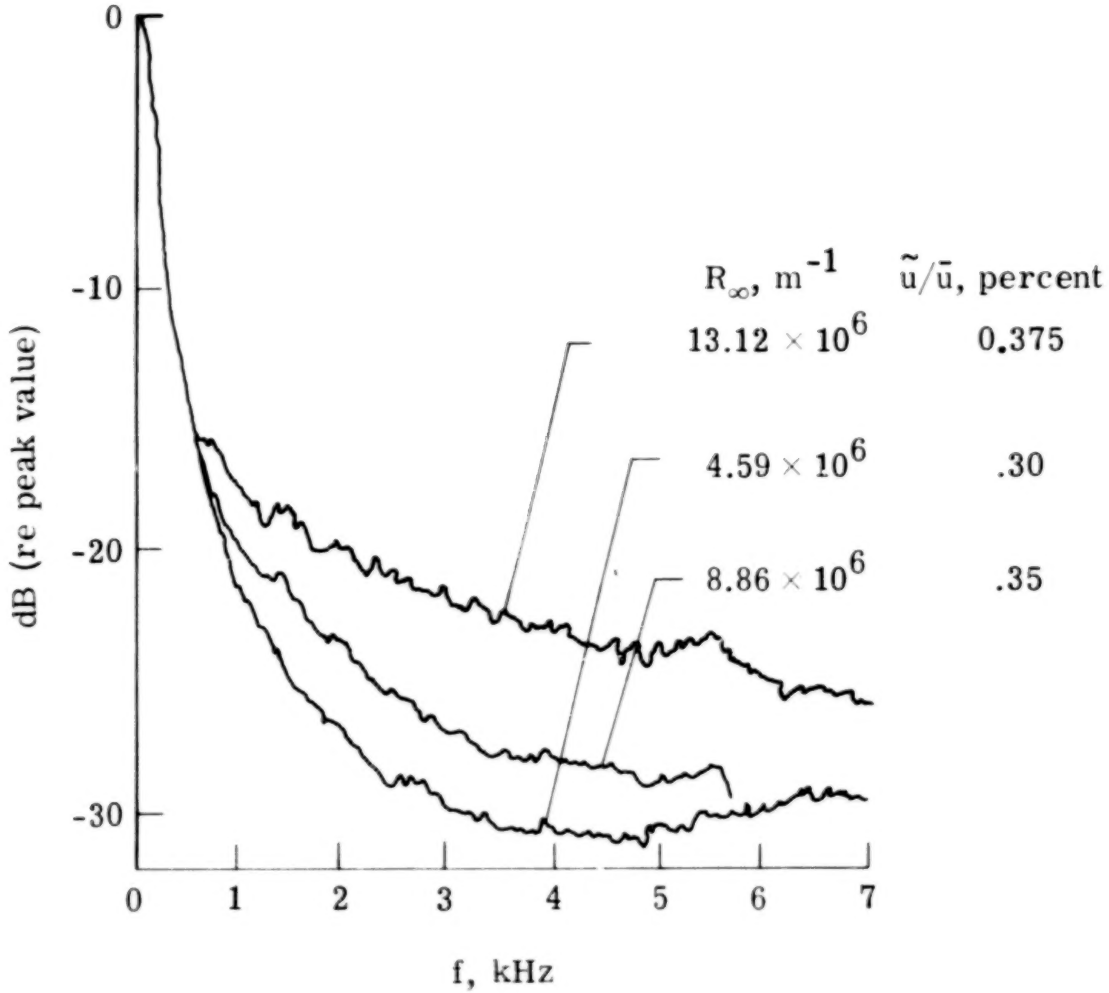

Figure 11.- Spectra from hot-wire measurements in test section of Langley 8-Foot Tunnel at $M_\infty = 0.8$.

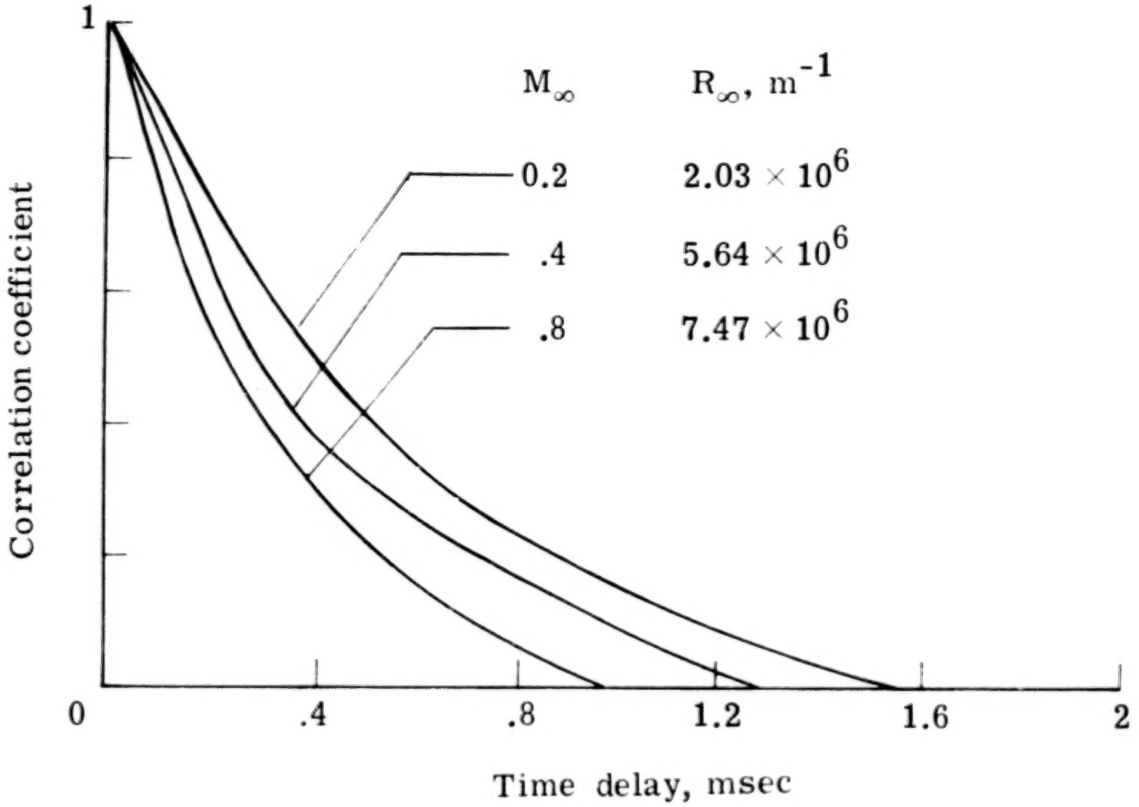

Figure 12.- Autocorrelations from hot-wire measurements in test section of Langley 8-Foot Tunnel.

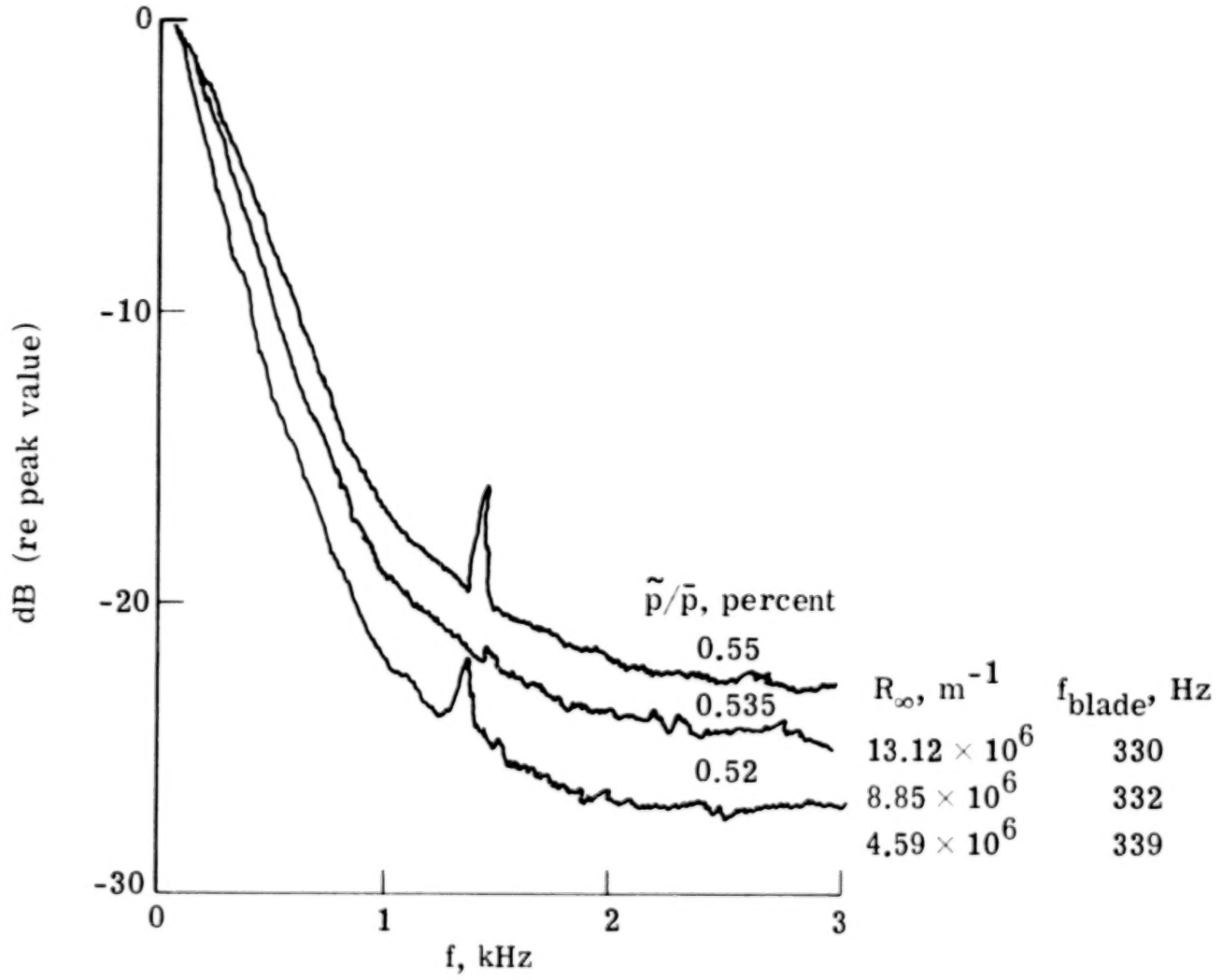

Figure 13.- Spectra from pressure measurements in test section of Langley 8-Foot Tunnel at $M_\infty = 0.8$.

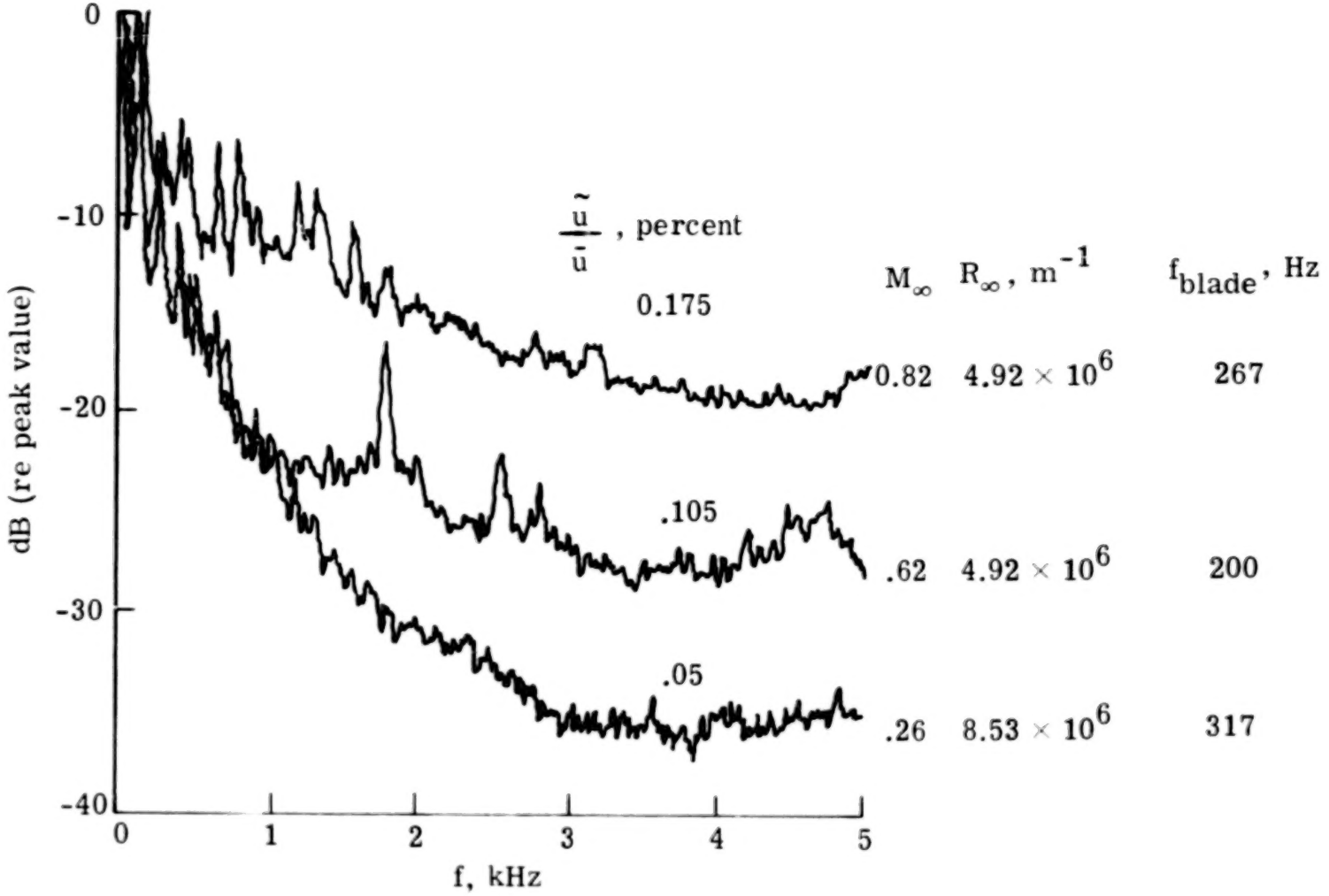

Figure 14.- Spectra from hot-wire measurements in test section of Ames 12-Foot Tunnel. Strut slots closed.

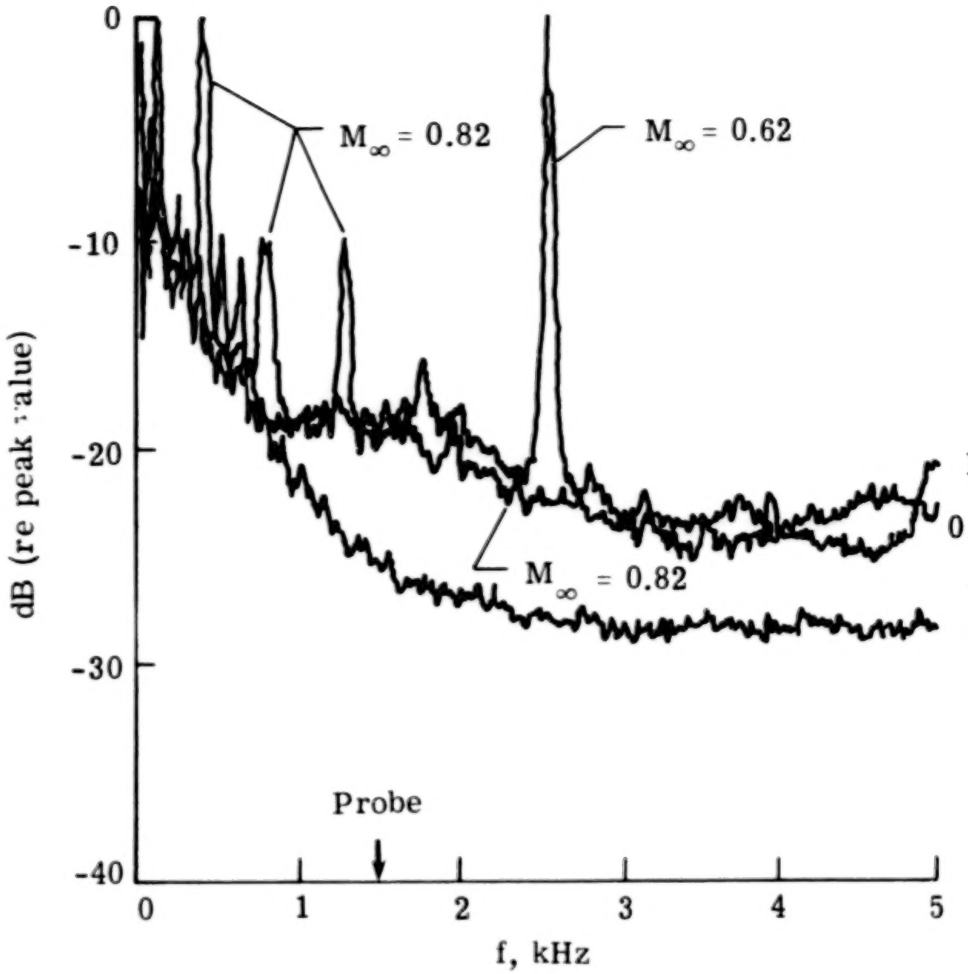

M_∞	R_∞, m^{-1}	$\frac{\tilde{p}}{p}$, percent	f_{blade}, Hz
0.82	4.92×10^6	0.16	267
.62	4.92×10^6	.095	200
.26	8.53×10^6	.0085	317

Figure 15.- Spectra from pressure measurements in test section of Ames 12-Foot Tunnel. Strut slots closed.

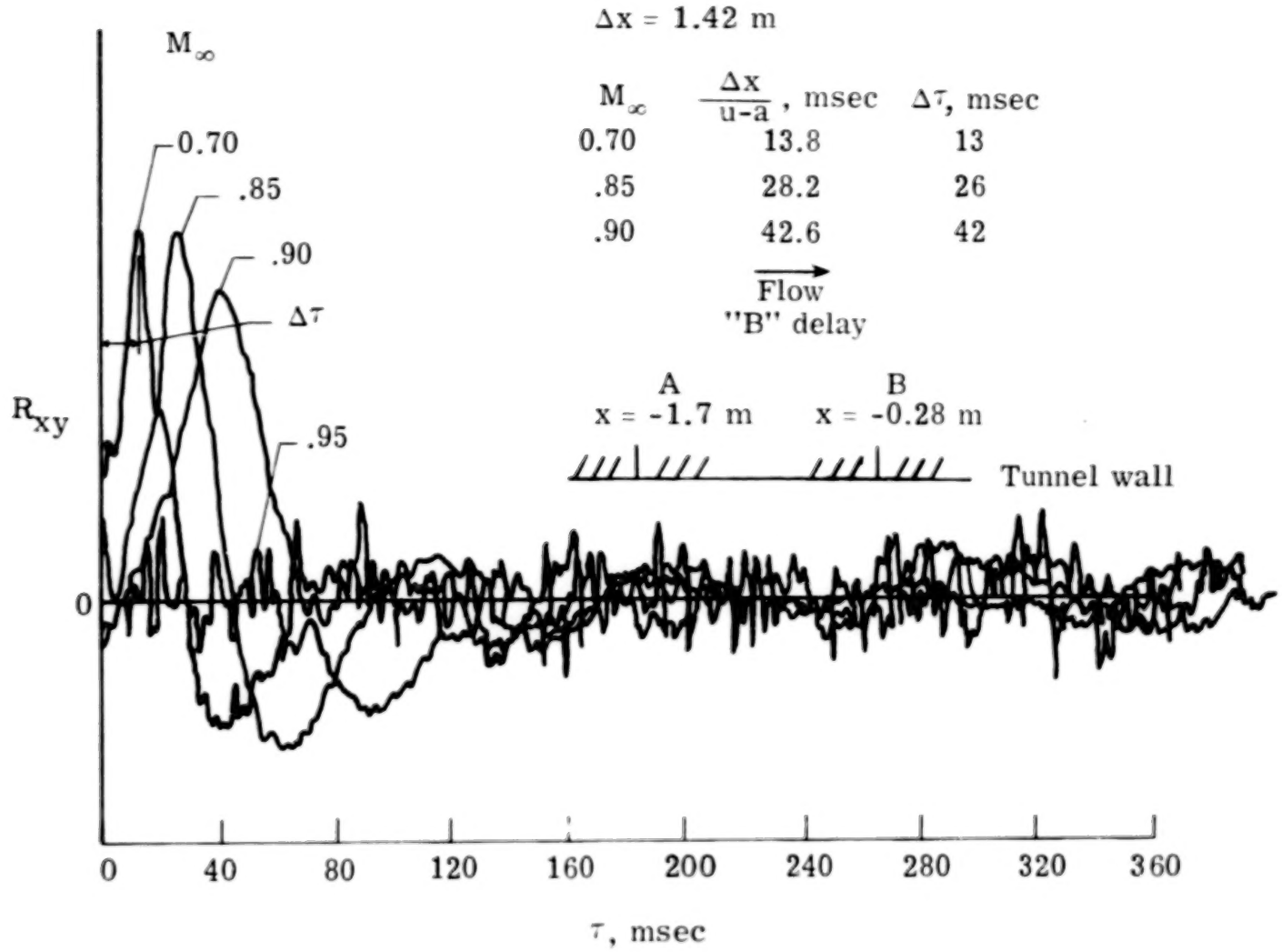

Figure 16.- Cross correlation of pressure fluctuations measured at test-section wall of Langley 8-Foot Tunnel.

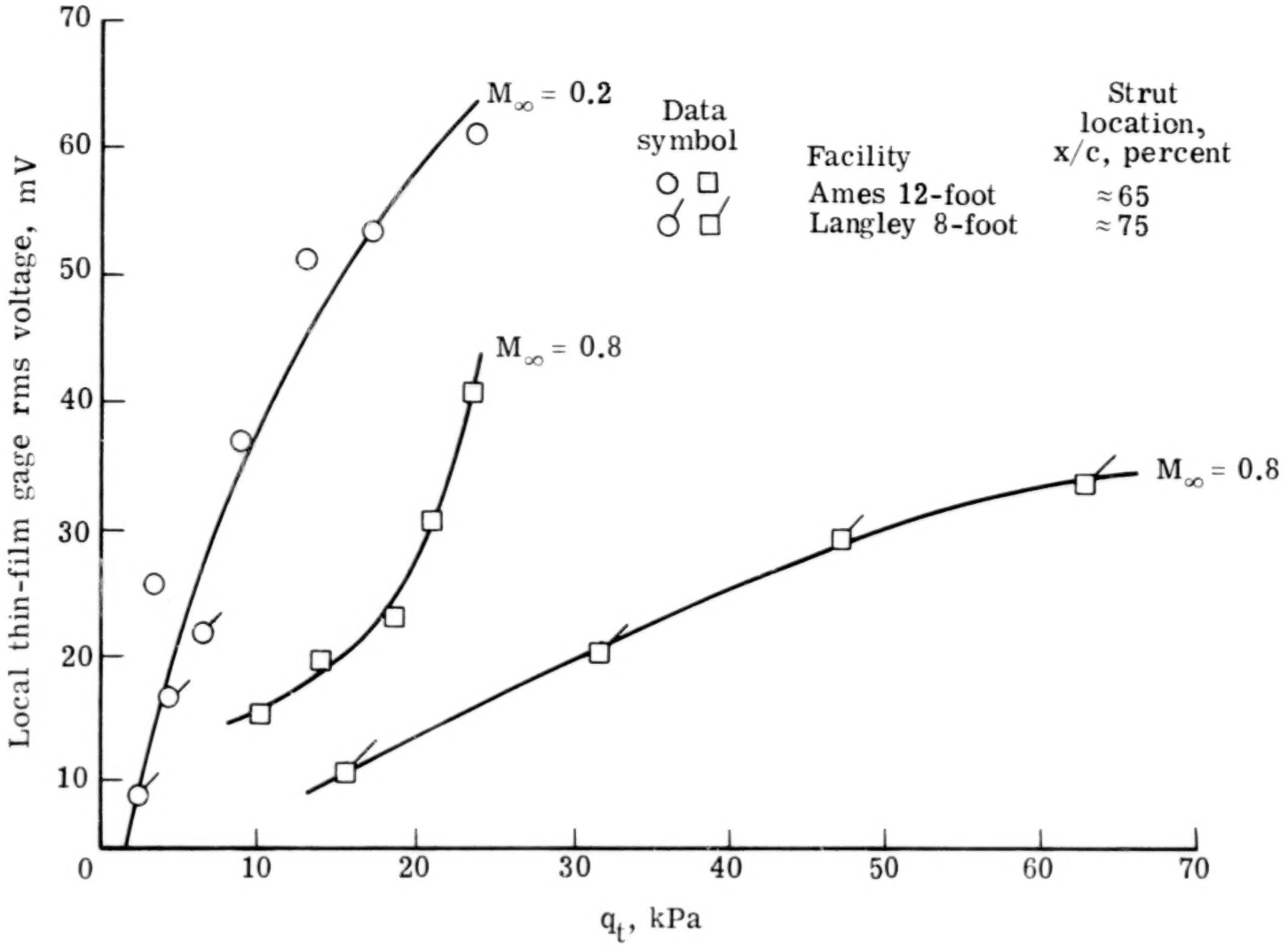

Figure 17.- Comparison between flow fluctuations on struts of Ames 12-Foot and Langley 8-Foot Tunnels.

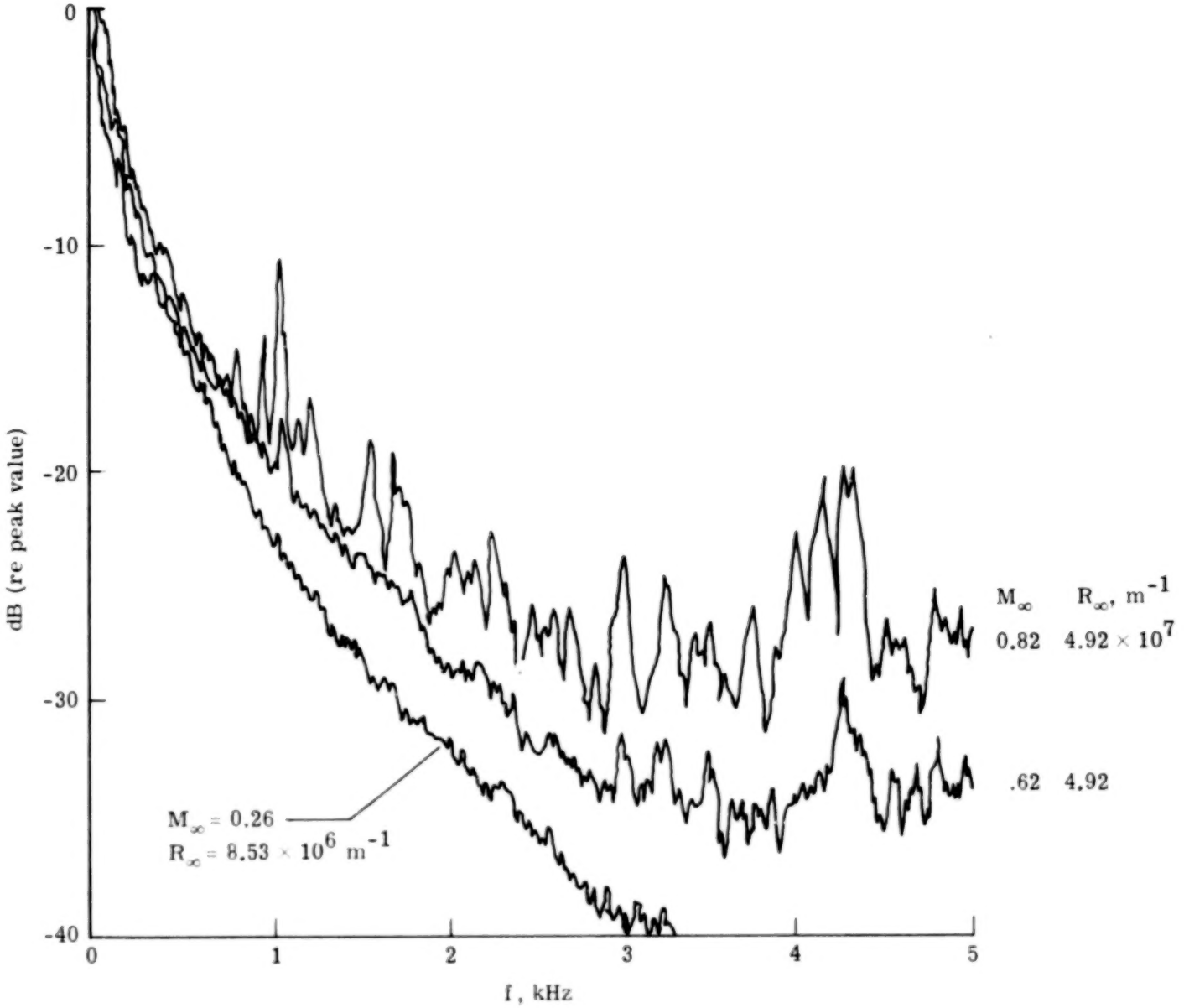

Figure 18.- Variation of thin-film spectra on strut in Ames 12-Foot Tunnel.

$\frac{x}{c} \approx 0.69$; strut slots covered.

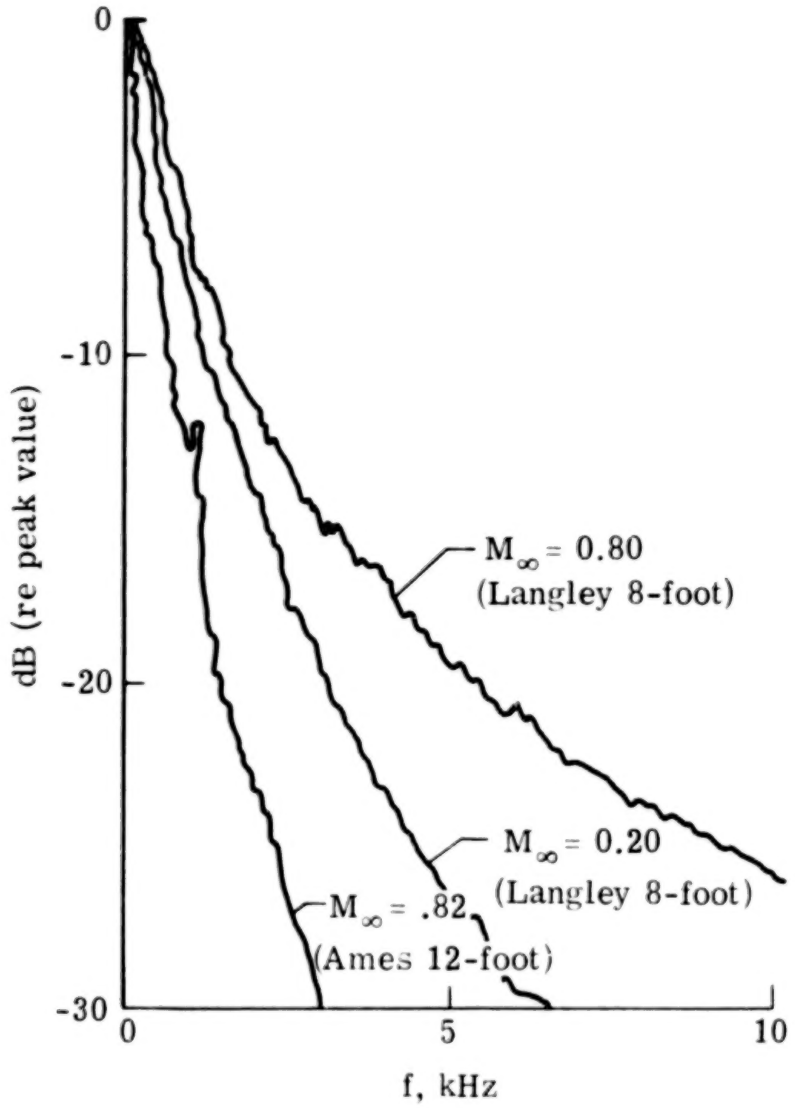

Figure 19.- Comparison of spectra measured with a thin film on the struts of the Ames 12-Foot and Langley 8-Foot Tunnels.

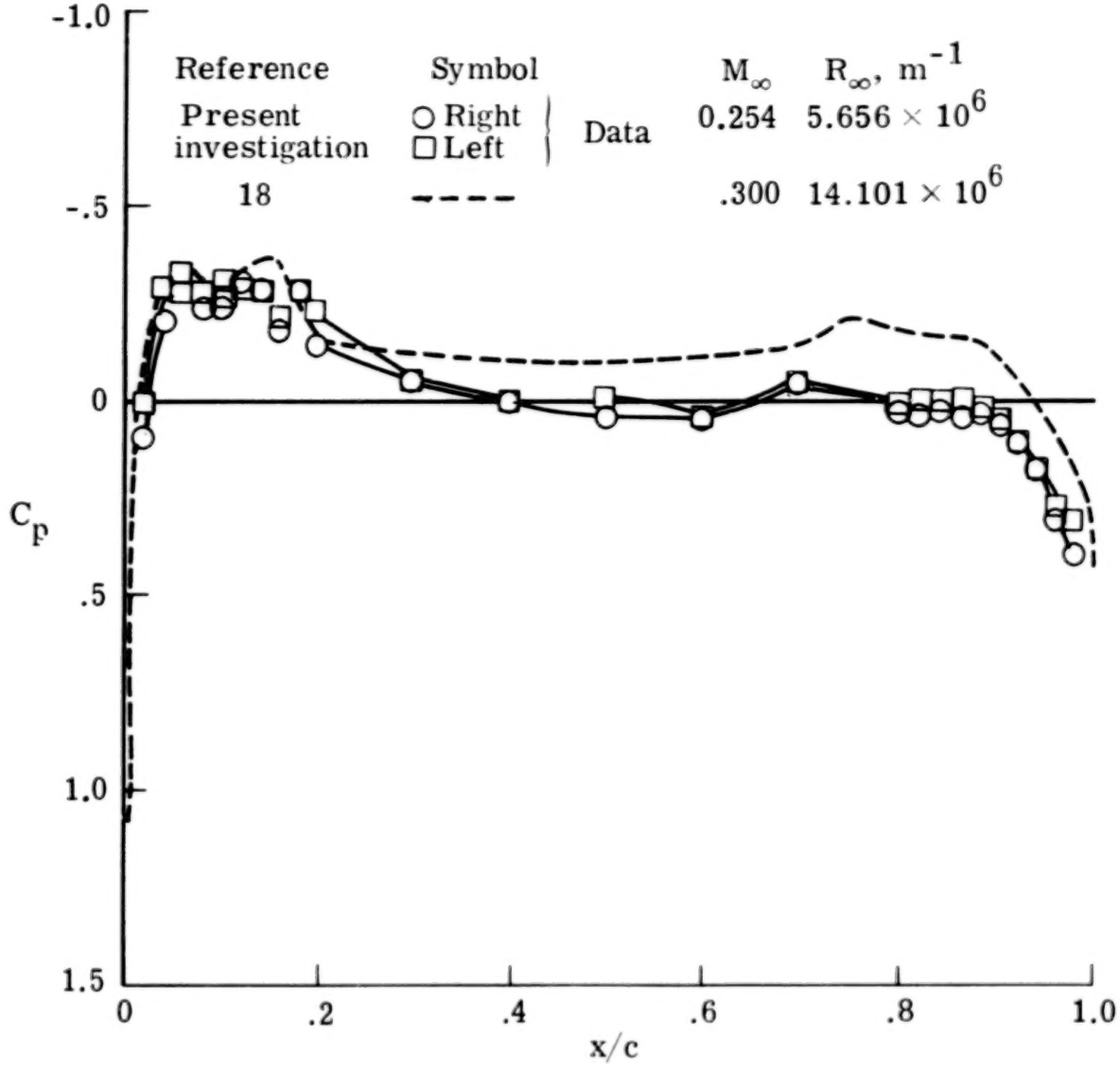

(a) $M_\infty = 0.25$.

Figure 20.- Comparison of measured pressure distribution with theory for Ames 12-Foot Tunnel model support strut. $\alpha = 0^\circ$; $C_L = 0$.

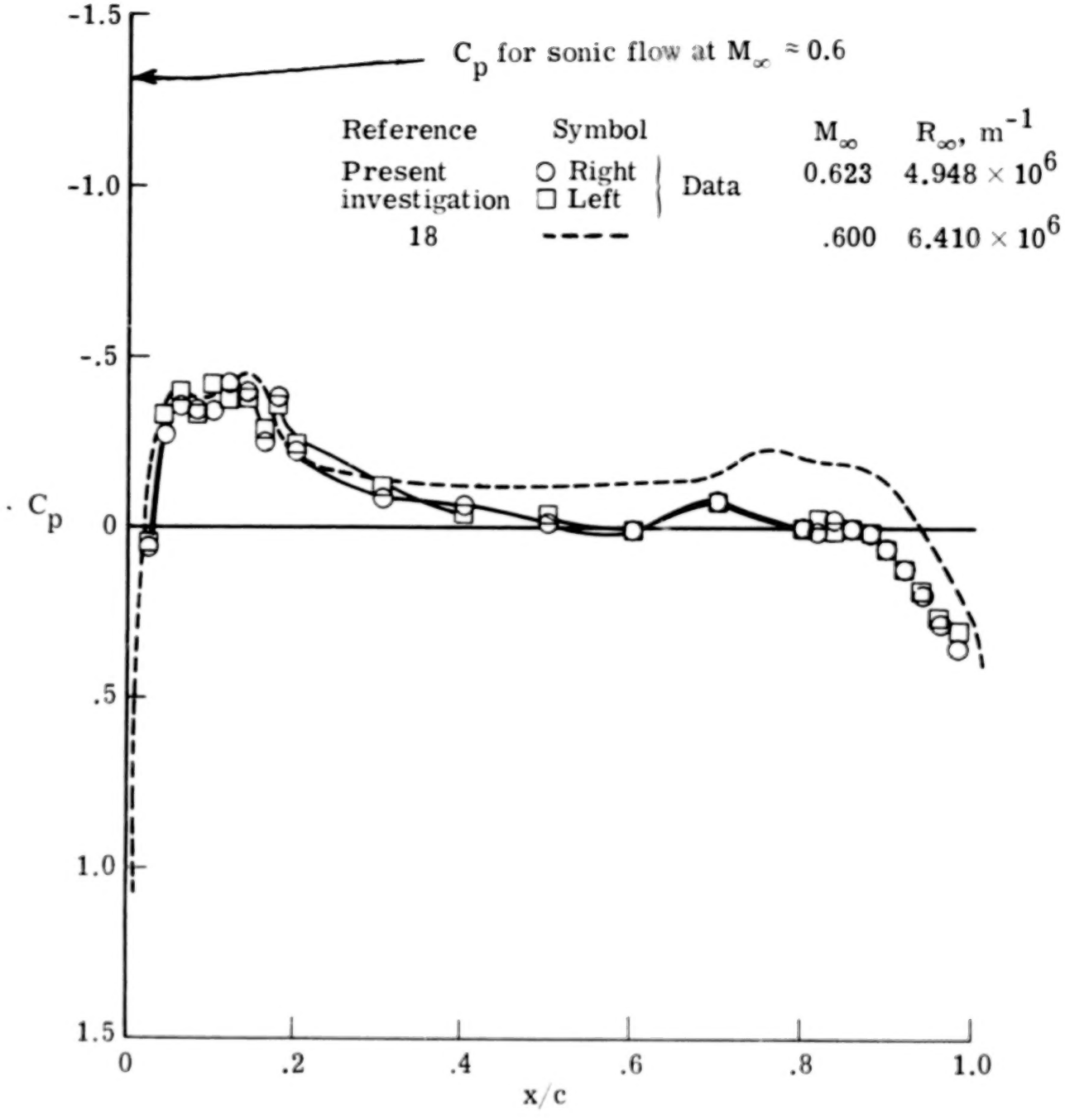

(b) $M_\infty = 0.62$.

Figure 20.- Continued.

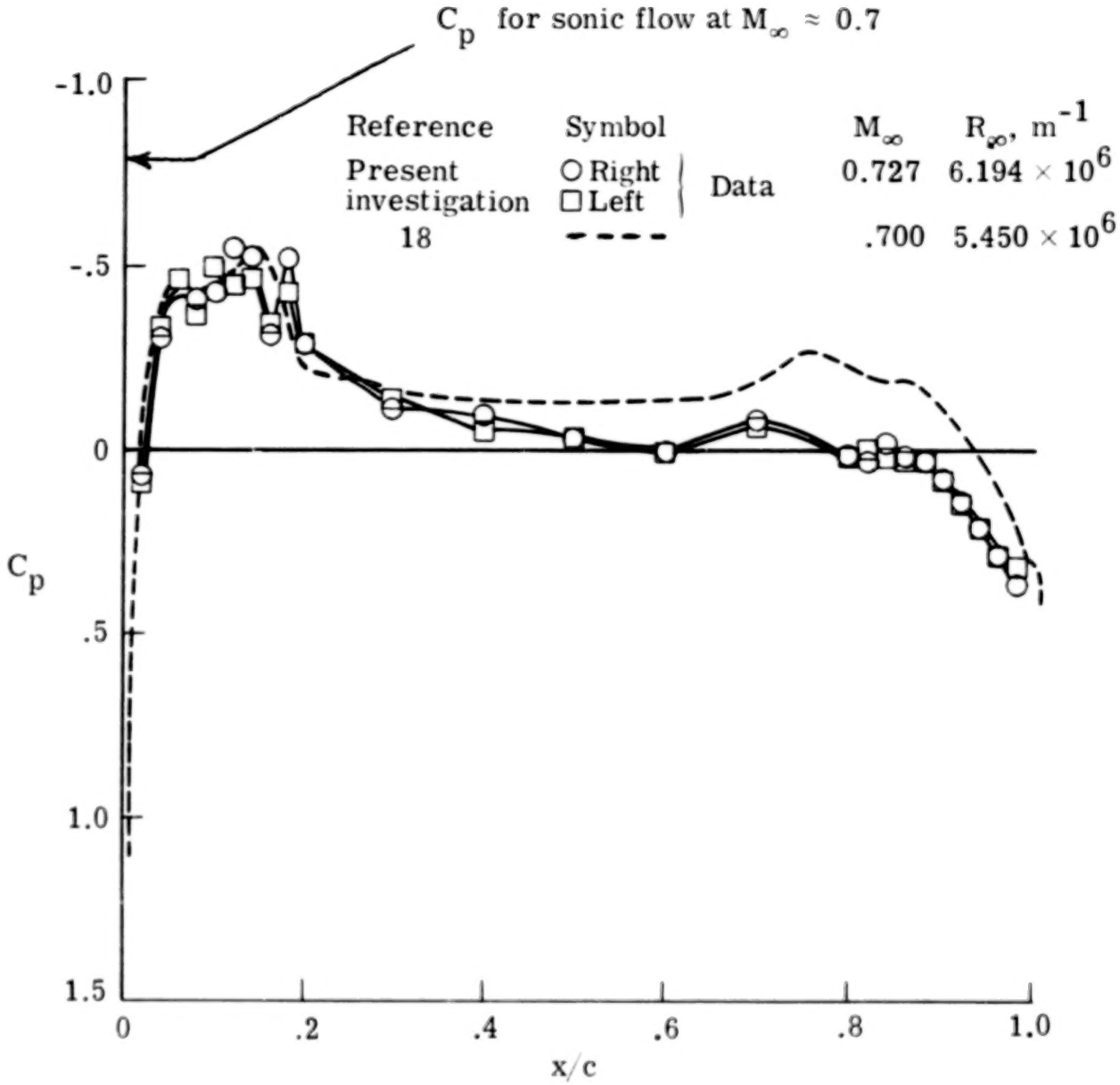

(c) $M_\infty = 0.73$.

Figure 20.- Continued.

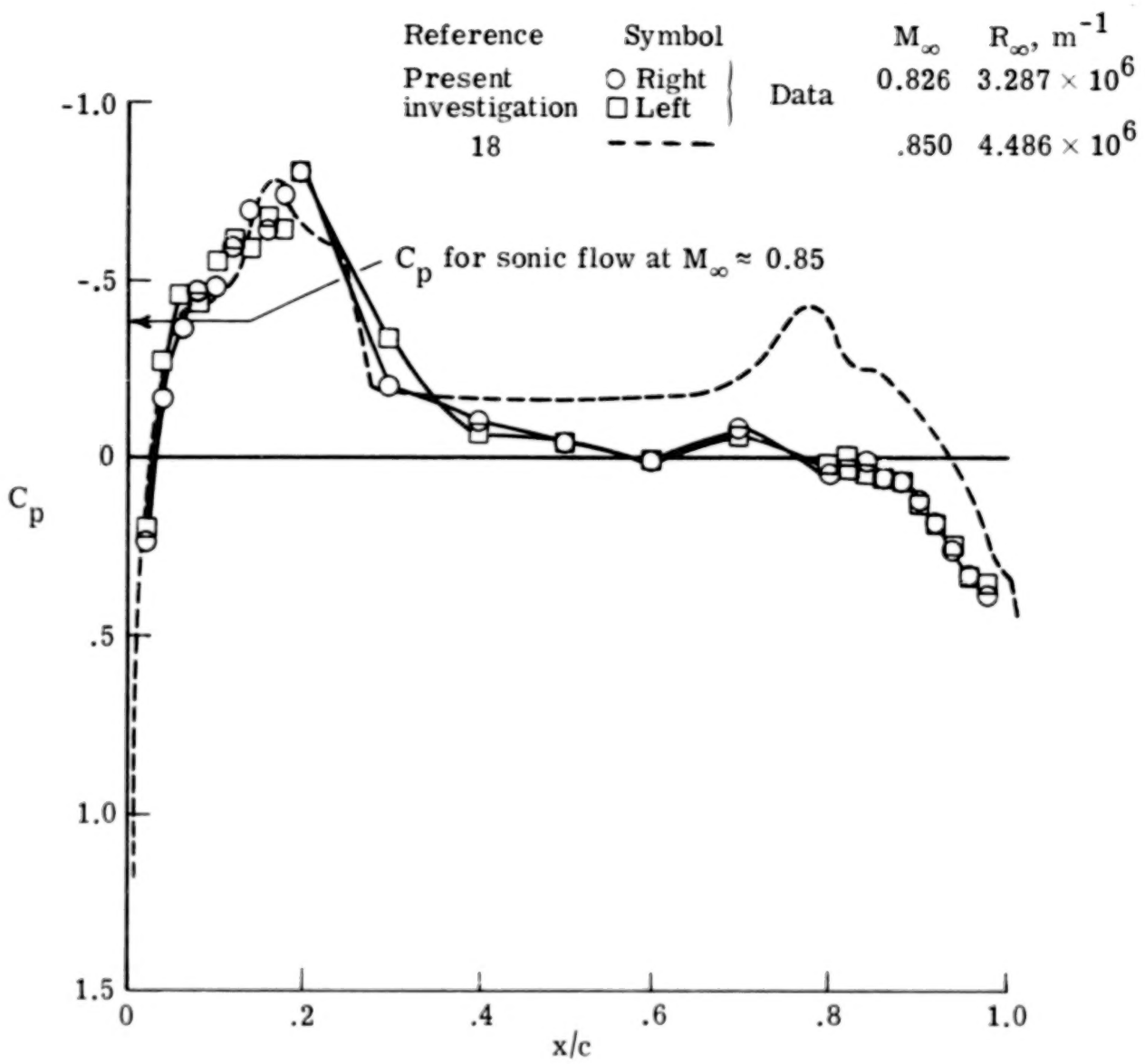

(d) $M_\infty = 0.83$.

Figure 20.- Concluded.

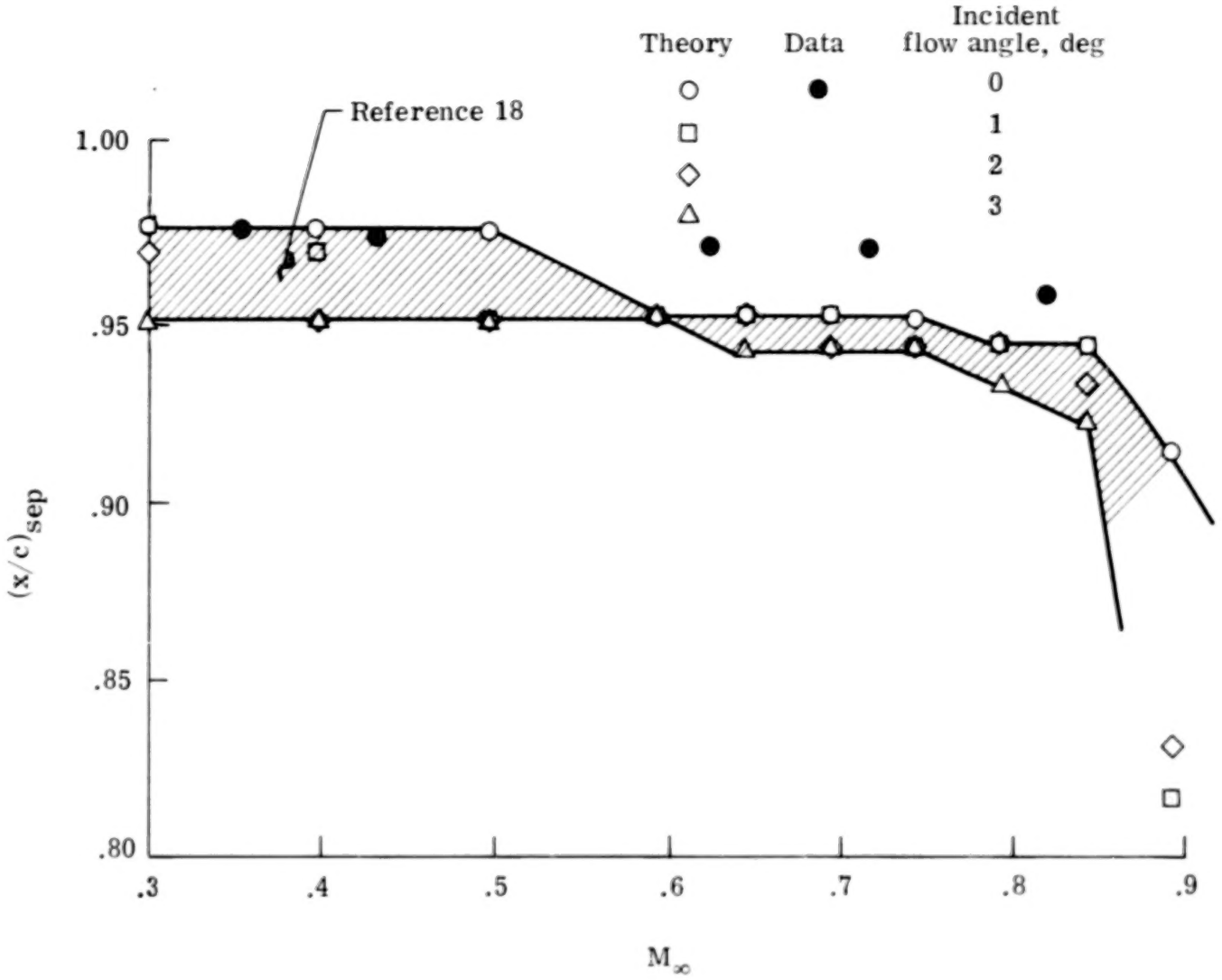

(a) Left surface.

Figure 21.- Comparison between experimental and theoretical flow separation on Ames 12-Foot Tunnel support strut. c = 2.18 m.

BLANK PAGE

BLANK PAGE

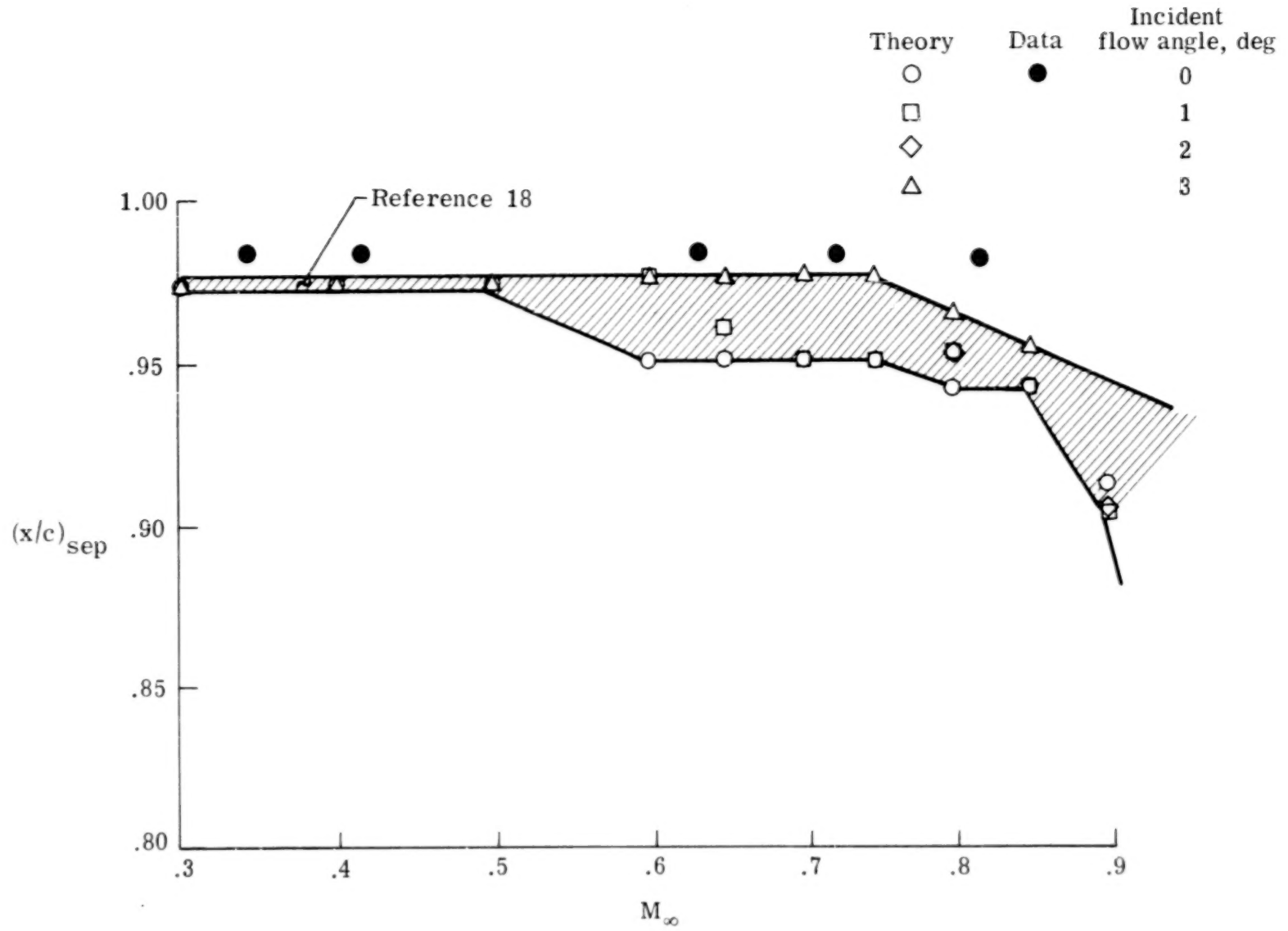

(b) Right surface.

Figure 21.- Concluded.

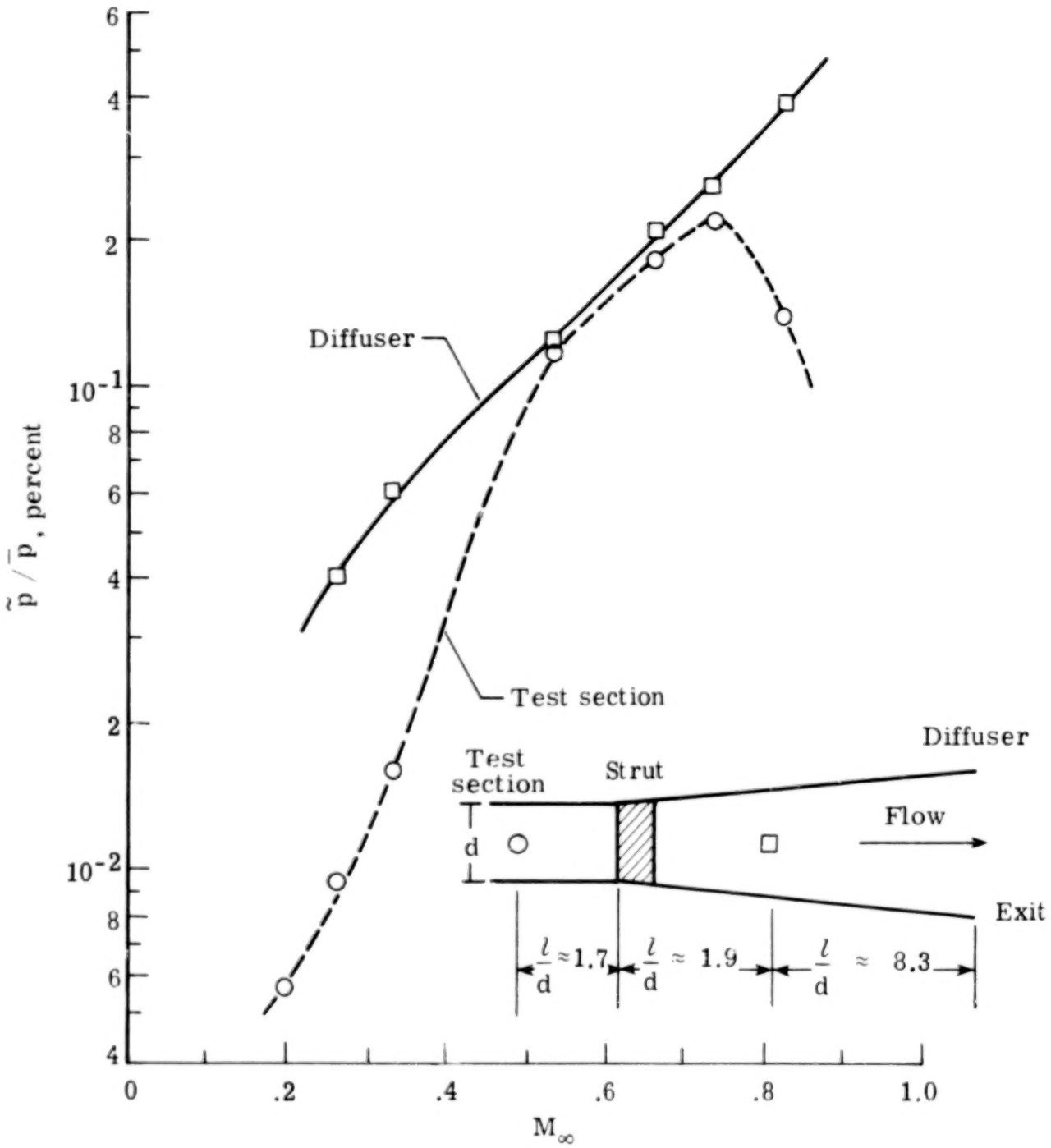

Figure 22.- Comparison of rms pressure fluctuations in Ames 12-Foot Tunnel test section with those in diffuser. $R_\infty \approx 6.56 \times 10^6$ m.

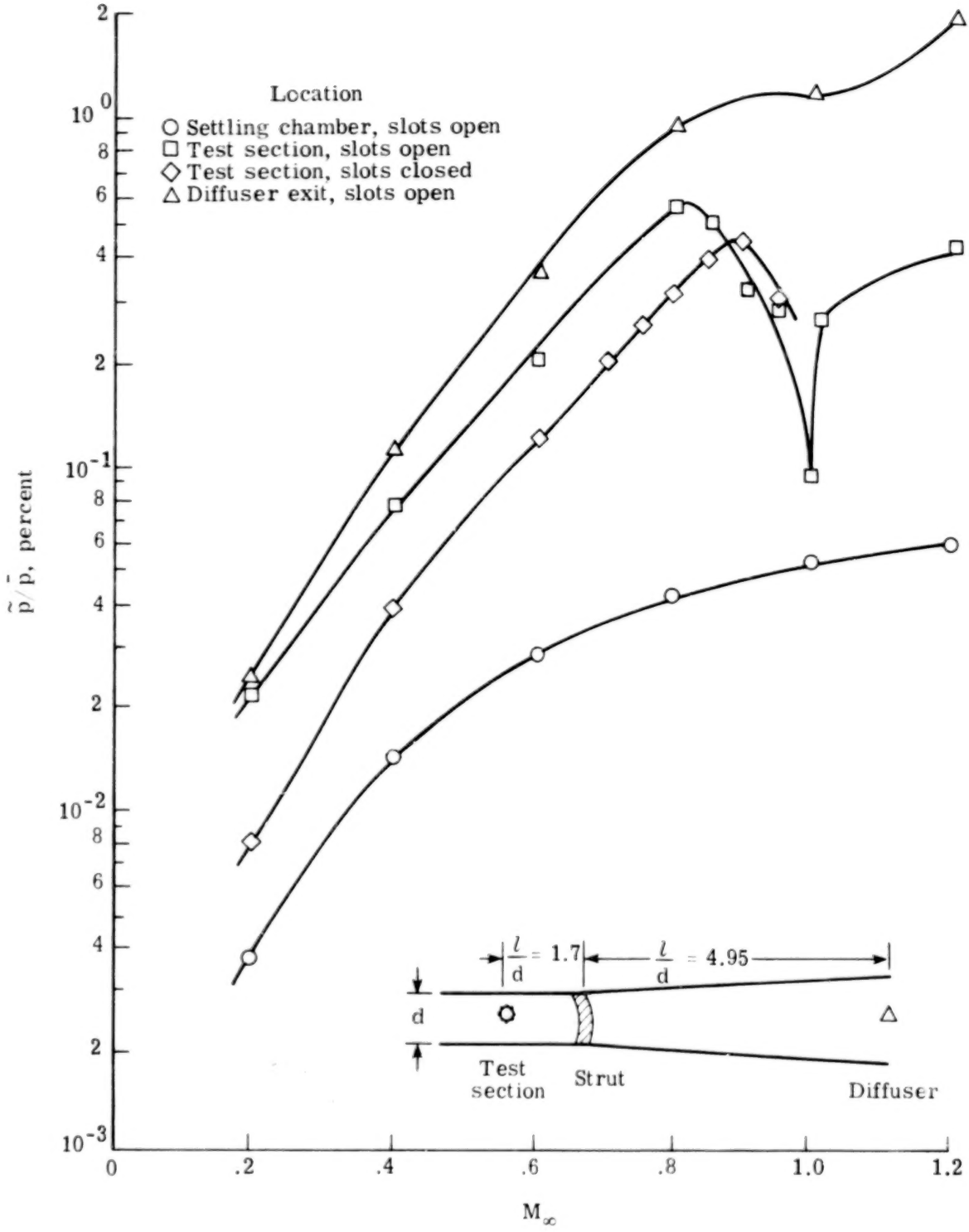

Figure 23.- Comparison between pressure fluctuations measured in Langley 8-Foot Tunnel settling chamber, diffuser, and test section with wall slots open and closed. $R_\infty \approx 6.56 \times 10^6$ m^{-1}.

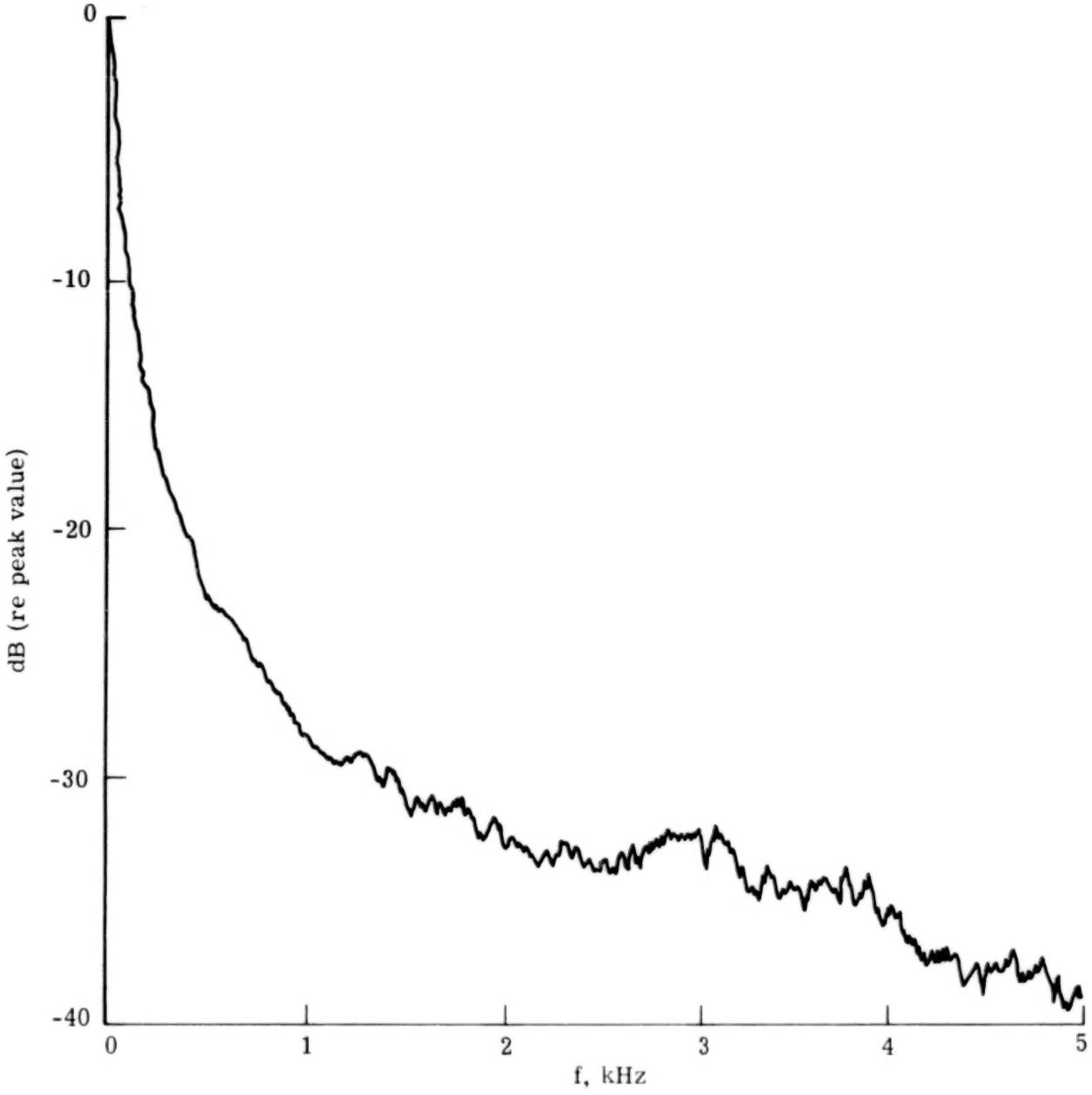

Figure 24.- Representative energy spectrum in Langley 8-Foot Tunnel diffuser exit obtained from pressure probe. $M_\infty = 0.8$; $\tilde{p}/\bar{p} = 1$ percent; $R_\infty \approx 6.56 \times 10^6\ m^{-1}$.

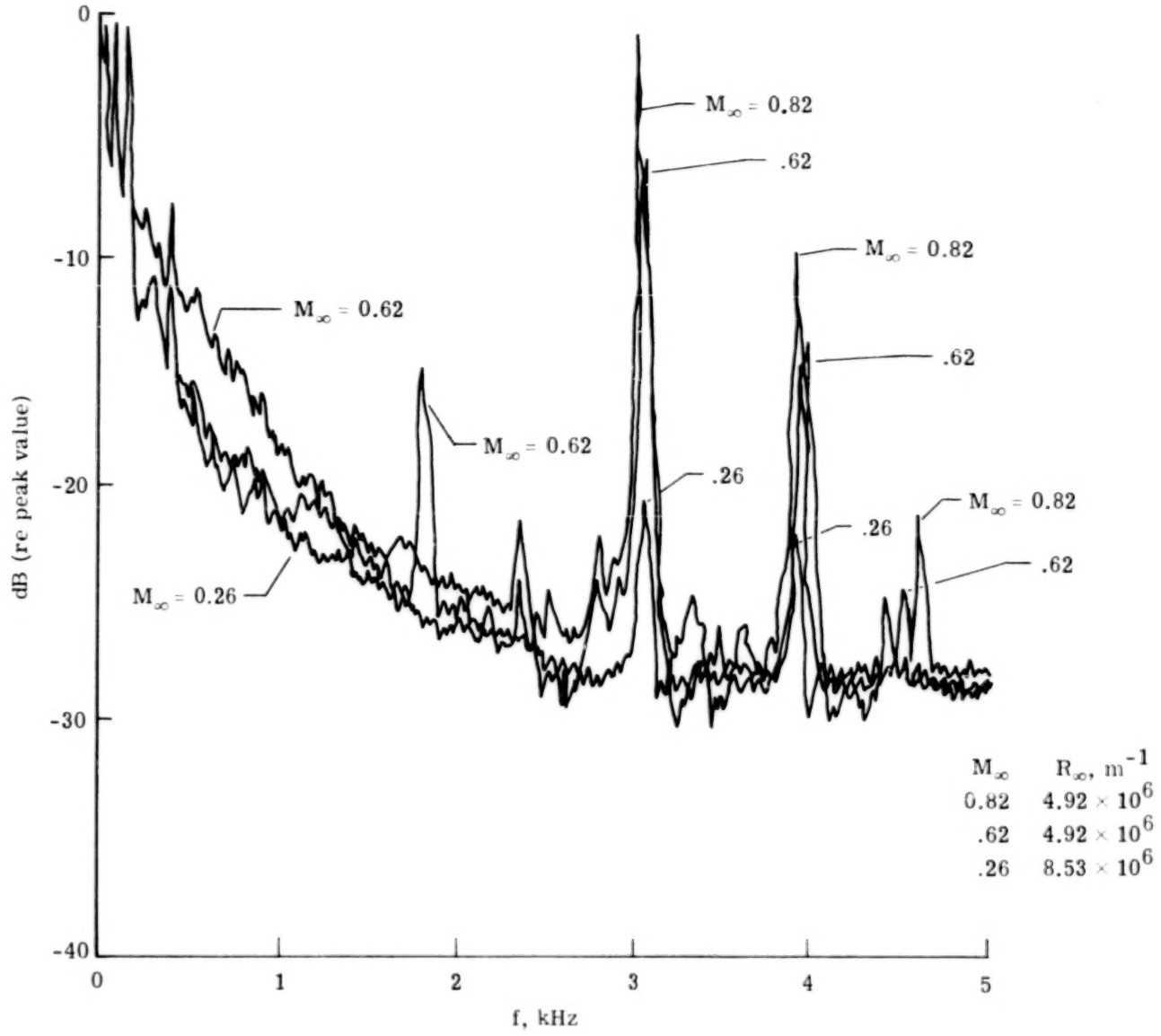

Figure 25.- Variation of acoustic spectra in Ames 12-Foot Tunnel diffuser. Strut slots closed.

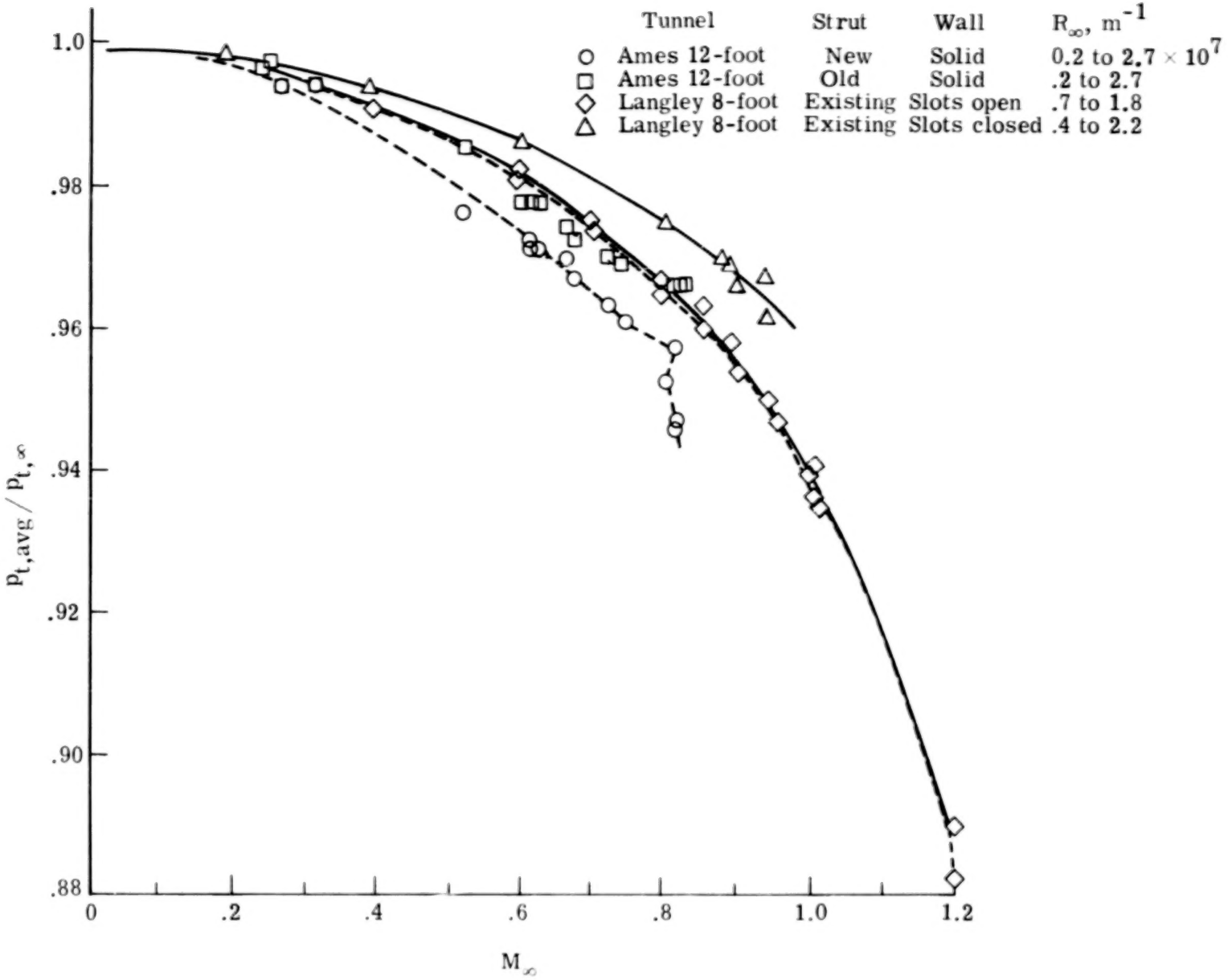

Figure 26.- Comparison between diffuser-exit losses in Ames 12-Foot and Langley 8-Foot Tunnels.

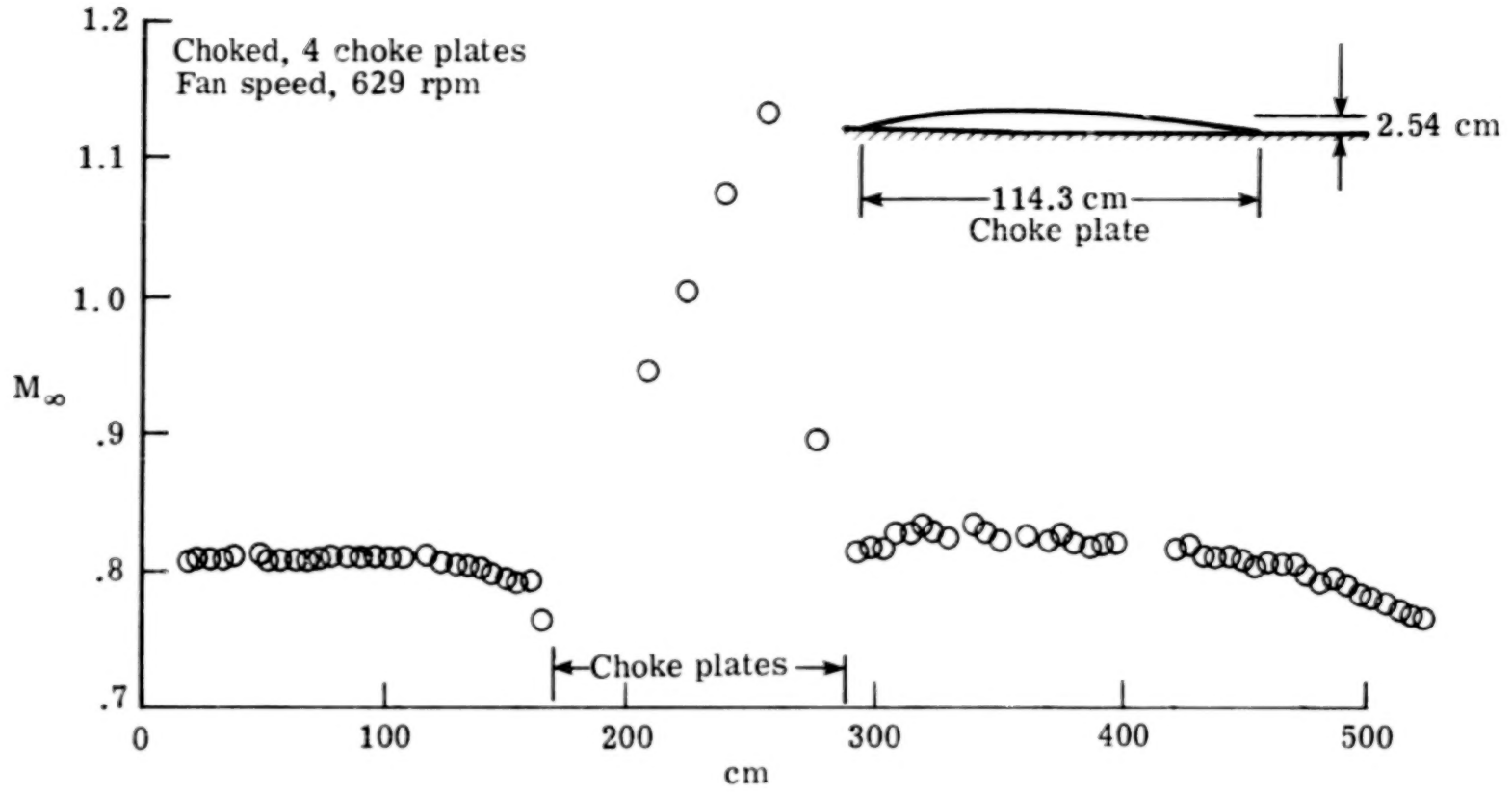

Figure 27.- Effect of choking the Langley 8-Foot Tunnel (using 4 choke plates) on test-section Mach number distribution with slots closed. M = 0.808. (From ref. 18.)

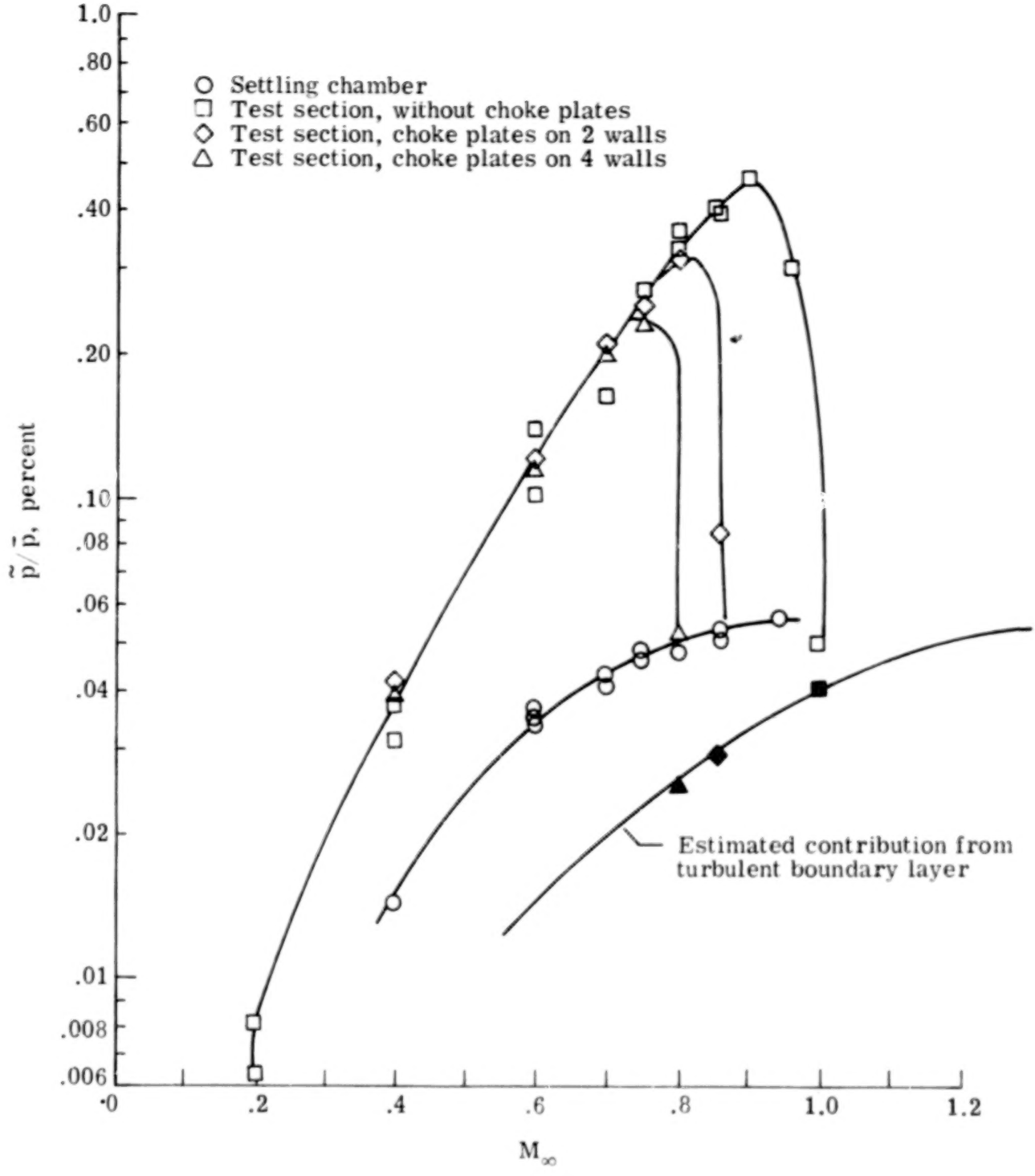

Figure 28.- Comparison between pressure fluctuations in Langley 8-Foot Tunnel with test section choked and slots closed.

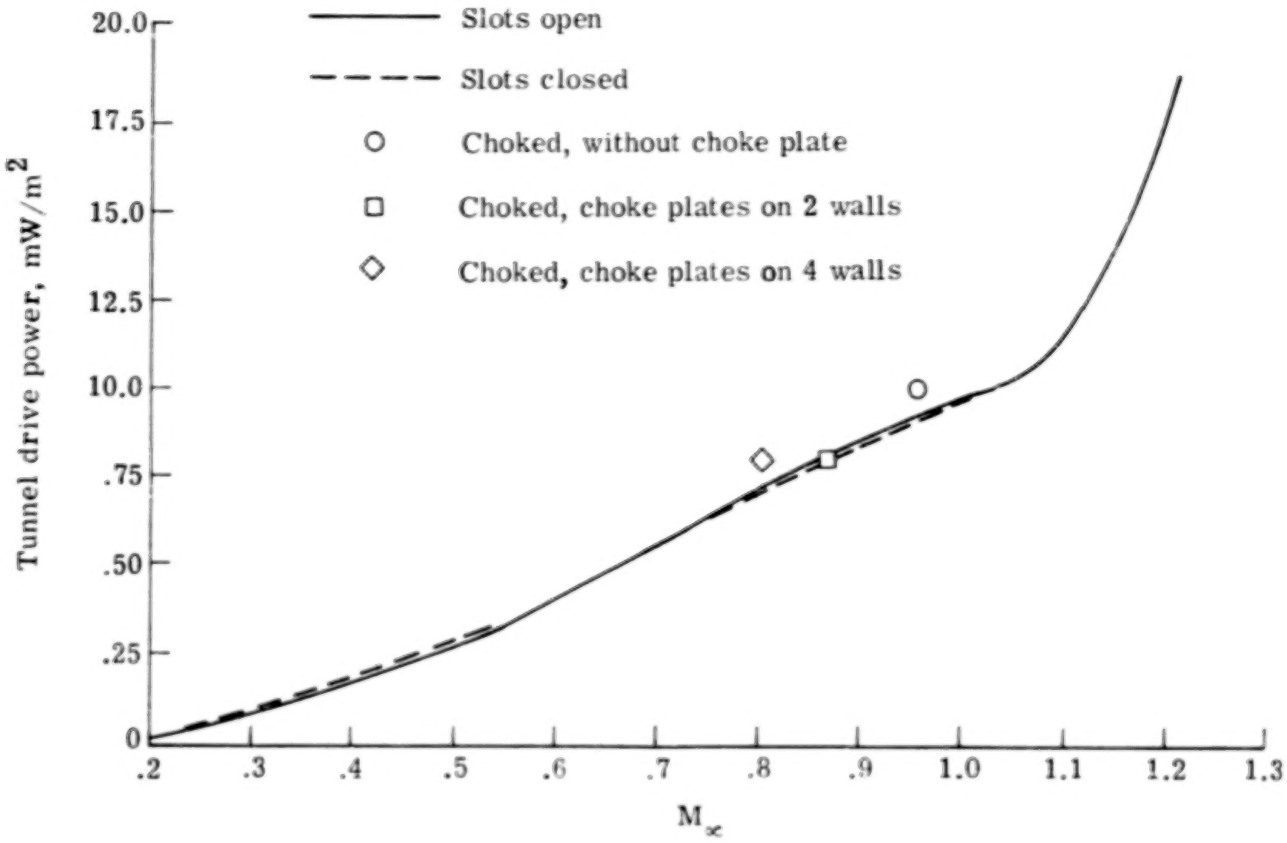

Figure 29.- Comparison between tunnel drive power required for operation in Langley 8-Foot Tunnel with and without choked flow and slots open or closed. p_t = 101.5 kPa; T_t = 322 K.

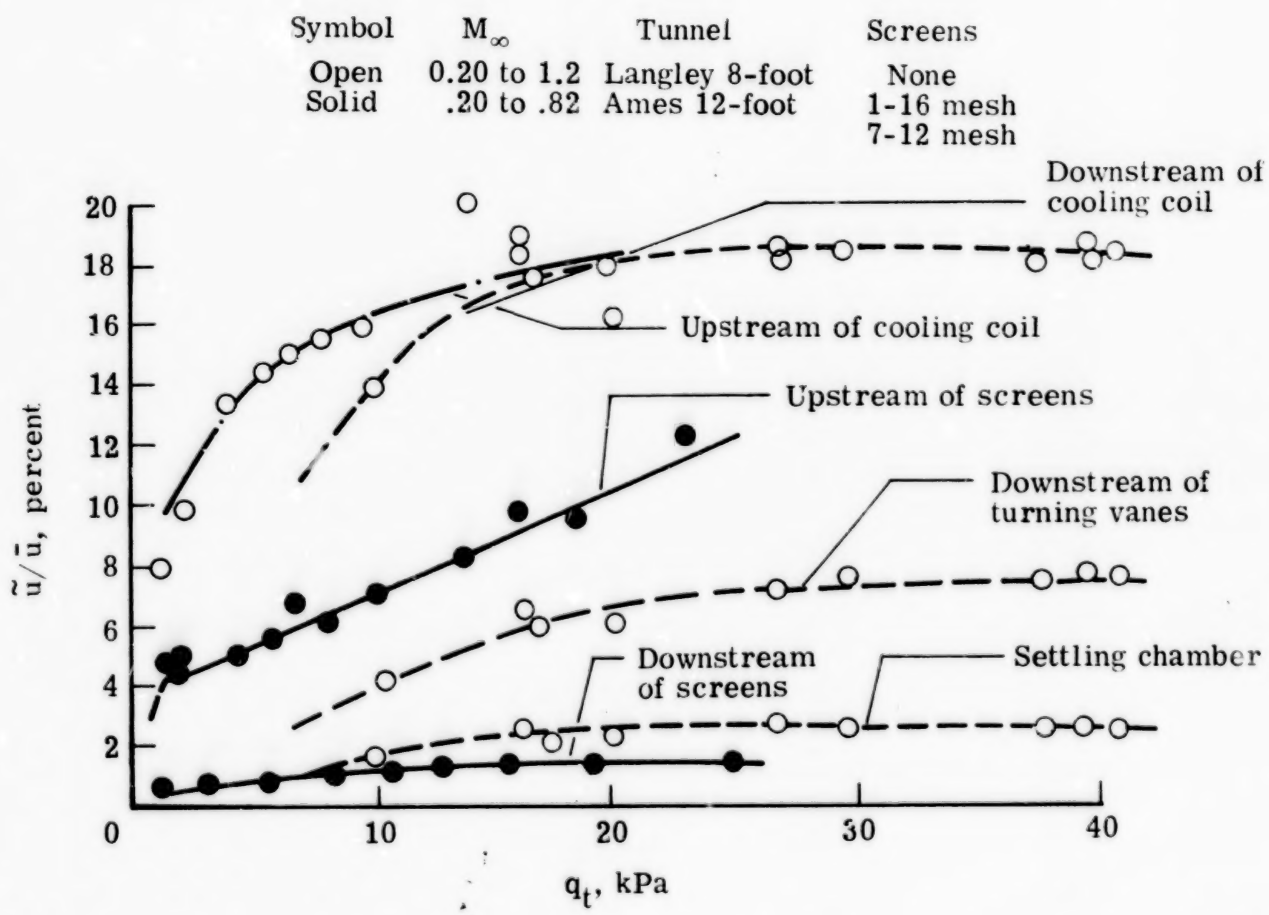

Figure 30.- Comparison between setting-chamber turbulence levels in Ames 12-Foot and Langley 8-Foot Tunnels.

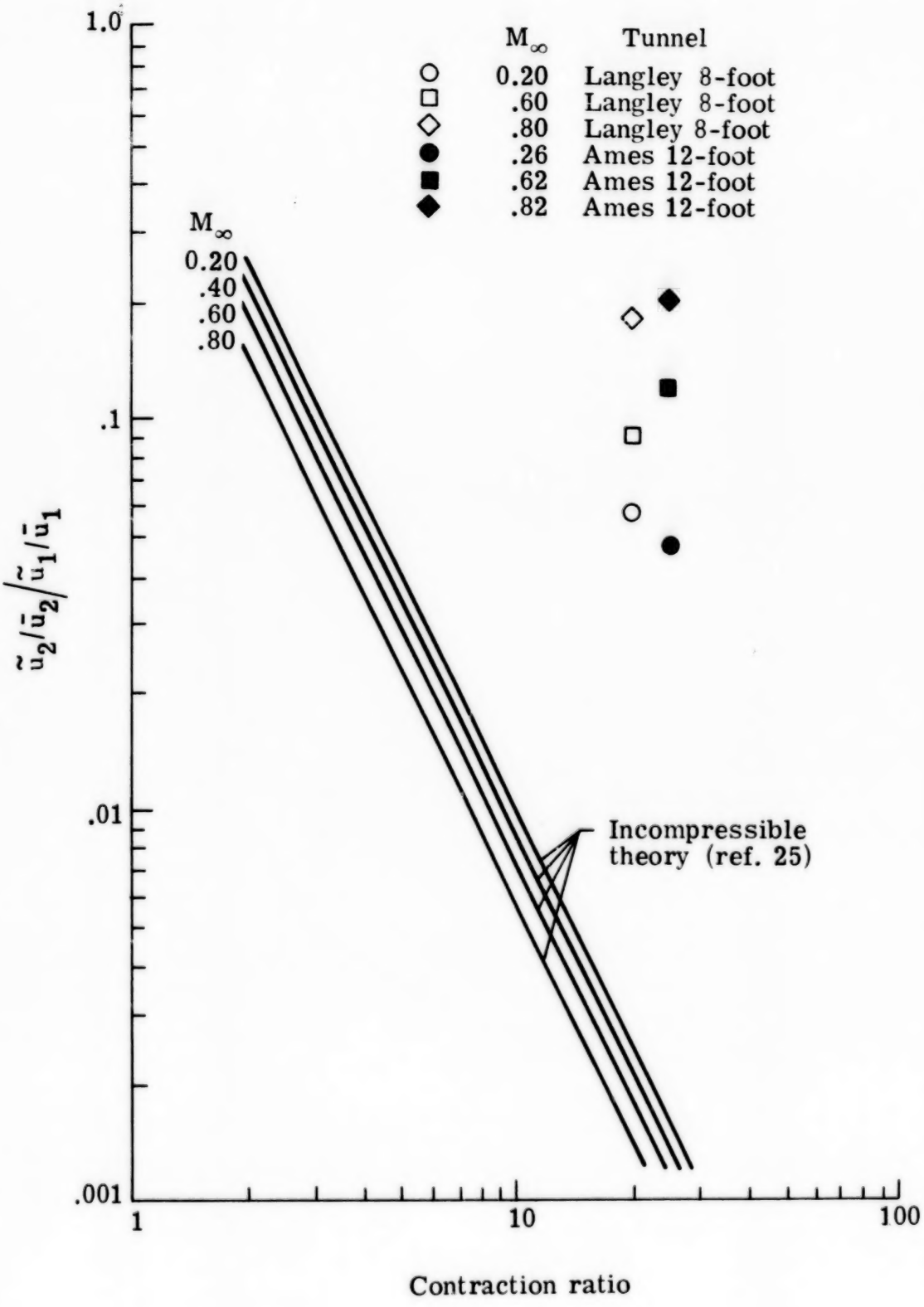

Figure 31.- Effect of nozzle contraction on turbulence transmissibility in Langley 8-Foot and Ames 12-Foot Tunnels compared with theory.

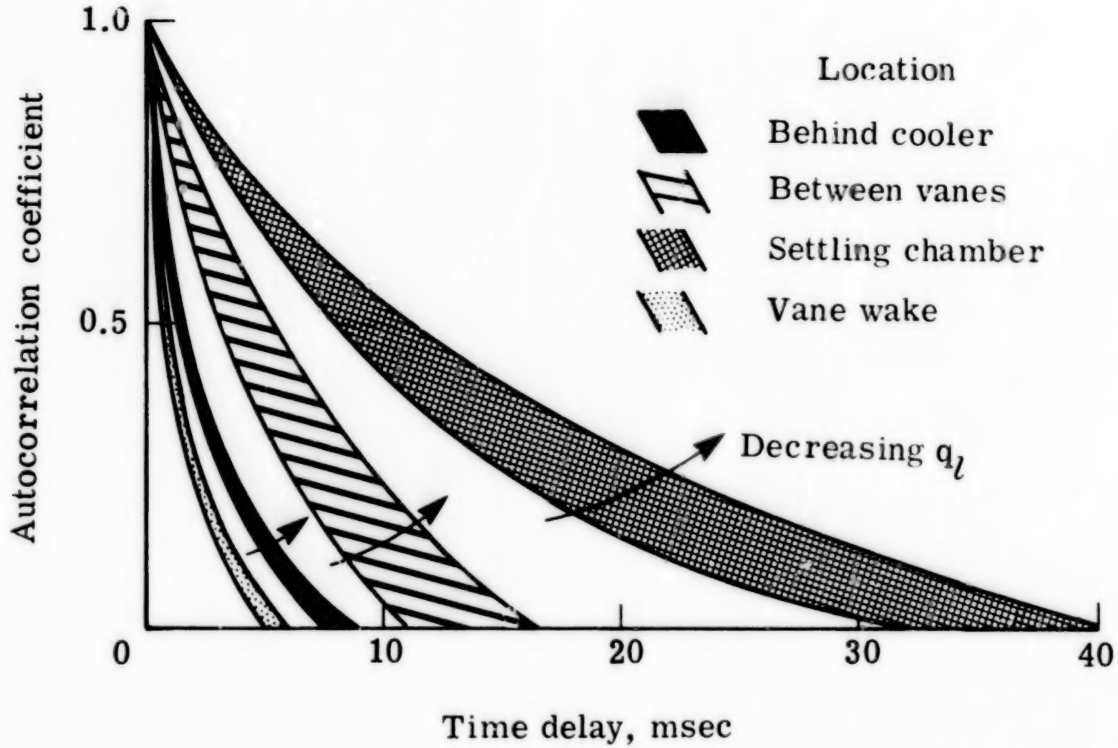

Figure 32.- Autocorrelations from hot-wire measurements in settling chamber of Langley 8-Foot Tunnel.

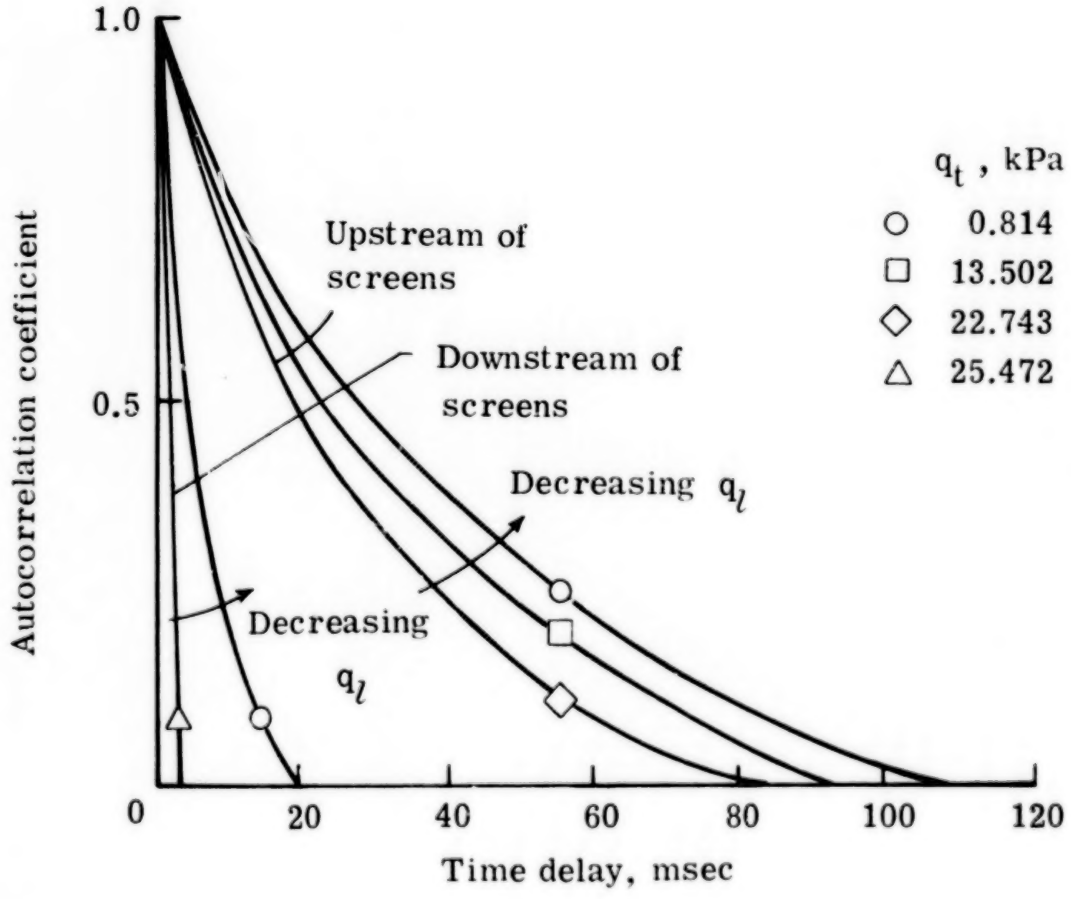

Figure 33.-Autocorrelations from hot-wire measurements in settling chamber of Ames 12-Foot Tunnel.

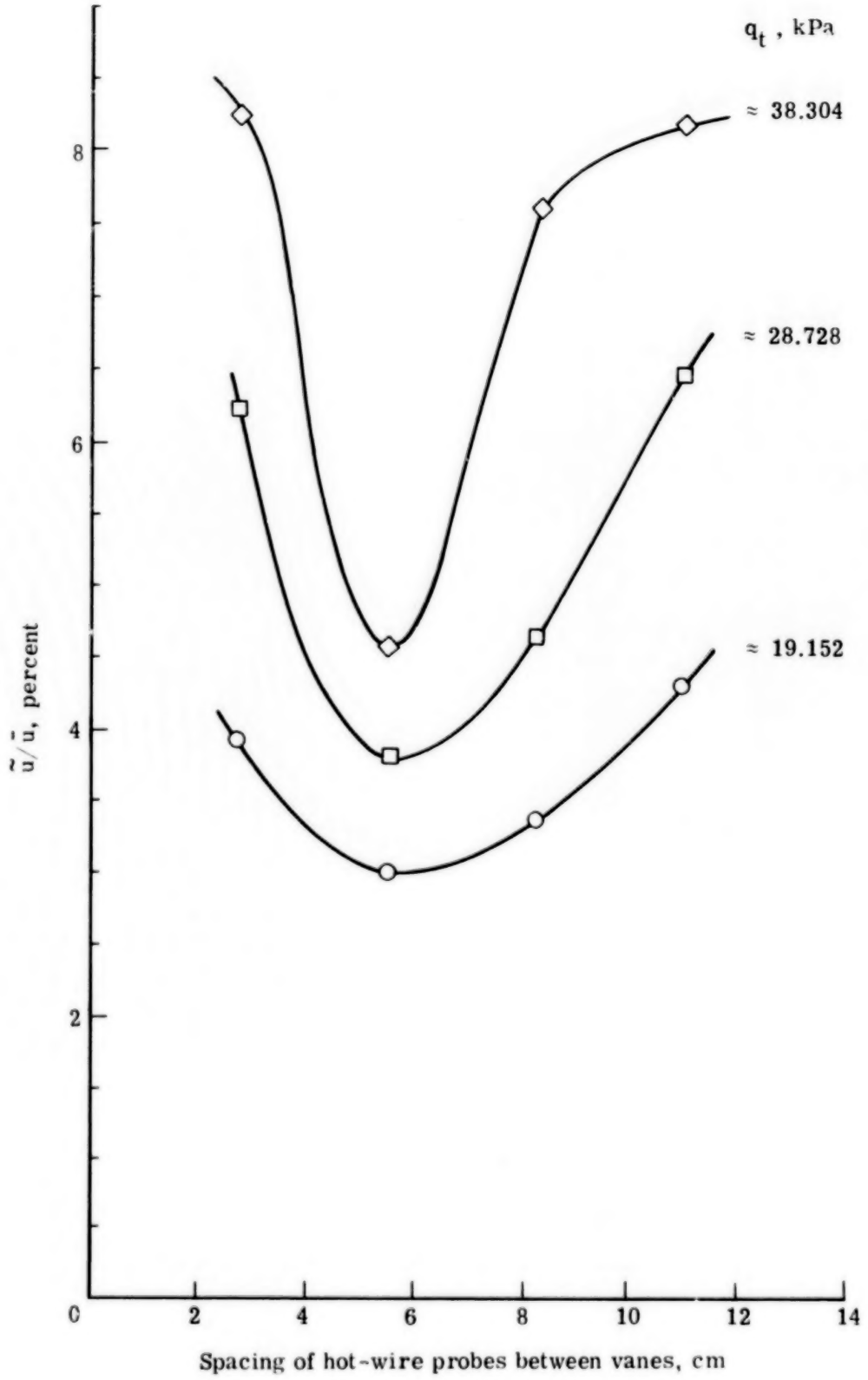

Figure 34.-Measured turbulence levels between turning vanes in settling chamber of Langley 8-Foot Tunnel. M_∞ = 0.80.

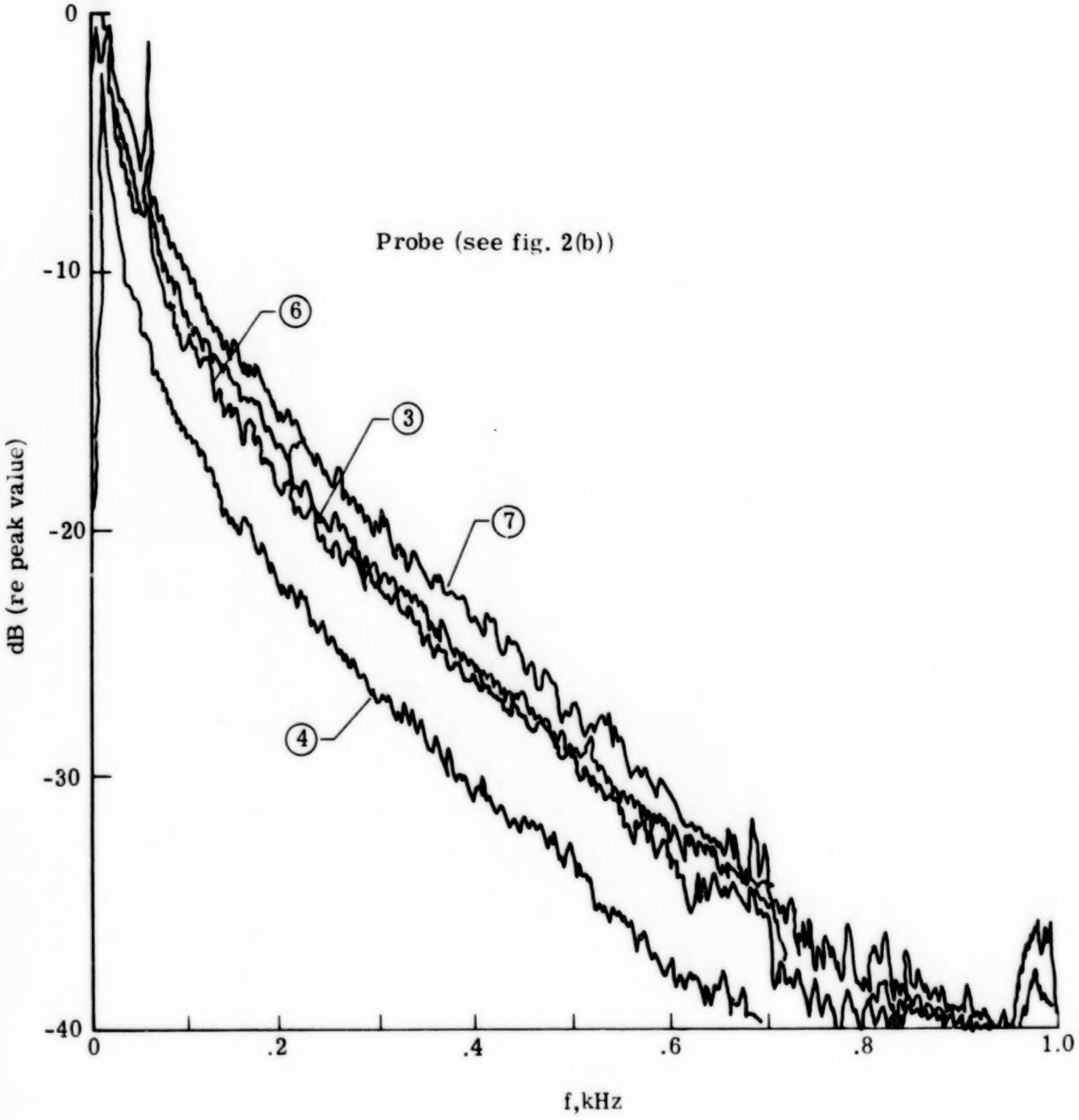

Figure 35.- Variation of hot-wire energy spectra between turning vanes in settling chamber of Langley 8-Foot Tunnel. $M_\infty = 0.8$.

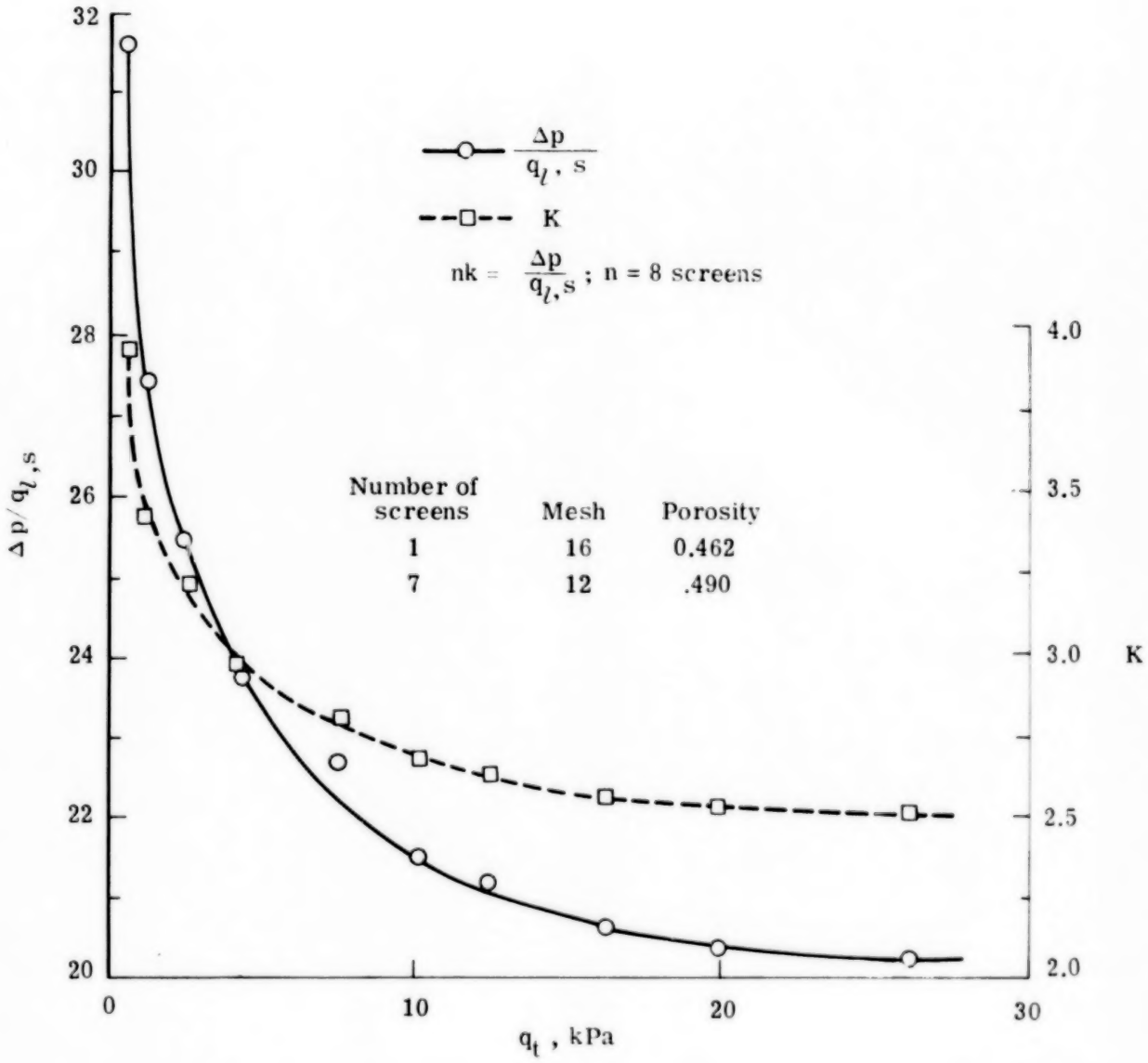

Figure 36.- Measured screen resistance coefficient in Ames 12-Foot Tunnel. M between 0.164 and 0.793.

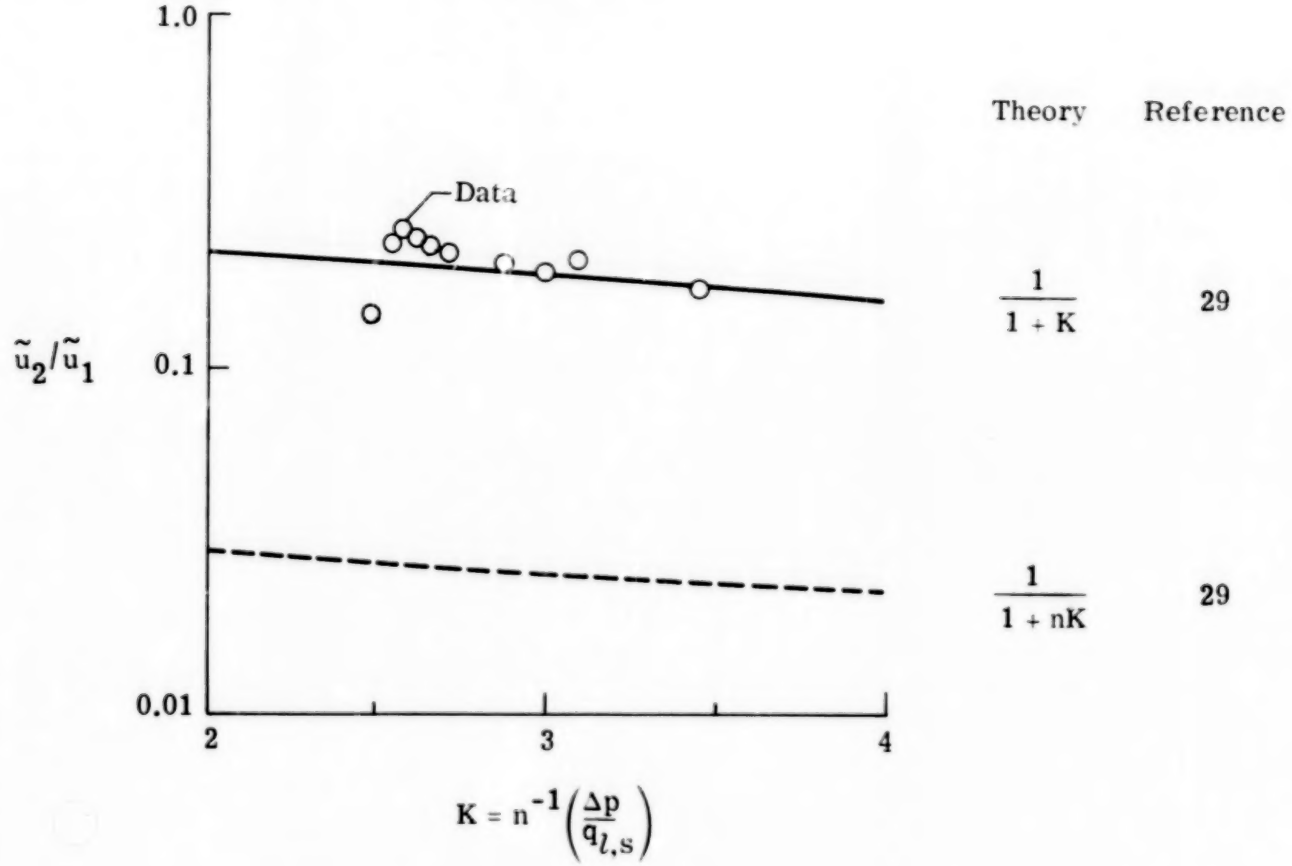

Figure 37.- Measured axial turbulence-reduction factor across settling-chamber screens in Ames 12-Foot Tunnel.

1. Report No.	2. Government Accession No.	3. Recipient's Catalog No.
NASA TP-1737		

4. Title and Subtitle	5. Report Date
EVALUATION OF FLOW QUALITY IN TWO LARGE NASA WIND TUNNELS AT TRANSONIC SPEEDS	December 1980
	6. Performing Organization Code 534-01-13-14

7. Author(s)	8. Performing Organization Report No.
William D. Harvey, P. Calvin Stainback and F. Kevin Owen	L-13448
	10. Work Unit No.

9. Performing Organization Name and Address	11. Contract or Grant No.
NASA Langley Research Center Hampton, VA 23665	
	13. Type of Report and Period Covered Technical Paper

12. Sponsoring Agency Name and Address	14. Sponsoring Agency Code
National Aeronautics and Space Administration Washington, DC 20546	

15. Supplementary Notes

William D. Harvey and P. Calvin Stainback: Langley Research Center, Hampton, VA.
F. Kevin Owen: COMPLERE, Inc., Palo Alto, California.

16. Abstract

Wind-tunnel testing of low-drag airfoils and basic transition studies at transonic speeds are designed to provide high quality aerodynamic data at high Reynolds numbers. This requires that the flow quality in facilities used for such research be excellent. To obtain a better understanding of the characteristics of facility disturbances and identification of their sources for possible facility modification, detailed flow quality measurements were made in two prospective NASA wind tunnels. This paper presents experimental results of an extensive and systematic flow-quality study of the settling chamber, test section, and diffuser in the Langley 8-Foot Transonic Pressure Tunnel (TPT) and the Ames 12-Foot Pressure Wind Tunnel (PWT). Results indicate that the free stream velocity and pressure fluctuation levels in both facilities are low ($\leq$0.1 percent) at subsonic speeds and are so high as to make it difficult to conduct meaningful boundary-layer control and transition studies at transonic speeds.

17. Key Words (Suggested by Author(s))	18. Distribution Statement
Flow quality Turbulence Flow noise Fluid mechanics Aerodynamics	Unclassified - Unlimited Subject Category 34

19. Security Classif. (of this report)	20. Security Classif. (of this page)	21. No. of Pages	22. Price
Unclassified	Unclassified	73	A04

For sale by the National Technical Information Service, Springfield, Virginia 22161

END

March 2, 1981